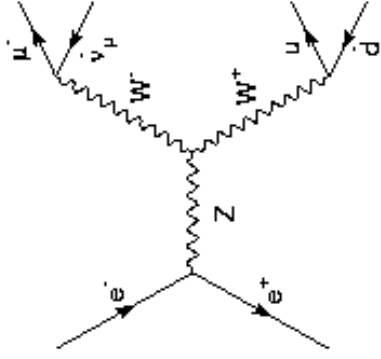
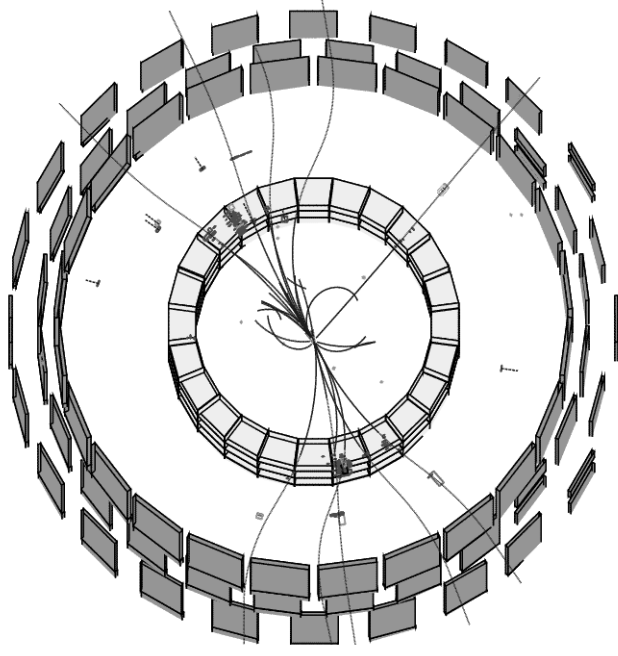


Particle Physics

experimental insight

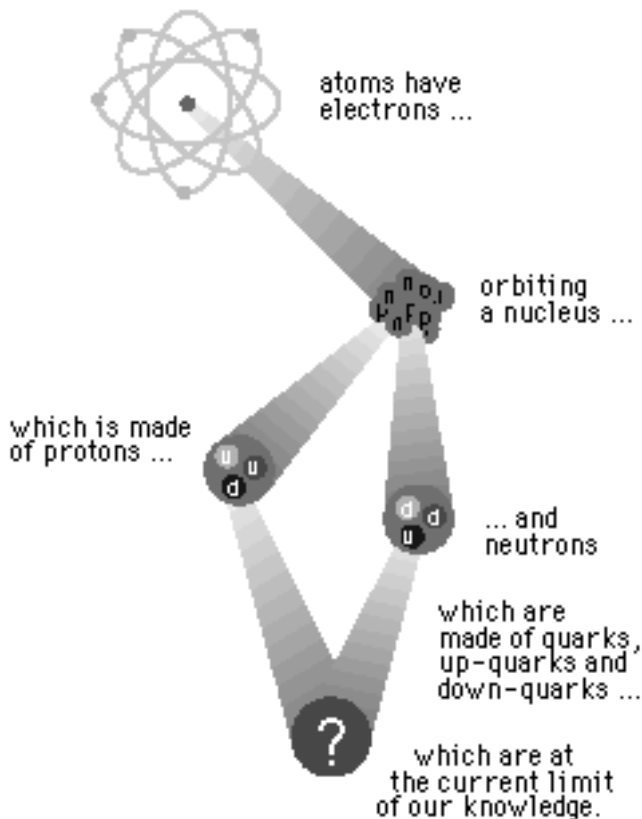


$$e^+e^- \rightarrow W^+W^- \rightarrow \mu\nu q\bar{q}$$



I. Basic concepts

- ▶▶▶▶ Particle physics studies the elementary “building blocks” of *matter* and interactions between them.
- ▶▶▶▶ Matter consists of *particles* and *fields*.
- ▶▶▶▶ Particles interact via *forces* caused by fields.
- ▶▶▶▶ Forces are being carried by specific particles, called *gauge* ['gejdʒ] *bosons*.



Forces of nature:

- 1) gravitational
- 2) weak
- 3) electromagnetic
- 4) strong

Forces of nature

| Name | Acts on: | Carrier | Range | Strength | Stable systems | Induced reaction |
|-------------------------|--------------------------------|----------------|---------------------------|-----------------|-----------------|--------------------|
| Gravity | all particles | graviton | long $F \propto 1/r^2$ | $\sim 10^{-39}$ | Solar system | Object falling |
| Weak force | fermions | bosons W and Z | $< 10^{-17}$ | 10^{-5} | None | β -decay |
| Electromagnetism | particles with electric charge | photon | long $F \propto 1/r^2$ | $1/137$ | Atoms, stones | Chemical reactions |
| Strong force | quarks and gluons | gluons | 10^{-15} m | 1 | Hadrons, nuclei | Nuclear reactions |

The Standard Model

- ▶▶▶▶ Electromagnetic and weak forces can be described by a single theory \Rightarrow the “*Electroweak Theory*” was developed in 1960s (Glashow, Weinberg, Salam).
- ▶▶▶▶ Theory of strong interactions appeared in 1970s: “*Quantum Chromodynamics*” (QCD).
- ▶▶▶▶ The “*Standard Model*” (SM) combines both.

Main postulates of SM:

- 1) Basic constituents of matter are *quarks* and *leptons* (spin 1/2).
- 2) They interact by means of gauge bosons (spin 1).
- 3) Quarks and leptons are subdivided into 3 *generations*.

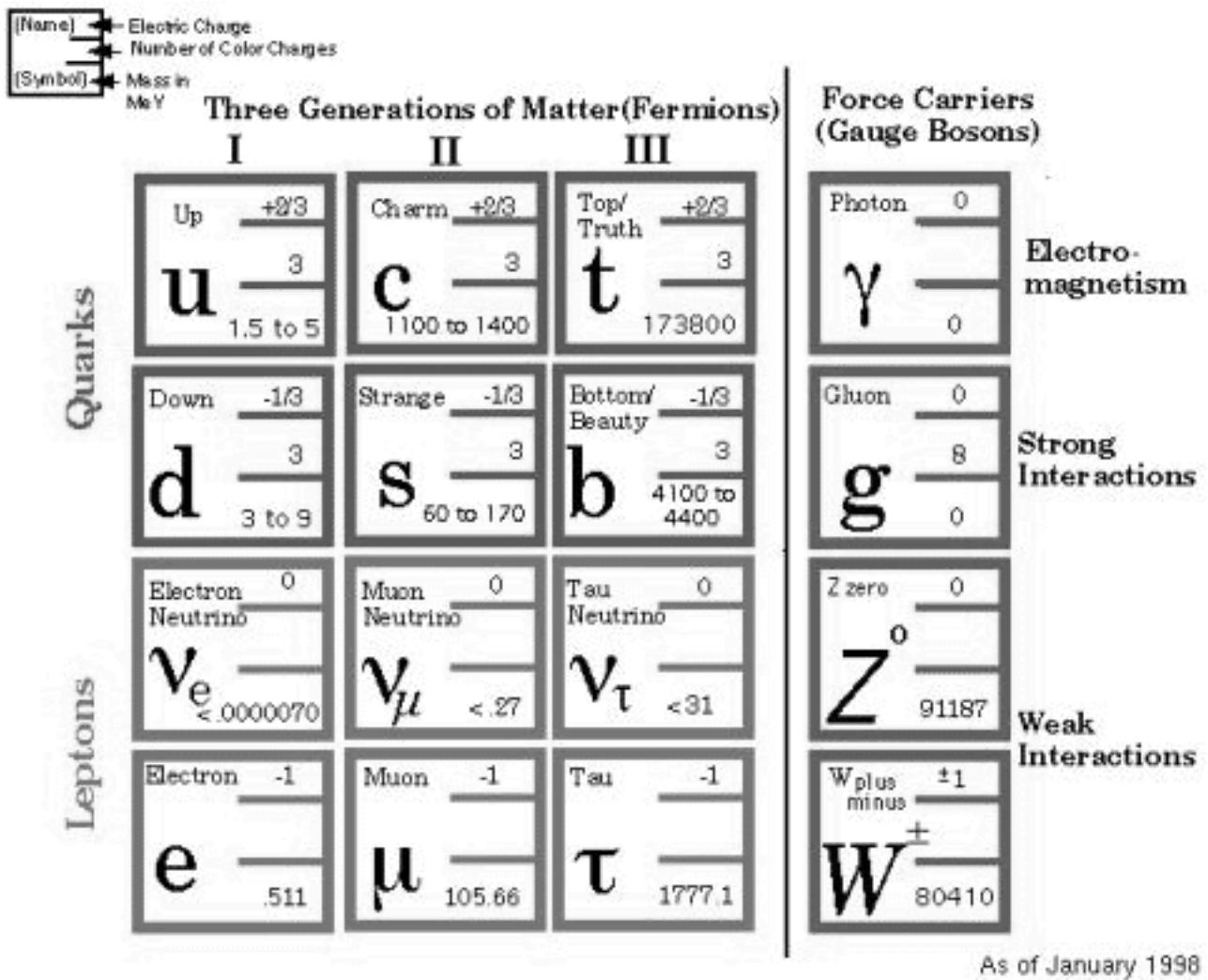


Figure 1: The Standard Model Chart

SM does not explain neither appearance of the mass nor the reason for existence of 3 generations.

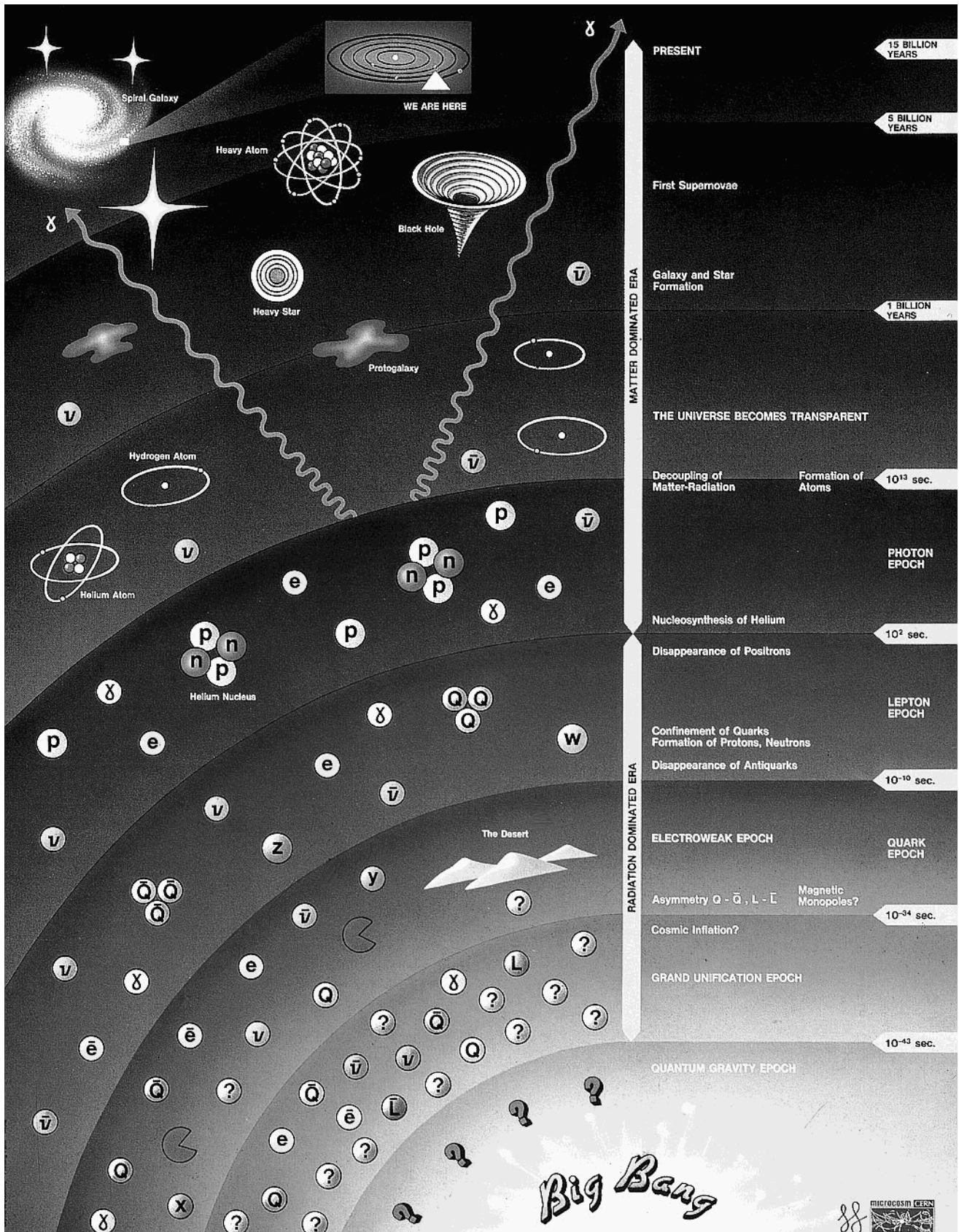


Figure 2: History of the Universe

Units and dimensions

►►► The energy is measured in *electron-volts*:

$$1 \text{ eV} \approx 1.602 \times 10^{-19} \text{ J}$$

$$1 \text{ keV} = 10^3 \text{ eV}; 1 \text{ MeV} = 10^6 \text{ eV}; 1 \text{ GeV} = 10^9 \text{ eV}$$

The Planck constant (reduced) is then:

$$\hbar \equiv h / 2\pi = 6.582 \times 10^{-22} \text{ MeV s}$$

and the “conversion constant” is:

$$\hbar c = 197.327 \times 10^{-15} \text{ MeV m}$$

►►► For simplicity, the *natural units* are used:

$$\hbar = 1 \quad \text{and} \quad c = 1$$

so that the unit of mass is eV/c^2 , and the unit of momentum is eV/c

Antiparticles

▣▣▣▣▣ Particles are described by a wavefunction:

$$\Psi(\vec{x}, t) = N e^{i(\vec{p}\vec{x} - Et)} \quad (1)$$

\vec{x} is the coordinate vector, \vec{p} - momentum vector, E and t are energy and time.

For relativistic particles, $E^2 = p^2 + m^2$, and the Schrödinger equation (2) is replaced by the Klein-Gordon equation (3):

$$i \frac{\partial}{\partial t} \Psi(\vec{x}, t) = -\frac{1}{2m} \nabla^2 \Psi(\vec{x}, t) \quad (2)$$

⇓

$$-\frac{\partial^2}{\partial t^2} \Psi = -\nabla^2 \Psi(\vec{x}, t) + m^2 \Psi(\vec{x}, t) \quad (3)$$

▣▣▣▣▣ There exist *negative* energy solutions!

$$\Psi^*(\vec{x}, t) = N^* \cdot e^{i(-\vec{p}\vec{x} + E_+ t)}$$

The problem with the Klein-Gordon equation: it is second order in derivatives. In 1928, Dirac found the first-order form having the same solutions:

$$i\frac{\partial\Psi}{\partial t} = -i\sum_i \alpha_i \frac{\partial\Psi}{\partial x_i} + \beta m\Psi \quad (4)$$

where α_i and β are 4×4 matrices and Ψ are four-component wavefunctions: *spinors* (for particles with spin 1/2).

$$\Psi(\vec{x}, t) = \begin{bmatrix} \Psi_1(\vec{x}, t) \\ \Psi_2(\vec{x}, t) \\ \Psi_3(\vec{x}, t) \\ \Psi_4(\vec{x}, t) \end{bmatrix}$$

Dirac-Pauli representation of matrices α_i and β :

$$\alpha_i = \begin{pmatrix} 0 & \sigma_i \\ \sigma_i & 0 \end{pmatrix}, \quad \beta = \begin{pmatrix} I & 0 \\ 0 & -I \end{pmatrix}$$

Here I is 2×2 unit matrix and σ_i are Pauli matrices:

$$\sigma_1 = \begin{pmatrix} 0 & 1 \\ 1 & 0 \end{pmatrix}, \quad \sigma_2 = \begin{pmatrix} 0 & -i \\ i & 0 \end{pmatrix}, \quad \sigma_3 = \begin{pmatrix} 1 & 0 \\ 0 & -1 \end{pmatrix}$$

Also possible is Weyl representation:

$$\alpha_i = \begin{pmatrix} -\sigma_i & 0 \\ 0 & \sigma_i \end{pmatrix}, \quad \beta = \begin{pmatrix} 0 & I \\ I & 0 \end{pmatrix}$$

Dirac's picture of vacuum

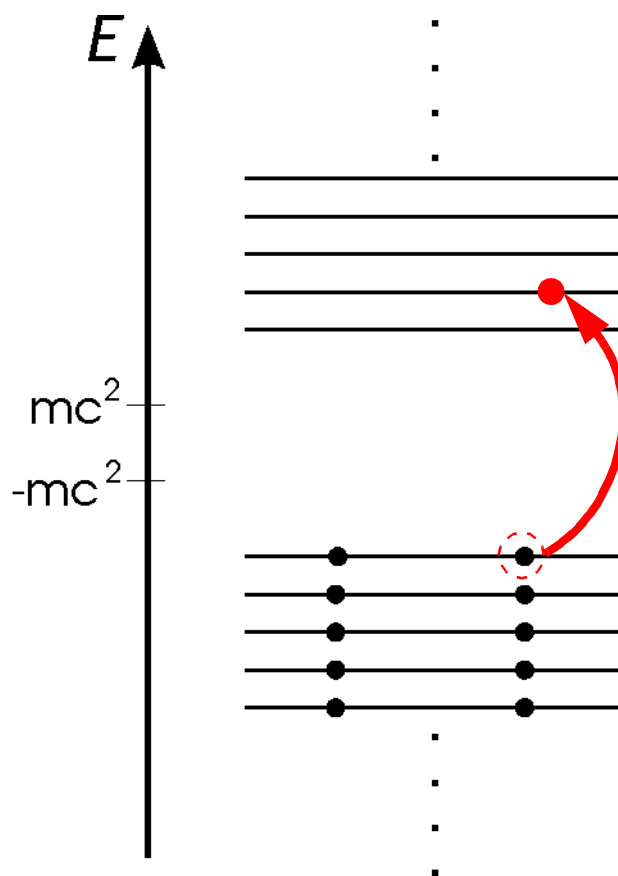


Figure 3: Fermions in Dirac's representation.

The “hole” created by the appearance of the electron with a positive energy is interpreted as the presence of electron's *antiparticle* with the opposite charge.

- ▣► Every charged particle has the antiparticle of the same mass and opposite charge.

Discovery of the positron

1933, C.D.Andersson, Univ. of California (Berkeley):
observed with the Wilson cloud chamber 15 tracks in
cosmic rays:

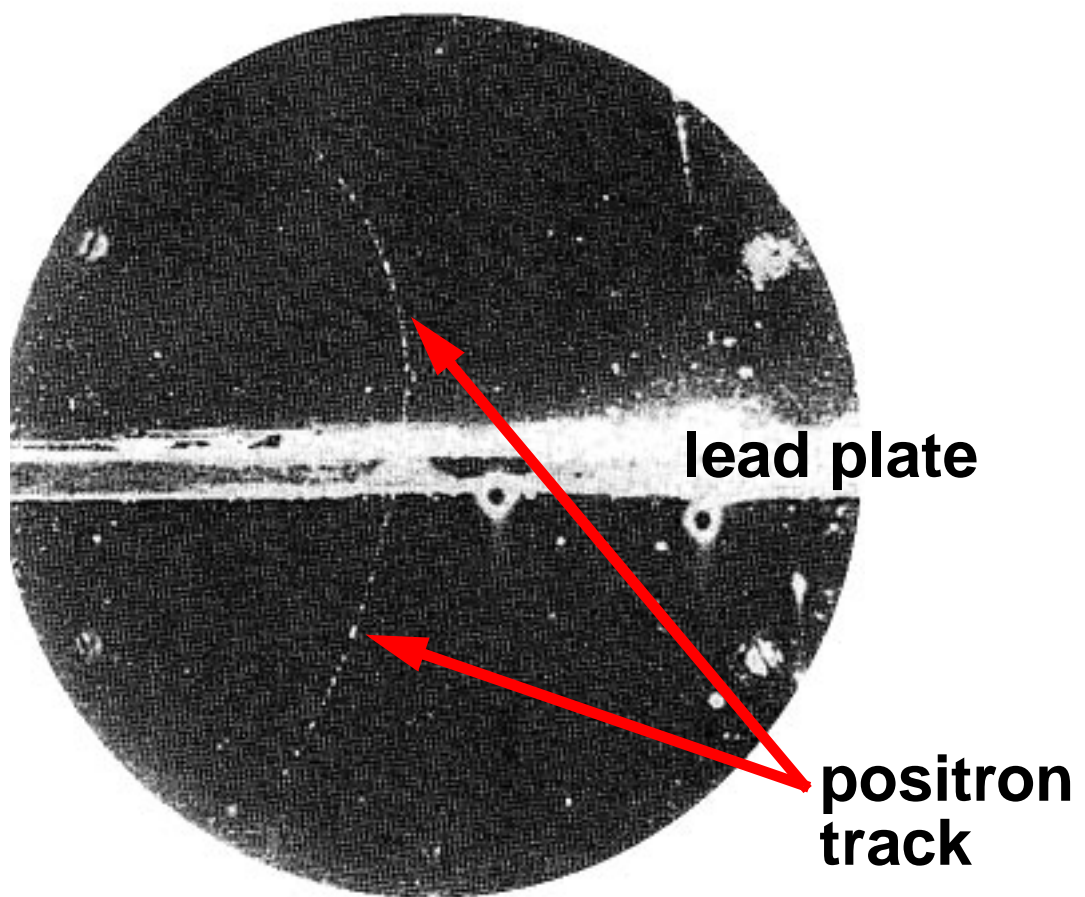


Figure 4: Photo of the track in the Wilson chamber

Feynman diagrams

In 1940s, R.Feynman developed a diagram technique for representing processes in particle physics.

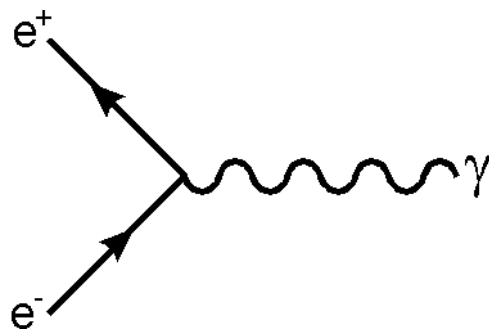


Figure 5: A Feynman diagram example

Main assumptions and requirements:

- ❖ Time runs from left to right
- ❖ Arrow directed towards the right indicates a particle, and otherwise - antiparticle
- ❖ At every vertex, momentum, angular momentum and charge are conserved (but not energy)
- ❖ Particles are usually denoted with solid lines, and gauge bosons - with helices or dashed lines

Virtual processes:

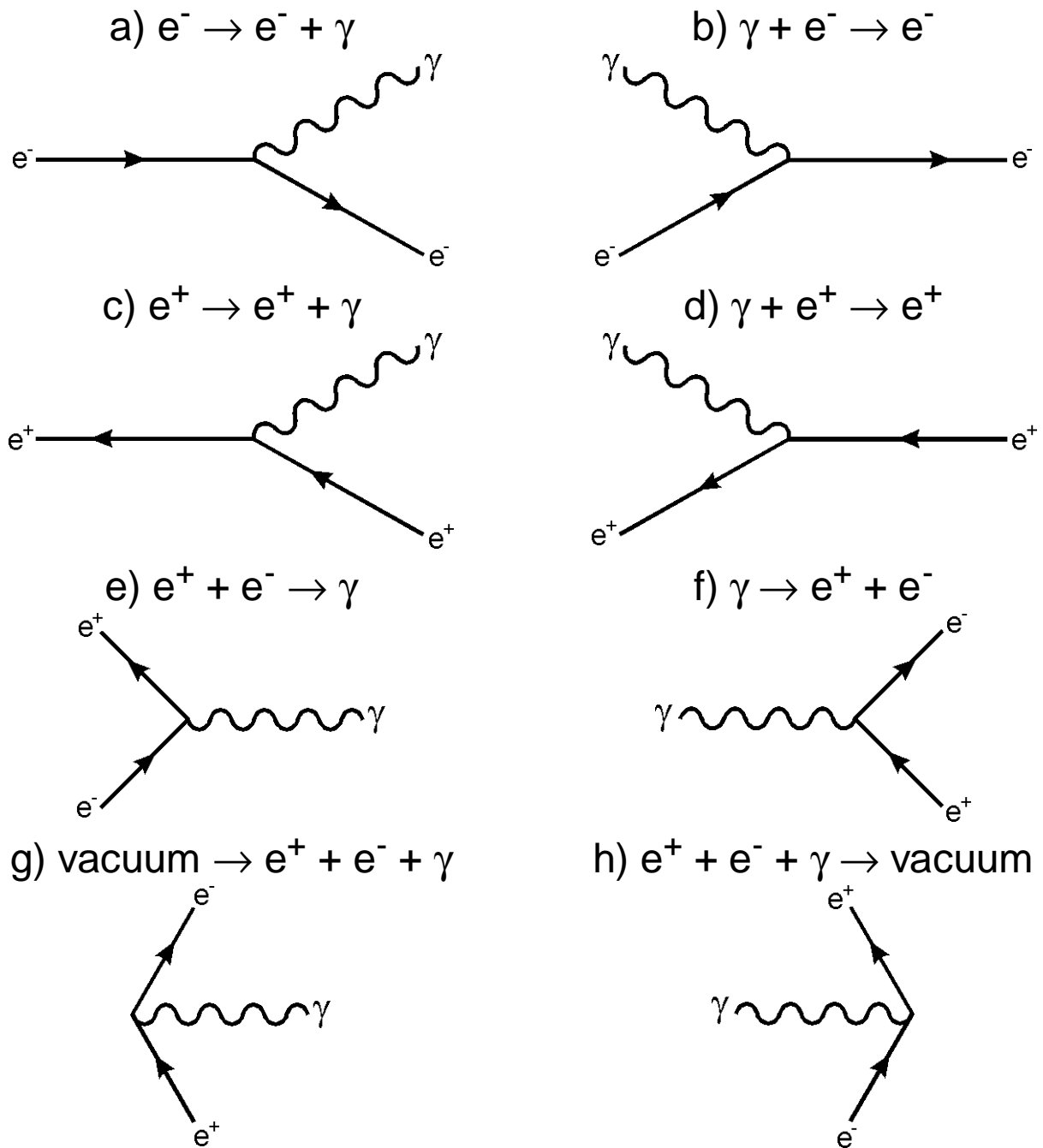


Figure 6: Feynman diagrams for basic processes involving electron, positron and photon

Real processes

- A real process demands energy conservation, hence is a combination of virtual processes.

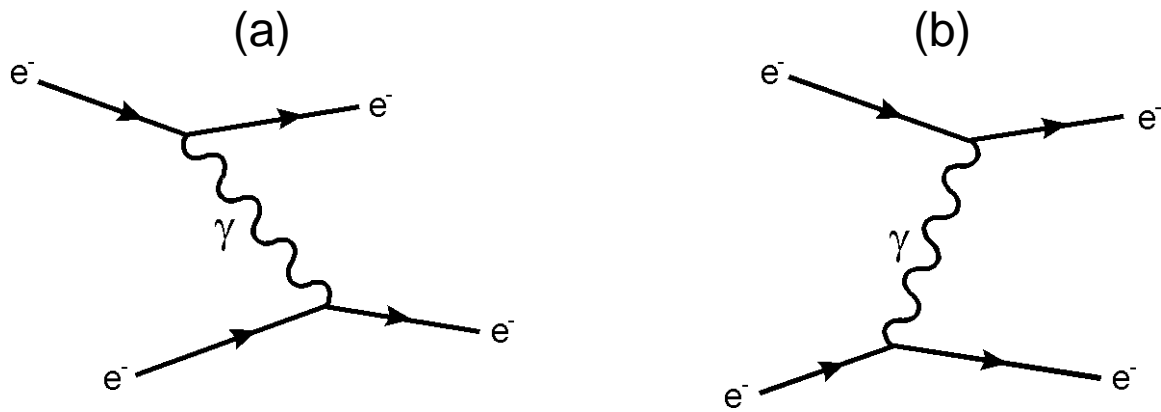


Figure 7: Electron-electron scattering, single photon exchange

- Any real process receives contributions from all possible virtual processes.

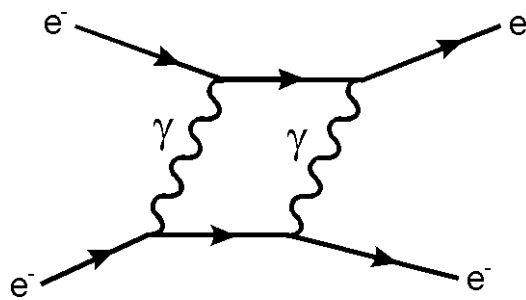


Figure 8: Two-photon exchange contribution

- ❖ Number of vertices in a diagram is called its *order*.
- ❖ Each vertex has an associated probability proportional to a *coupling constant*, usually denoted as “ α ”. In discussed processes this constant is

$$\alpha_{em} = \frac{e^2}{4\pi\epsilon_0} \approx \frac{1}{137}$$

- ❖ For the real processes, a diagram of order n gives a contribution to probability of order α^n .

Provided sufficiently small α , high order contributions to many real processes can be neglected, allowing rather precise calculations of probability amplitudes of physical processes.

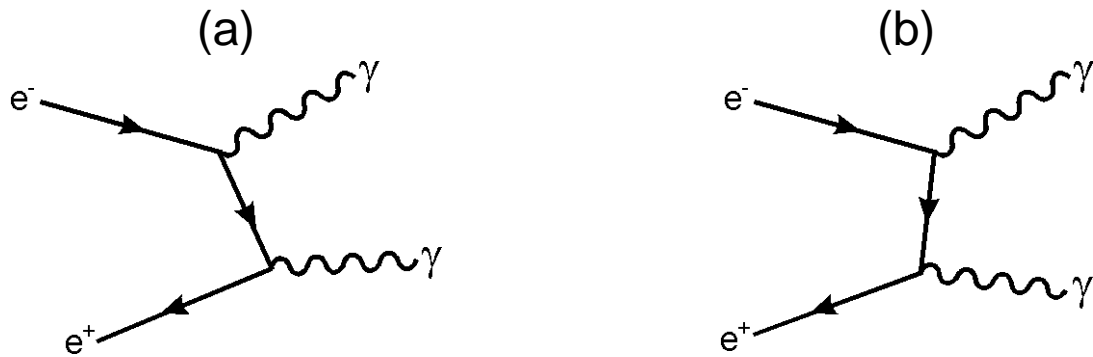


Figure 9: Lowest order contributions to
 $e^+e^- \rightarrow \gamma\gamma$

Diagrams which differ only by time-ordering are usually implied by drawing only one of them

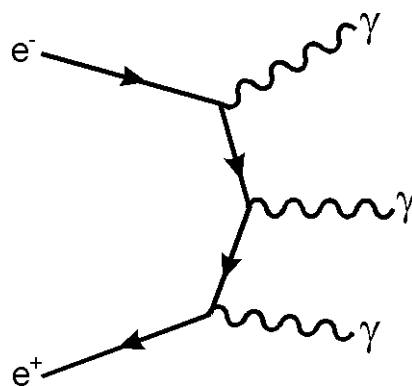


Figure 10: Lowest order of the process
 $e^+e^- \rightarrow \gamma\gamma\gamma$

This kind of process implies $3!=6$ different time orderings

⇒ Only from the order of diagrams one can estimate the ratio of appearance rates of processes:

$$R \equiv \frac{\text{Rate}(e^+e^- \rightarrow \gamma\gamma\gamma)}{\text{Rate}(e^+e^- \rightarrow \gamma\gamma)} = O(\alpha)$$

This ratio can be measured experimentally; it appears to be $R = 0.9 \times 10^{-3}$, which is smaller than α_{em} , but the equation above is only a first order prediction.

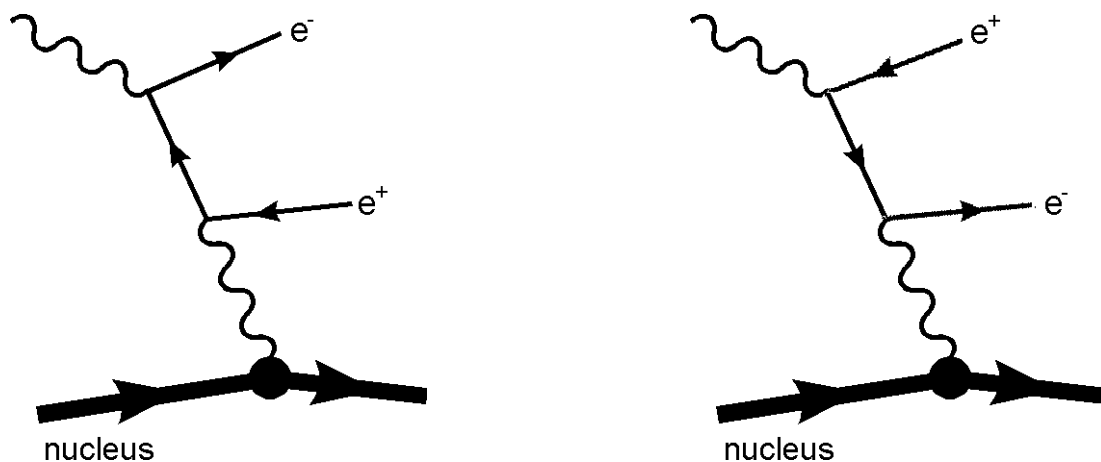


Figure 11: Diagrams are not related by time ordering

For nucleus, the coupling is proportional to $Z^2\alpha$, hence the rate of this process is of order $Z^2\alpha^3$

Exchange of a massive boson

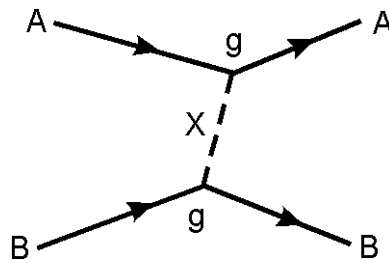


Figure 12: Exchange of a massive particle X

In the rest frame of particle A:

$$A(E_0, \vec{p}_0) \rightarrow A(E_A, \vec{p}) + X(E_x, -\vec{p})$$

where $E_0 = M_A$, $\vec{p}_0 = (0, 0, 0)$,

$$E_A = \sqrt{p^2 + M_A^2}, \quad E_X = \sqrt{p^2 + M_X^2}$$

From this one can estimate the maximum distance over which X can propagate before being absorbed:

$\Delta E = E_X + E_A - M_A \geq M_X$, and this energy violation

can exist only for a period of time $\Delta t \approx \hbar / \Delta E$, hence the *range of the interaction* is

$$r \approx R \equiv \hbar M_X c$$

- ▣▣▣▣ For a massless exchanged particle, the interaction has an infinite range (e.g., electromagnetic)
- ▣▣▣▣ In case of a very heavy exchanged particle (e.g., a W boson in weak interaction), the interaction can be approximated by a *zero-range*, or *point interaction*:

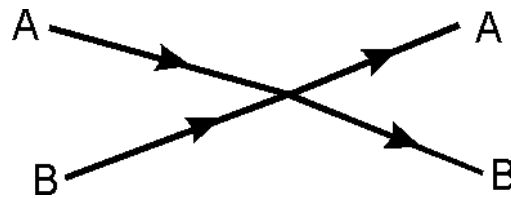


Figure 13: Point interaction as a result of $M_X \rightarrow \infty$

$$R_W = \hbar/M_W = \hbar/(80.4 \text{ GeV}/c^2) \approx 2 \times 10^{-18} \text{ m}$$

Considering particle X as an electrostatic potential $V(r)$, the Klein-Gordon equation (3) for it will look like

$$\nabla^2 V(r) = \frac{1}{r^2} \frac{\partial}{\partial r} \left(r^2 \frac{\partial V}{\partial r} \right) = M_X^2 V(r) \quad (5)$$

Yukawa potential (1935)

Integration of the equation (5) gives the solution of

$$V(r) = -\frac{g^2}{4\pi r} e^{-r/R} \quad (6)$$

Here g is an integration constant, and it is interpreted as the coupling strength for particle X to the particles A and B.

▣ In Yukawa theory, g is analogous to the electric charge in QED, and the analogue of α_{em} is

$$\alpha_X = \frac{g^2}{4\pi}$$

α_X characterizes the strength of the interaction at distances $r \leq R$.

Consider a particle being scattered by the potential (6), thus receiving a momentum transfer \vec{q}

▣ Potential (6) has the corresponding amplitude,

which is its Fourier-transform (like in optics):

$$f(\vec{q}) = \int V(\vec{x}) e^{i\vec{q}\vec{x}} d^3\vec{x} \quad (7)$$

Using polar coordinates, $d^3\vec{x} = r^2 \sin\theta d\theta dr d\phi$, and assuming $V(\vec{x}) = V(r)$, the amplitude is

$$f(\vec{q}) = 4\pi g \int_0^\infty V(r) \frac{\sin(qr)}{qr} r^2 dr = \frac{-g^2}{q^2 + M_X^2} \quad (8)$$

►► For the point interaction, $M_X^2 \gg q^2$, hence $f(\vec{q})$ becomes a constant:

$$f(\vec{q}) = -G = \frac{-4\pi\alpha_X}{M_X^2}$$

That means that the point interaction is characterized not only by α_X , but by M_X as well.

II. Leptons, quarks and hadrons

▣▣▣▣ \rightarrow *Leptons* are spin-1/2 fermions, not subject to strong interaction

$$\begin{pmatrix} \nu_e \\ e^- \end{pmatrix}, \begin{pmatrix} \nu_\mu \\ \mu^- \end{pmatrix}, \begin{pmatrix} \nu_\tau \\ \tau^- \end{pmatrix}$$

$$M_e < M_\mu < M_\tau$$

- ❖ Electron e^- , muon μ^- and tauon τ^- have corresponding neutrinos ν_e , ν_μ and ν_τ .
- ❖ Electron, muon and tauon have electric charge of $-e$. Neutrinos are neutral.
- ❖ Neutrinos *possibly* have zero masses.
- ❖ For neutrinos, only weak interactions have been observed so far

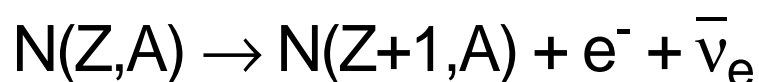
- Antileptons are positron e^+ , positive muon and tauon (pronounced *mju-plus* and *tau-plus*), and antineutrinos:

$$\begin{pmatrix} e^+ \\ \bar{\nu}_e \end{pmatrix}, \begin{pmatrix} \mu^+ \\ \bar{\nu}_\mu \end{pmatrix}, \begin{pmatrix} \tau^+ \\ \bar{\nu}_\tau \end{pmatrix}$$

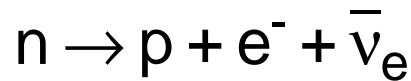
- Neutrinos and antineutrinos differ by the *lepton number*. Leptons possess lepton numbers $L_\alpha=1$ (α stands for e , μ or τ), and antileptons have $L_\alpha=-1$.
- Lepton numbers are conserved in any interaction

Neutrinos can not be registered by any detector, there are only indirect indications of their quantities.

- ❖ First indication of neutrino existence came from β -decays of a nucleus N :



β -decay is nothing but a neutron decay:



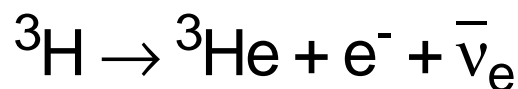
❖ Necessity of a neutrino existence comes from the apparent energy and angular momentum non-conservation in observed reactions

➡ Note that for the sake of the lepton number conservation, electron must be accompanied by an antineutrino and not neutrino!

Mass limit for $\bar{\nu}_e$ can be estimated from the precise measurements of the β -decay:

$$m_e \leq E_e \leq \Delta M_N - m_{\bar{\nu}_e}$$

The best results are obtained from the tritium decay:



It gives $m_{\bar{\nu}_e} \leq 15 \text{ eV}/c^2$, which usually is considered as a zero mass.

▣▣▣▣ An inverse β -decay also takes place:

$$\nu_e + n \rightarrow e^- + p \quad (9)$$

or

$$\bar{\nu}_e + p \rightarrow e^+ + n \quad (10)$$

However, the probability of these processes is very low, therefore to register it one needs a very intense flux of neutrinos

Reines and Cowan experiment (1956)

- ❖ Using antineutrinos produced in a nuclear reactor, it is possible to obtain around 2 events (10) per hour.
- ❖ Aqueous solution of $CdCl_2$ used as the target (Cd used to capture neutrons)
- ❖ To separate the signal from the background, the “delayed coincidence” scheme was used: signal from neutron comes later than one from positron

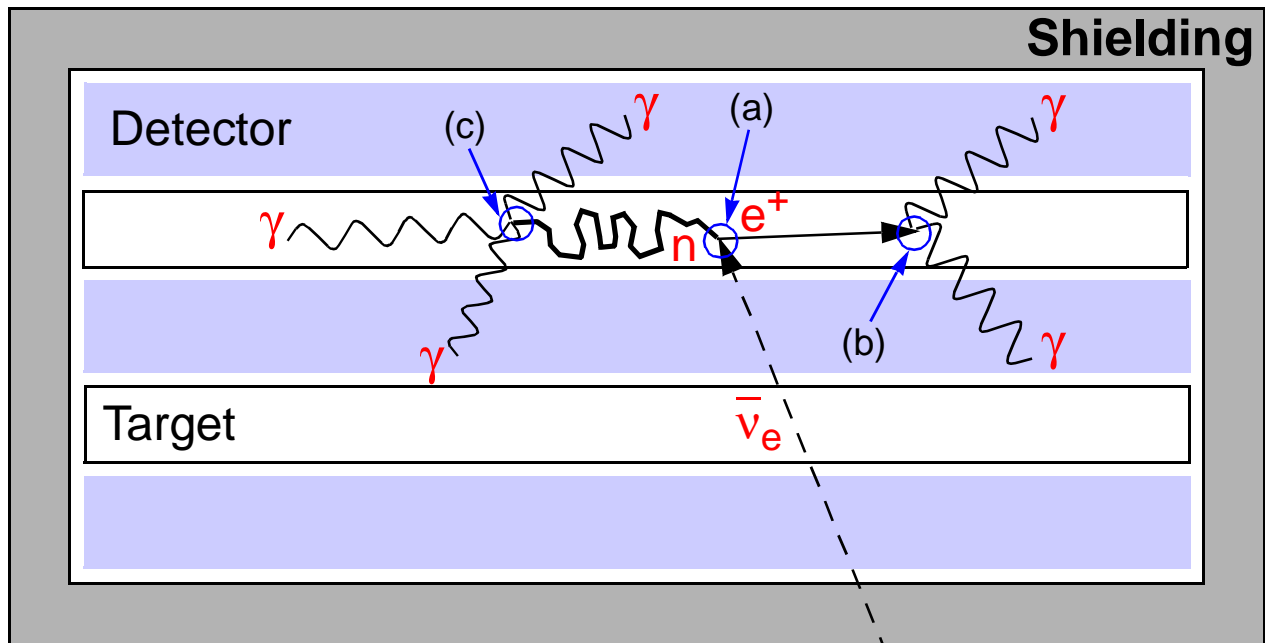


Figure 14: Schematic representation of the Reines and Cowan experiment

Main stages:

- (a) Antineutrino interacts with proton, producing neutron and positron
- (b) Positron annihilates with an atomic electron, produces fast photon which gives rise to softer photons through the Compton effect
- (c) Neutron captured by a Cd nucleus, releasing more photons

▣▣▣▣ Muons were first observed in 1936, in *cosmic rays*

Cosmic rays have two components:

- 1) *primaries*, which are high-energy particles coming from the outer space, mostly hydrogen nuclei
- 2) *secondaries*, the particles which are produced in collisions of primaries with nuclei in the Earth atmosphere; muons belong to this component

❖ Muons are 200 times heavier than electrons and are very penetrating particles.

❖ Electromagnetic properties of muon are identical to those of electron (upon the proper account of the mass difference)

▣▣▣▣ Tauon is the heaviest of leptons, was discovered in e^+e^- annihilation experiments in 1975

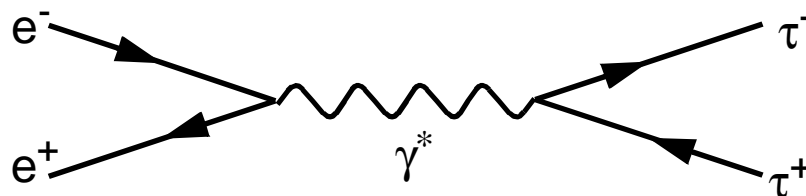


Figure 15: τ pair production in e^+e^- annihilation

⇒ Electron is a stable particle, while muon and tauon have a finite lifetime:

$$\tau_{\mu} = 2.2 \times 10^{-6} \text{ s} \quad \text{and} \quad \tau_{\tau} = 2.9 \times 10^{-13} \text{ s}$$

Muon decays in a purely leptonic mode:

$$\mu^{-} \rightarrow e^{-} + \bar{\nu}_e + \nu_{\mu} \quad (11)$$

Tauon has a mass sufficient to produce even hadrons, but has leptonic decay modes as well:

$$\tau^{-} \rightarrow e^{-} + \bar{\nu}_e + \nu_{\tau} \quad (12)$$

$$\tau^{-} \rightarrow \mu^{-} + \bar{\nu}_{\mu} + \nu_{\tau} \quad (13)$$

⇒ Fraction of a particular decay mode with respect to all possible decays is called *branching ratio*.

Branching ratio of the process (12) is 17.81%, and of (13) -- 17.37%.

⇒ **Note: lepton numbers are conserved in all reactions ever observed**

Important assumptions:

- 1) Weak interactions of leptons are identical, just like electromagnetic ones (*“interactions universality”*)
- 2) One can neglect final state lepton masses for many basic calculations

The *decay rate* of a muon is given by expression:

$$\Gamma(\mu^- \rightarrow e^- + \bar{\nu}_e + \nu_\mu) = \frac{G_F^2 m_\mu^5}{195\pi^3} \quad (14)$$

Here G_F is the *Fermi constant*.

Substituting m_μ with m_τ one obtains decay rates of tauon leptonic decays, equal for both processes (12) and (13). It explains why branching ratios of these processes have very close values.

Using the decay rate, the lifetime of a lepton is:

$$\tau_l = \frac{B(l^- \rightarrow e^- \bar{\nu}_e \nu_l)}{\Gamma(l^- \rightarrow e^- \bar{\nu}_e \nu_l)} \quad (15)$$

Here l stands for μ or τ . Since muons have basically only one decay mode, $B=1$ in their case. Using experimental values of B and formula (14), one obtains the ratio of muon and tauon lifetimes:

$$\frac{\tau_\tau}{\tau_\mu} \approx 0.178 \cdot \left(\frac{m_\mu}{m_\tau} \right)^5 \approx 1.3 \times 10^{-7}$$

This again is in a very good agreement with independent experimental measurements

►►► **Universality of lepton interactions is proved to big extent. That means that there is basically no difference between lepton generations, **apart of the mass.****

▣▣▣▣▣ **Quarks** are spin-1/2 fermions, subject to all kind of interactions; possess fractional electric charges

Quarks and their bound states are the only particles which interact strongly

Some historical background:

- ❖ Proton and neutron (“nucleons”) were known to interact strongly
- ❖ In 1947, in cosmic rays, new heavy particles were detected (“hadrons”)
- ❖ By 1960s, in accelerator experiments, many dozens of hadrons were discovered
- ❖ An urge to find a kind of “periodic system” lead to the “Eightfold Way” classification, invented by Gell-Mann and Ne‘eman in 1961, based on the SU(3) symmetry group and describing hadrons in terms of “building blocks”
- ❖ In 1964, Gell-Mann invented quarks as the building blocks (and Zweig invented “aces”)

➡ The quark model: *baryons* and *antibaryons* are bound states of three quarks, and *mesons* are bound states of a quark and antiquark.

Analogously to leptons, quarks occur in three generations:

$$\begin{pmatrix} u \\ d \end{pmatrix}, \begin{pmatrix} c \\ s \end{pmatrix}, \begin{pmatrix} t \\ b \end{pmatrix}$$

Corresponding antiquarks are:

$$\begin{pmatrix} \bar{d} \\ \bar{u} \end{pmatrix}, \begin{pmatrix} \bar{s} \\ \bar{c} \end{pmatrix}, \begin{pmatrix} \bar{b} \\ \bar{t} \end{pmatrix}$$

| Name ("Flavour") | Symbol | Charge (units of e) | Mass (GeV/c ²) |
|---------------------|--------|------------------------|-------------------------------|
| Down | d | -1/3 | ≈ 0.35 |
| Up | u | +2/3 | ≈ 0.35 |
| Strange | s | -1/3 | ≈ 0.5 |
| Charmed | c | +2/3 | ≈ 1.5 |
| Bottom | b | -1/3 | ≈ 4.5 |
| Top | t | +2/3 | ≈ 170 |

Free quarks can never be observed

There is an elegant explanation for this:

- Every quark possesses a new quantum number: the *colour*. There are three different colours, thus each quark can have three distinct colour states.
- Coloured objects can not be observed.
- Therefore quarks must confine into hadrons immediately upon appearance.

Three colours are usually called *red*, *green* and *blue*. Baryons thus are bound states of three quarks of different colours, which add up to a colourless state. Mesons are represented by colour-anticolour quark pairs.

Strange, charmed, bottom and top quarks each have an additional quantum number: *strangeness* S , *charm* C , *beauty* \tilde{B} and *truth* T respectively. All these quantum numbers are conserved in strong interactions, but not in weak ones.

Some examples of baryons:

| Particle | Mass (Gev/c ²) | Quark composition | Q (units of e) | S | C | \tilde{B} |
|-------------|-------------------------------|----------------------|----------------------|----|---|-------------|
| p | 0.938 | uud | 1 | 0 | 0 | 0 |
| n | 0.940 | udd | 0 | 0 | 0 | 0 |
| Λ | 1.116 | uds | 0 | -1 | 0 | 0 |
| Λ_c | 2.285 | udc | 1 | 0 | 1 | 0 |

Strangeness is defined so that $S=-1$ for s-quark and $S=1$ for \bar{s} respectively. Further, $C=1$ for c-quark, $\tilde{B}=-1$ for b-quark, and $T=1$ for t-quark.

❖ Since the top-quark is a very short-living one, there are no hadrons containing it, i.e., $T=0$ for all hadrons.

Quark numbers for up and down quarks have no name, but just like any other flavour, they are conserved in strong and electromagnetic interactions.

Baryons are assigned own quantum number B : $B=1$ for baryons, $B=-1$ for antibaryons and $B=0$ for mesons.

Some examples of mesons:

| Particle | Mass (Gev/c ²) | Quark composition | Q (units of e) | S | C | \tilde{B} |
|----------|-------------------------------|----------------------|----------------------|----|----|-------------|
| π^+ | 0.140 | $u\bar{d}$ | 1 | 0 | 0 | 0 |
| K^- | 0.494 | $s\bar{u}$ | -1 | -1 | 0 | 0 |
| D^- | 1.869 | $d\bar{c}$ | -1 | 0 | -1 | 0 |
| D_s^+ | 1.969 | $c\bar{s}$ | 1 | 1 | 1 | 0 |
| B^- | 5.279 | $b\bar{u}$ | -1 | 0 | 0 | -1 |
| Y | 9.460 | $b\bar{b}$ | 0 | 0 | 0 | 0 |

❖ Majority of hadrons are unstable and tend to decay by the strong interaction to the state with the lowest possible mass (lifetime about 10^{-23} s).

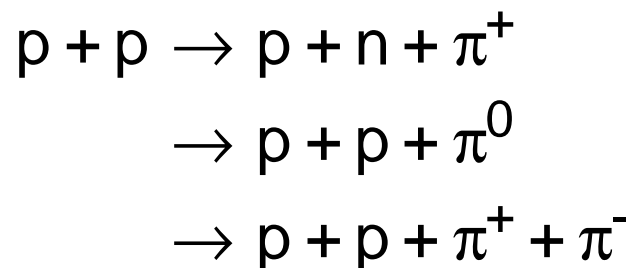
❖ Hadrons with the lowest possible mass for each quark number (S, C, etc.) may live significantly longer before decaying weakly (lifetimes 10^{-7} - 10^{-13} s) or electromagnetically (mesons, lifetimes 10^{-16} - 10^{-21} s). Such hadrons are called *stable particles*.

Brief history of hadron discoveries

- ❖ First known hadrons were proton and neutron
 - ❖ The lightest are pions π (pi-mesons). There are charged pions π^+ , π^- with mass of $0.140 \text{ GeV}/c^2$, and neutral ones π^0 , mass $0.135 \text{ GeV}/c^2$.
- ➡ Pions and nucleons are the lightest particles containing u- and d-quarks only.

Pions were discovered in 1947 in cosmic rays, using photoemulsions to detect particles.

Some reactions induced by cosmic rays primaries:



Same reactions can be reproduced in accelerators, with higher rates, although cosmic rays may provide higher energies.



Figure 16: First observed pions: a π^+ stops in the emulsion and decays to a μ^+ and ν_μ , followed by the decay of μ^+

In emulsions, pions were identified by much more dense ionization along the track, as compared to electrons

Figure 16 shows examples of the reaction

$$\pi^+ \rightarrow \mu^+ + \nu_\mu \quad (16)$$

where pion comes to the rest, producing muons having equal energies, which in turn decay by the reaction $\mu^+ \rightarrow e^+ \nu_e \bar{\nu}_\mu$.

- ▣▣▣▣ Charged pions decay mainly to the muon-neutrino pair (branching ratio about 99.99%), having lifetimes of 2.6×10^{-8} s. In quark terms:

$$(u\bar{d}) \rightarrow \mu^+ + \nu_\mu$$

- ▣▣▣▣ Neutral pions decay mostly by the electromagnetic interaction, having shorter lifetime of 0.8×10^{-16} s:

$$\pi^0 \rightarrow \gamma + \gamma$$

Discovered pions were fitting very well into Yukawa's theory -- they were supposed to be responsible for the nuclear forces:

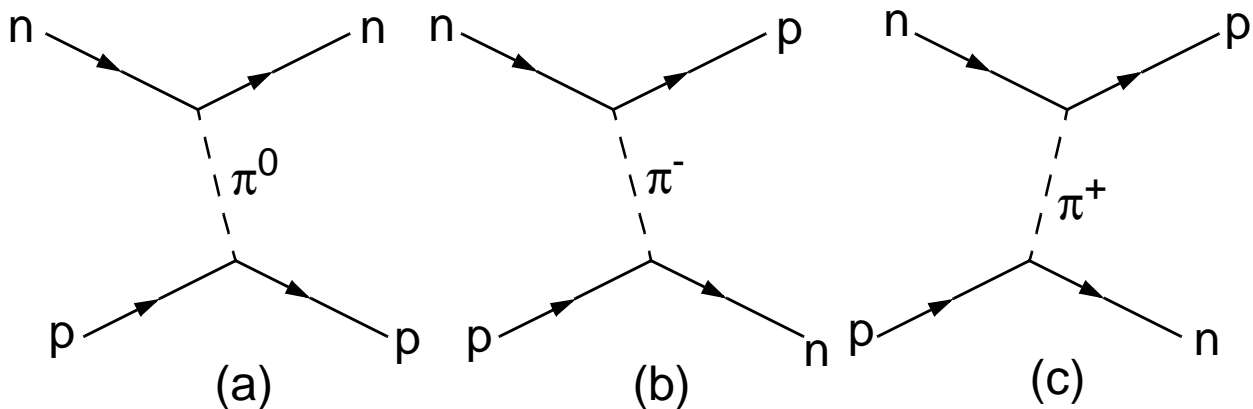


Figure 17: Yukawa model of direct (a) and exchange (b,c) nuclear forces

- ❖ The resulting potential for this kind of exchange is of Yukawa type (6), and at the longest range reproduces observed nuclear forces very well, including even spin effects.
- ❖ However, at the ranges comparable with the size of nucleons, this description **fails**, and the internal structure of hadrons must be taken into account.

Strange mesons and baryons

were called so because, being produced in strong interactions, had quite long lifetimes and decayed weakly rather than strongly.

The most light particles containing s-quark are:

- ❖ mesons K^+ , K^- and K^0 , \bar{K}^0 : "kaons", lifetime of K^+ is 1.2×10^{-8} s
- ❖ baryon Λ , lifetime of 2.6×10^{-10} s

Principal decay modes of strange hadrons:

$$K^+ \rightarrow \mu^+ + \nu_\mu \quad (B=0.64)$$

$$K^+ \rightarrow \pi^+ + \pi^0 \quad (B=0.21)$$

$$\Lambda \rightarrow \pi^- + p \quad (B=0.64)$$

$$\Lambda \rightarrow \pi^0 + n \quad (B=0.36)$$

While the first decay in the list is clearly a weak one, decays of Λ can be very well described as strong ones, if not the long lifetime: $(udd) \rightarrow (d\bar{u}) + (uud)$ must have a lifetime of order 10^{-23} s, thus Λ can not be another sort of neutron...

Solution: to invent a new “*strange*” quark, bearing a new quark number -- “*strangeness*”, which does not have to be conserved in weak interactions

| $S=1$ | $S=-1$ |
|-----------------------|-----------------------------|
| $K^+(494) = u\bar{s}$ | $\Lambda(1116) = uds$ |
| $K^0(498) = d\bar{s}$ | $K^-(494) = s\bar{u}$ |
| | $\bar{K}^0(498) = s\bar{d}$ |

⇒ In strong interactions, strange particles have to be produced in pairs in order to conserve total strangeness (“*associated production*”):



In 1952, *bubble chambers* were invented as particle detectors, and also worked as *targets*, providing, for instance, the proton target for reaction (17).

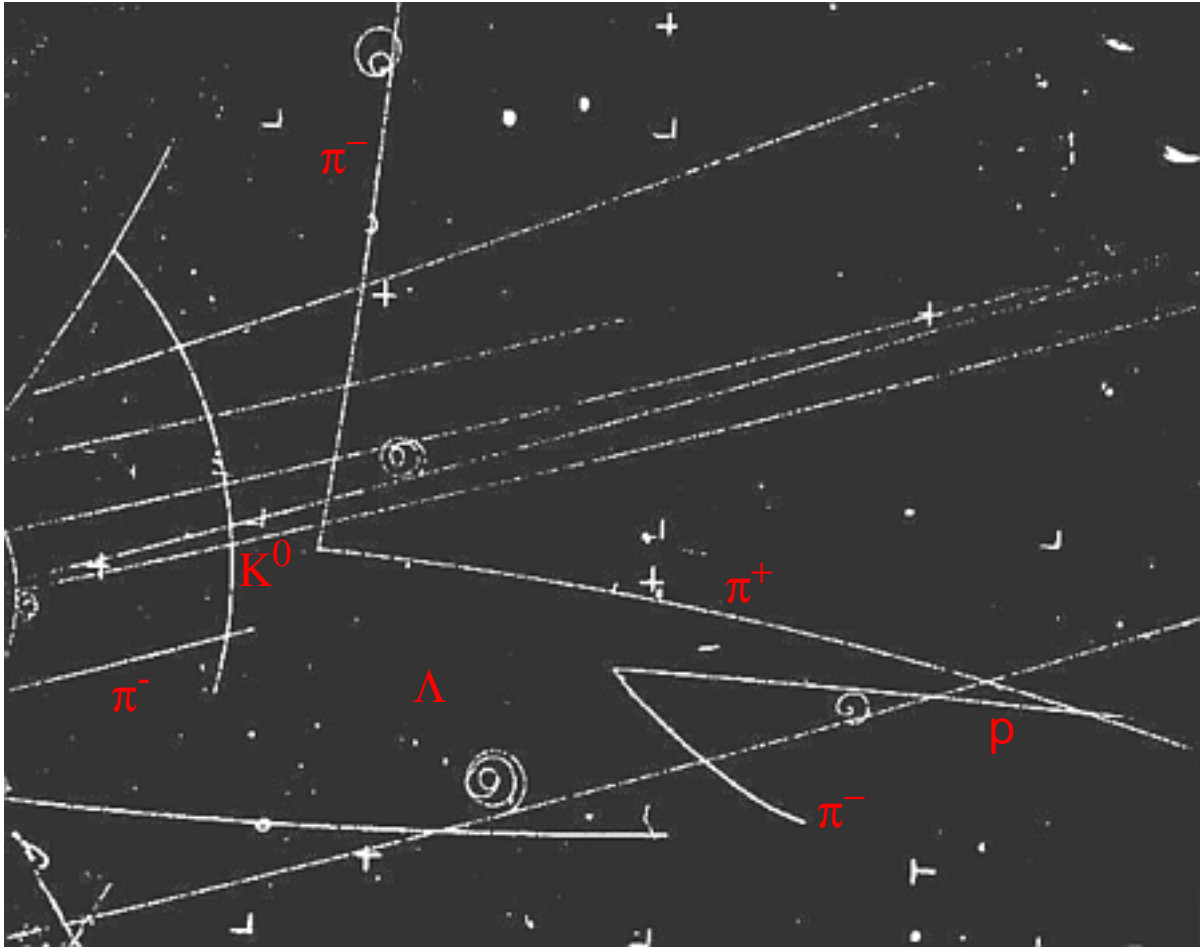


Figure 18: A bubble chamber picture of the reaction (17)

How does a bubble chamber work:

- It is filled with a liquid under pressure (hydrogen)
- Particles ionize the liquid along their passage
- When pressure drops, liquid boils preferentially along the ionization trails

- ❖ Bubble chambers were great tools of particle discovery, providing physicists with numerous hadrons, all of them fitting u-d-s quark scheme until 1974.
- ❖ In 1974, a new particle was discovered, which demanded a new flavour to be introduced. Since it was detected simultaneously by two rival groups in Brookhaven (BNL) and Stanford (SLAC), it received a double name: "*dzei-psai*"

$$J/\psi (3097) = c\bar{c}$$

The new quark was called "*charmed*", and the corresponding quark number is *charm*, C . Since J/ψ itself has $C=0$, it is said to contain "hidden charm".

Shortly after that particles with "naked charm" were discovered as well:

$$D^+(1869) = c\bar{d}, D^0(1865) = c\bar{u}$$

$$D^-(1869) = d\bar{c}, \bar{D}^0(1865) = u\bar{c}$$

$$\Lambda_c^+ (2285) = udc$$

Even heavier charmed mesons were found -- those which contained strange quark as well:

$$D_s^+ (1969) = c\bar{s}, D_s^- (1969) = s\bar{c}$$

Lifetimes of the lightest charmed particles are of order 10^{-13} s, well in the expected range of weak decays.

❖ Discovery of “charmed” particles was a triumph for the electroweak theory, which demanded number of quarks and leptons to be equal.

In 1977, “*beautiful*” mesons were discovered:

$$Y(9460) = b\bar{b}$$

$$B^+(5279) = u\bar{b}, B^0(5279) = d\bar{b}$$

$$B^-(5279) = b\bar{u}, \bar{B}^0(5279) = b\bar{d}$$

and the lightest b-baryon: $\Lambda_b^0(5461) = udb$

And this is the limit: top-quark is too unstable to form observable hadrons

III. Experimental methods

Before 1950s, cosmic rays were source of high energy particles, and cloud chambers and photo-emulsions were the means to detect them.

The quest for heavier particles and more precise measurements lead to the increasing importance of *accelerators* to produce particles and complicated *detectors* to observe them.

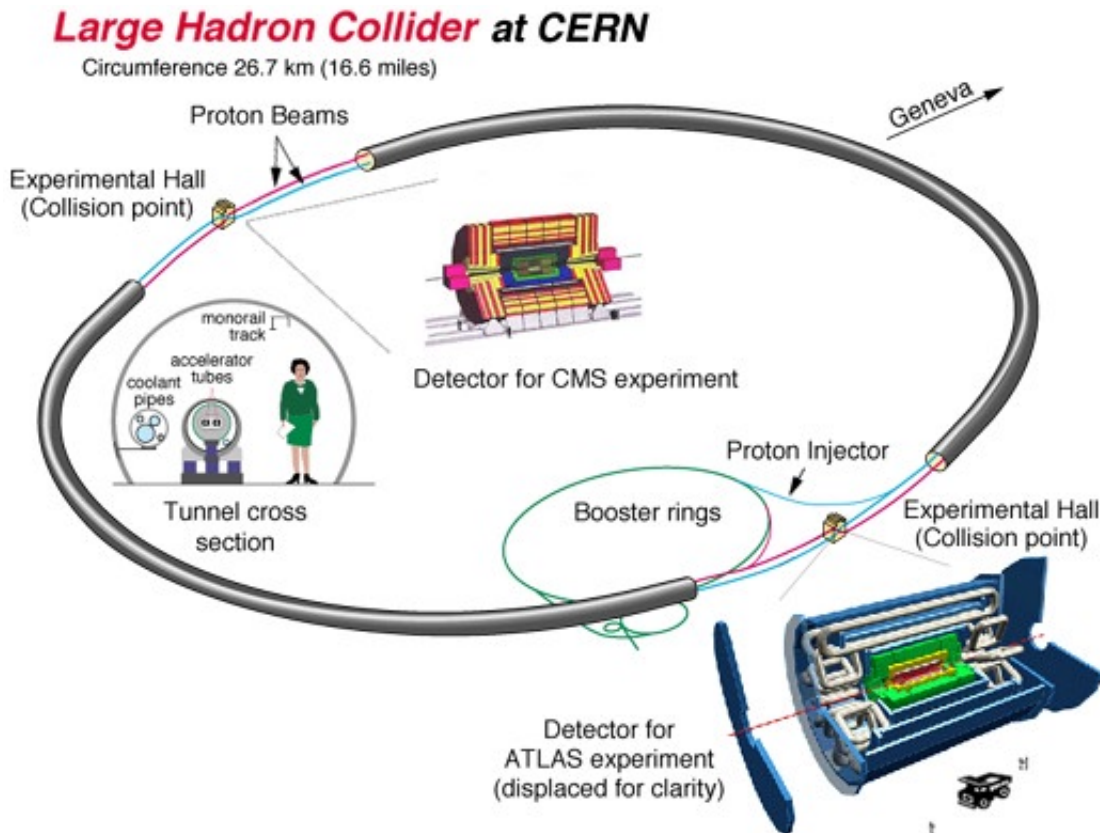


Figure 19: A future accelerator

Accelerators

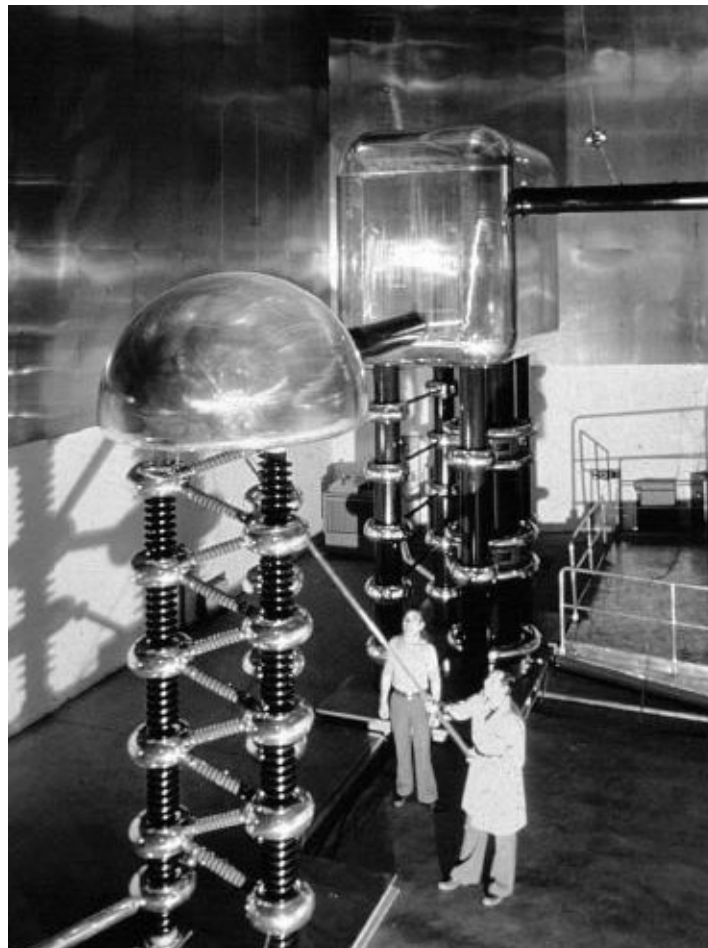


Figure 20: The Cockcroft-Walton generator at CERN: accelerates particles by an electrostatic field

➡ **Basic idea of all accelerators: apply a voltage to accelerate particles**

Main varieties of accelerators are:

- Linear (*“linacs”*)
- Cyclic (*“cyclotrons”, “synchrotrons”*)

[Linear accelerators](#)

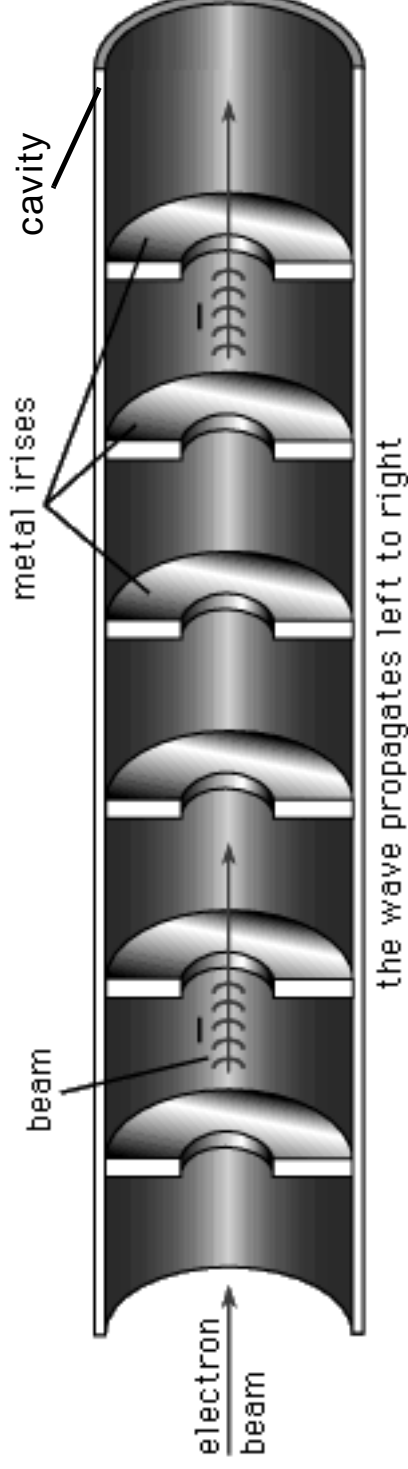


Figure 21: A traveling-wave linear accelerator schematics

- ❖ Linacs are used mostly to accelerate electrons
- Electrons are accelerated along a sequence of cylindrical vacuum cavities
- Inside cavities, an electromagnetic field is created with a frequency near 3,000 MHz (radio-frequency) and electric component along the beam axis
- Electrons arrive into each cavity at the same phase of the electric wave

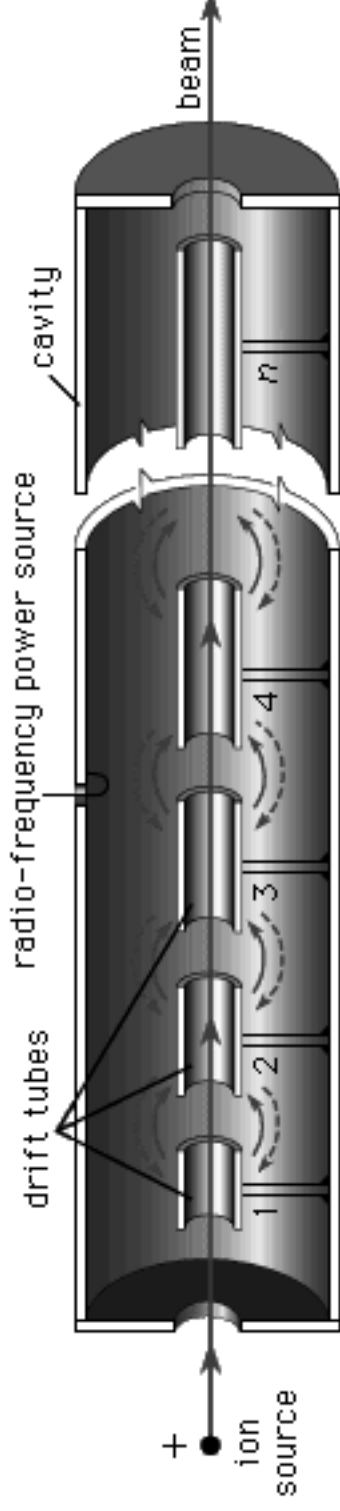


Figure 22: Standing-wave linac

- ❖ Standing-wave linacs are used to accelerate heavier particles, like protons
 - Typical frequency of the field is about 200 MHz
 - Drift tubes screen particles from the electromagnetic field for the periods when the field has decelerating effect
 - Lengths of drift tubes are proportional to particles' speed

Cyclic accelerators.

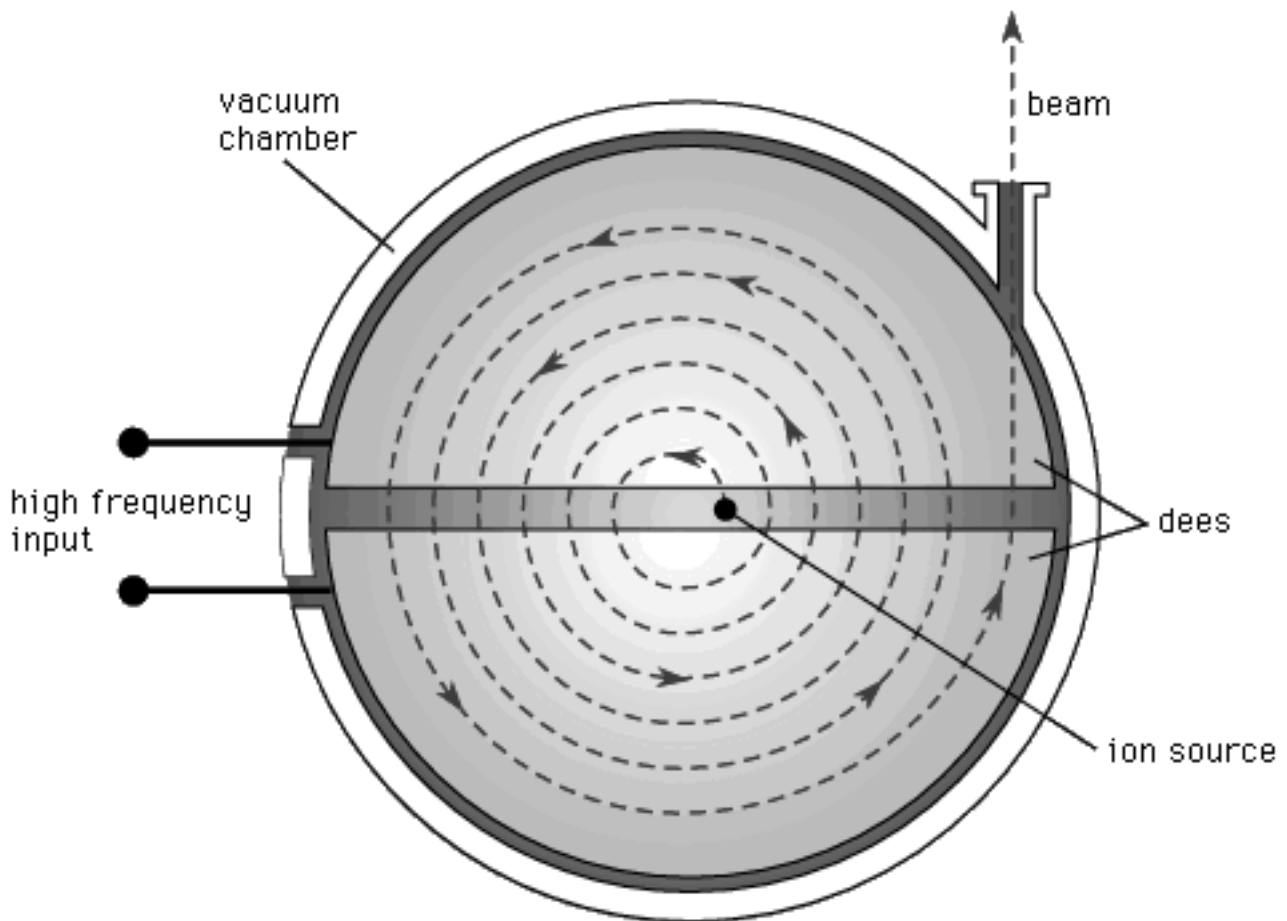


Figure 23: Cyclotron, the first resonance accelerator

- The vacuum chamber is placed inside a magnetic field, perpendicular to the rotation plane
- Dees (for “D”) are empty “boxes” working as electrodes; there is no electric field inside them
- Particle is accelerated by the high frequency field between the dees (maximal energy achieved for protons: 25 MeV)

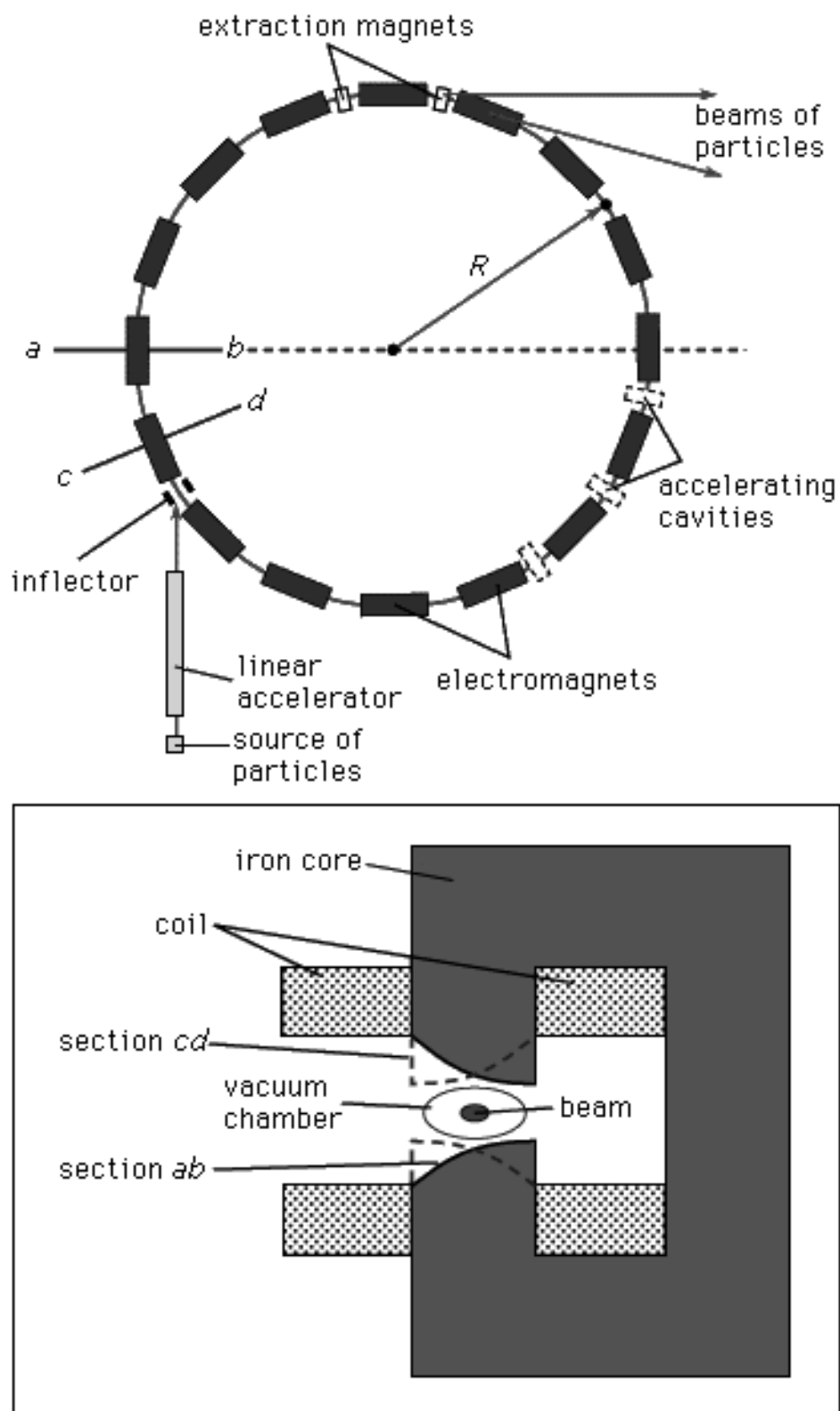


Figure 24: Schematic layout of a synchrotron

Synchrotrons are the most widely used accelerators

- Beam of particles is constrained in a circular path by bending dipole magnets
- Accelerating cavities are placed along the ring
- Charged particles which travel in a circular orbit with relativistic speeds emit *synchrotron radiation*

Amount of energy radiated per turn is:

$$\Delta E = \frac{q^2 \beta^3 \gamma^4}{3 \epsilon_0 \rho} \quad (18)$$

Here q is electric charge of a particle, $\beta \equiv v/c$, $\gamma \equiv (1 - \beta^2)^{-1/2}$, and ρ is the radius of the orbit.

►►► For relativistic particles, $\gamma = E/mc^2$, hence energy loss grows dramatically with particle mass decreasing, being especially big for electrons

Limits on the amounts of the radio-frequency power mean that electron synchrotrons can not produce beams with energies more than 100 GeV

From the standard expression for the centrifugal force, momentum of the particle with the unit charge in a synchrotron is

$$p = 0.3B\rho$$

Hence the magnetic field B has to increase, given that ρ must be constant and the goal is to increase momentum.

▣▣▣▣ **Maximal momentum is therefore limited by both the maximal available magnetic field and the size of the ring.**

❖ To keep particles well contained inside the beam pipe and to achieve the stable orbit, particles are accelerated in *bunches*, synchronized with the radio-frequency field

Analogously to linacs, all particles in a bunch has to move with the circulation frequency in phase with the radio-frequency field.

Requirement of precise synchronisation, however, is not very tight: particles behind the radio-frequency phase will receive lower momentum increase, and other way around.

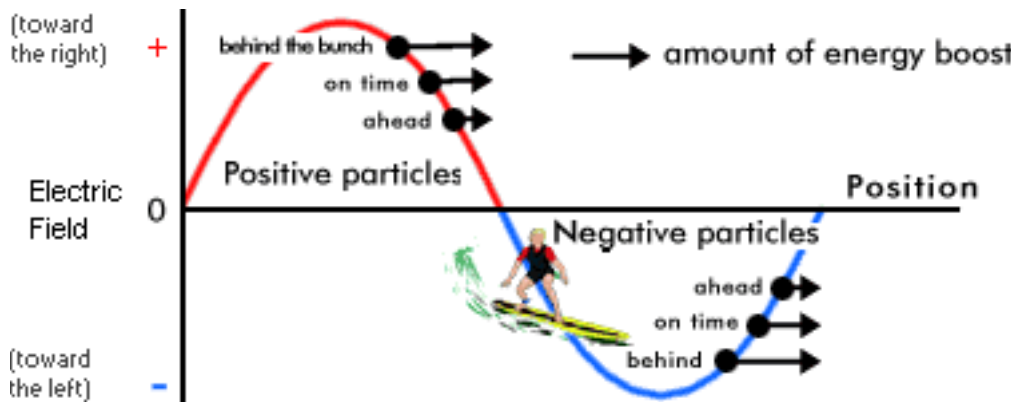


Figure 25: Effect of the electric field onto the particles in accelerator cavities

Therefore all particles in a bunch stay basically on the same orbit, slightly oscillating

To keep particle beams focused, quadrupol and sextupol magnets are placed along the ring and act like optical lenses

Depending on whether beam is deposited onto a fixed target or is collided with another beam, both linear and cyclic accelerators are subdivided into two types:

- ❖ “fixed-target” machines
- ❖ “colliders” (“storage rings” in case of cyclic machines)

Some fixed target accelerators:

| Machine | Type | Particles | E_{beam} (GeV) |
|--------------------------------------|-------------|-----------|-------------------------|
| KEK, Tokyo, Japan | synchrotron | p | 12 |
| SLAC, Stanford, California, USA | linac | e^- | 25 |
| SPS, CERN, Geneva, Switzerland | synchrotron | p | 450 |
| Tevatron II, Fermilab, Illinois, USA | synchrotron | p | 1000 |

Much higher energies for protons comparing to electrons are achieved due to smaller losses caused by synchrotron radiation

Fixed-target machines can be used to produce secondary beams of neutral or unstable particles.

❖ Centre-of-mass energy, i.e., energy available for particle production during the collision of a beam of energy E_L with a target is :

$$E_{CM} = \sqrt{m_b^2 c^4 + m_t^2 c^4 + 2m_t c^2 E_L} \quad (19)$$

Here m_b and m_t are masses of the beam and target particles respectively, and increase of E_L does not lead to big gains in E_{MC} .

More efficiently high centre-of-mass energies can be achieved by colliding two beams of energies E_A and E_B (at an optional crossing angle θ), so that

$$E_{CM}^2 = 2E_A E_B (1 + \cos\theta) \quad (20)$$

Some colliders:

| Machine | Particles(E_{beam} , GeV) |
|--|-------------------------------------|
| TRISTAN, Tokyo, Japan | $e^+(32) + e^-(32)$ |
| SLC, Stanford, California, USA | $e^+(50) + e^-(50)$ |
| LEP, CERN, Geneva, Switzerland | $e^+(94.5) + e^-(94.5)$ |
| HERA, Hamburg, Germany | $e^-(30) + p(820)$ |
| Tevatron I, Fermilab, Illinois, USA | $p(1000) + \bar{p}(1000)$ |
| LHC, CERN, Geneva, Switzerland (planned) | $p(7000) + p(7000)$ |

Particle interactions with matter

- ▣▣▣▣▣ All particle detecting techniques are based on the properties of interactions of particles in question with different materials

Short-range interaction with nuclei

- ❖ Probability of a particle to interact (with a nucleus or another particle) is called *cross-section*.

Cross-sections are normally measured in *millibarns*:

$$1\text{mb} \equiv 10^{-31} \text{m}^2$$

Total cross-section of a reaction is sum over all possible processes

There are two main kinds of scattering processes:

- *elastic scattering*: only momenta of incident particles are changed, for example, $\pi^- p \rightarrow \pi^- p$
- *inelastic scattering*: final state particles differ from those in initial state, like in $\pi^- p \rightarrow K^0 \Lambda$

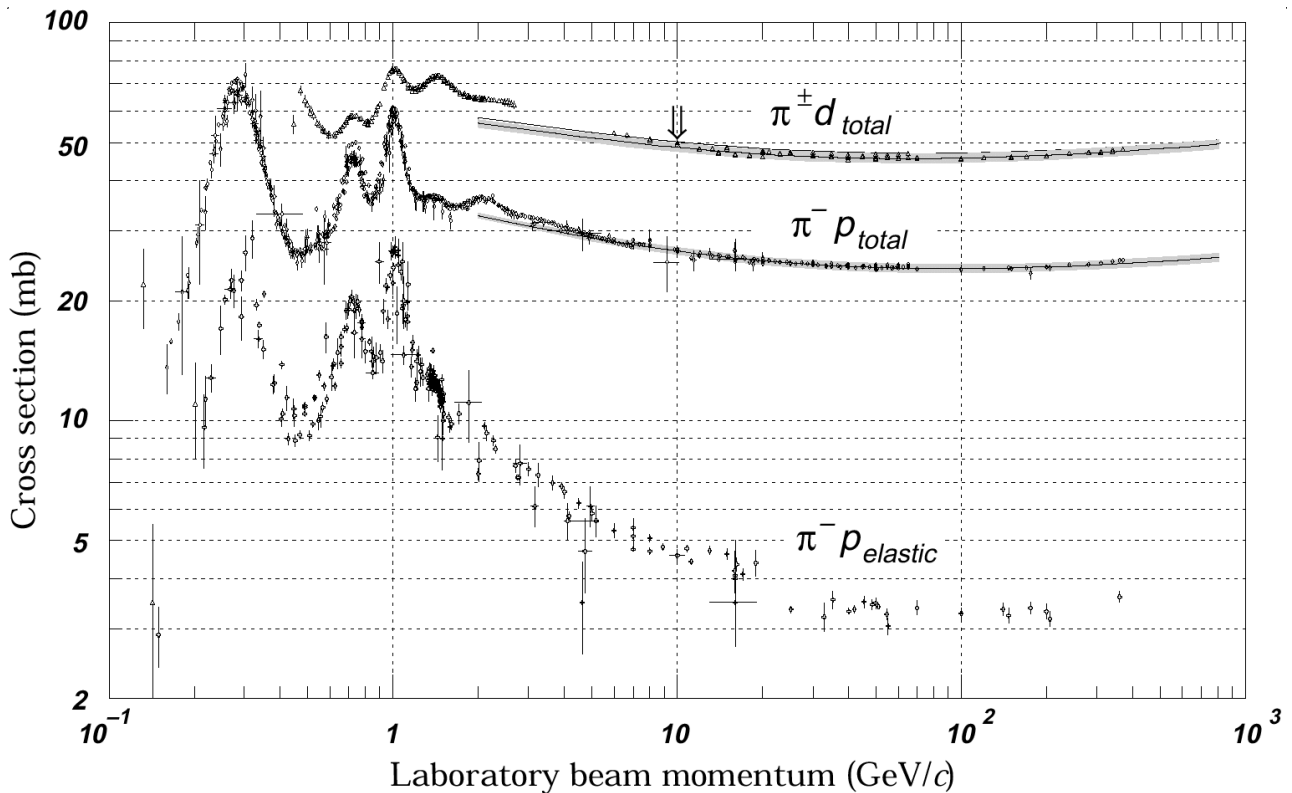


Figure 26: Cross sections of π^- on a fixed proton target

For hadron-hadron scattering, cross-sections are of the same order with the geometrical “cross-sections” of hadrons: assuming their sizes are of order $1 \text{ fm} \equiv 10^{-15} \text{ m} \Rightarrow \pi r^2 \approx 30 \text{ mb}$

For complex nuclei, obviously, cross-sections are bigger, and elastic scattering on one of the nucleons can lead to nuclear excitation or break-up -- so-called *quasi-elastic scattering*.

Knowing cross-sections and number of nuclei per unit volume in a given material n , one can introduce two important characteristics:

$$\text{collision length} : l_c \equiv 1/n\sigma_{\text{tot}}$$

$$\text{absorption length} : l_a \equiv 1/n\sigma_{\text{inel}}$$

At high energies, hadrons comprise majority of particles subject to detection.

Neutrinos and photons have much smaller cross-sections of interactions with nuclei, since former interact only weakly and latter -- only electromagnetically

Ionization energy losses

► Appear predominantly due to Coulomb scattering of particles from atomic electrons

Energy loss per travelled distance: dE/dx

Bethe-Bloch formula for spin-0 bosons with charge $\pm e$:

$$-\frac{dE}{dx} = \frac{Dn_e}{\beta^2} \left[\ln \left(\left(\frac{2mc^2\beta^2\gamma^2}{I} \right) - \beta^2 - \frac{\delta(\gamma)}{2} \right) \right] \quad (21)$$

$$D = \frac{4\pi\alpha^2\hbar^2}{m} = 5.1 \times 10^{-25} \text{ MeV cm}^2$$

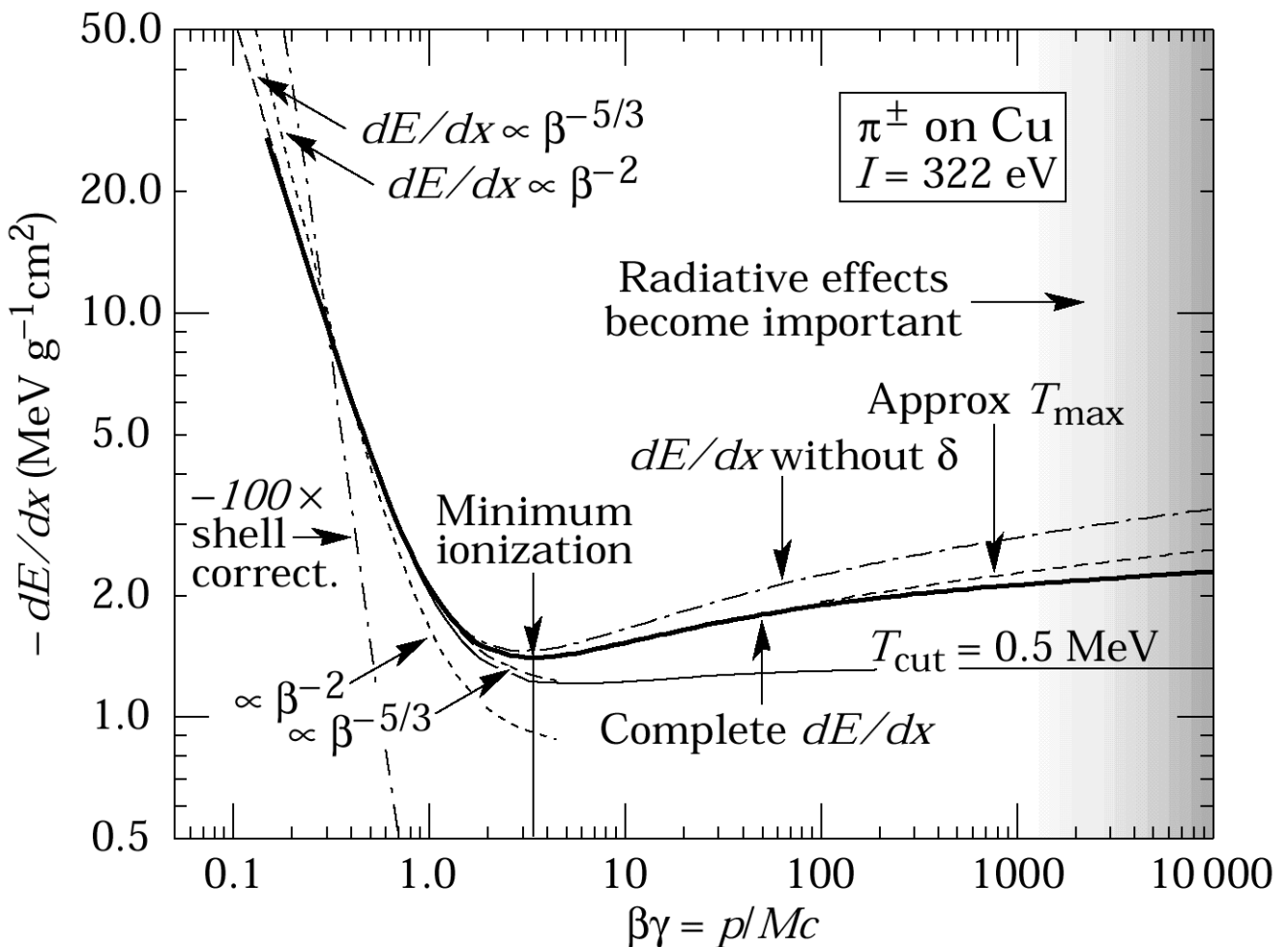


Figure 27: Energy loss rate for pions in copper

In Equation (21), n_e , I and $\delta(\gamma)$ are constants which are characteristic to the medium:

- ❖ n_e is the electron density, $n_e = \rho N_A Z / \tilde{A}$, where ρ is the mass density of the medium and \tilde{A} is its atomic weight. Hence, energy loss is strongly *proportional to the density* of the medium
- ❖ I is the mean ionization potential, $I \approx 10Z$ eV for $Z > 20$
- ❖ $\delta(\gamma)$ is a dielectric screening correction, important only for very energetic particles

Radiation energy losses

- ▣▶ Electric field of a nucleus accelerates or decelerates particles, causing them to radiate photons, hence, lose energy : *bremsstrahlung*

Bremsstrahlung is a very important contribution to the energy loss of light particles like electrons.

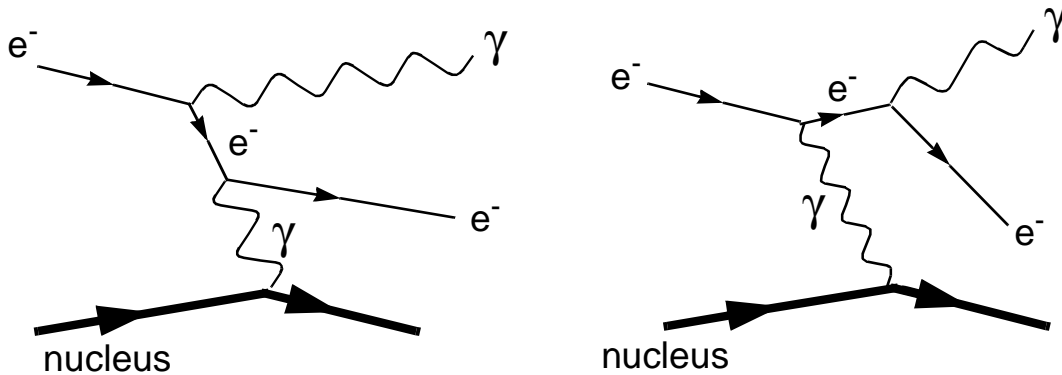


Figure 28: The dominant Feynman diagrams for the bremsstrahlung process $e^- + (Z,A) \rightarrow e^- + \gamma + (Z,A)$

- ❖ Contribution to bremsstrahlung from the field of nucleus is of order $Z^2\alpha^3$, and from atomic electrons -- of order $Z\alpha^3$ (α^3 from each electron).
- ❖ For relativistic electrons, average rate of bremsstrahlung energy loss is given by

$$-\frac{dE}{dx} = \frac{E}{L_R} \tag{22}$$

The constant L_R is called the **radiation length**:

$$\frac{1}{L_R} = 4\left(\frac{\hbar}{mc}\right)^2 Z(Z+1)\alpha^3 n_a \ln\left(\frac{183}{Z^{1/3}}\right) \tag{23}$$

In Equation (23), n_a is the density of atoms per cm^3 in medium.

➡ Radiation length is a very important characteristics of a medium, meaning the average thickness of material which reduces the mean energy of the particle (electron or positron) by a factor e .

❖ Bremsstrahlung is an important component of energy loss only for high-energetic electrons and positrons

Interactions of photons in matter

Main contributing processes to the total cross-section of photon interaction with atom are (see Fig.29):

- 1) Photoelectric effect ($\sigma_{\text{p.e.}}$)
- 2) Compton effect (σ_{incoh})
- 3) Pair production in nuclear and electron field (κ_N and κ_e)

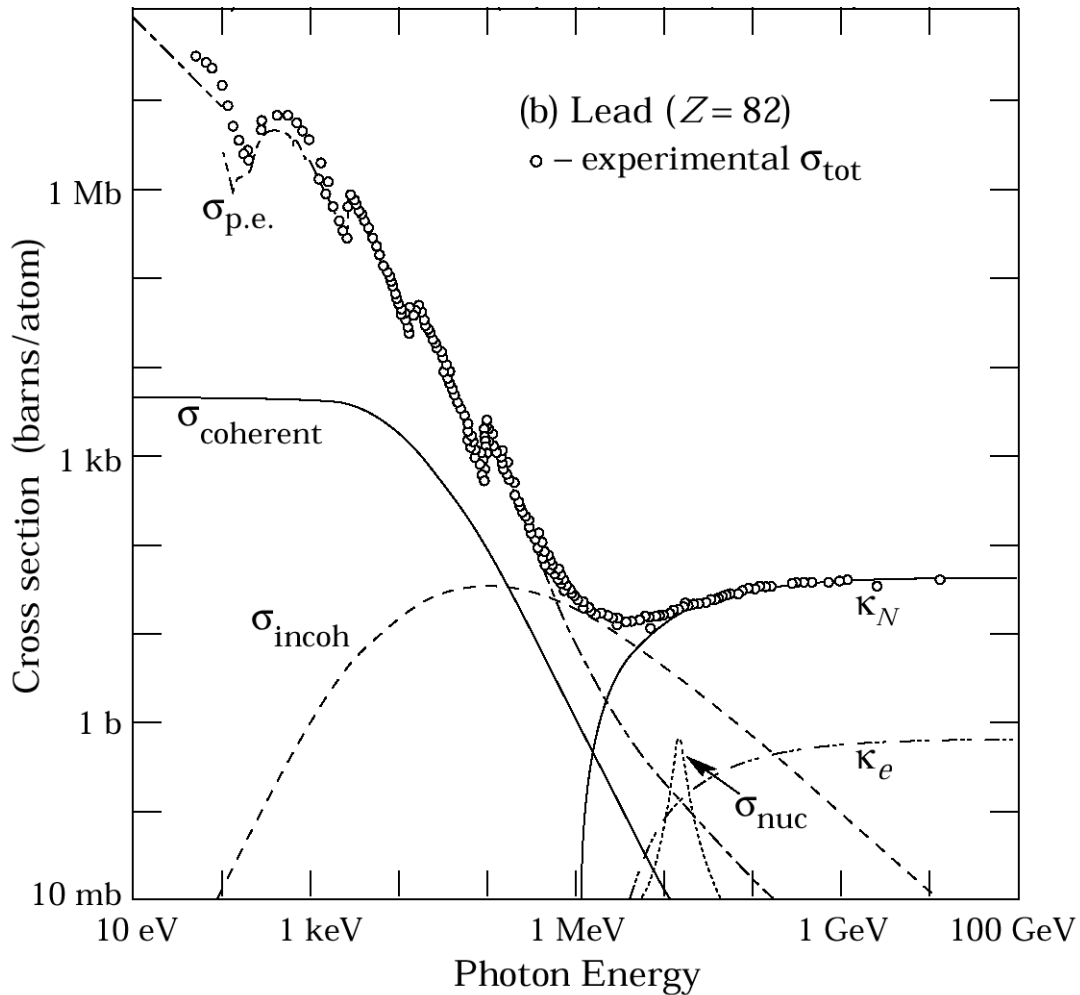


Figure 29: Photon interaction cross-section on a lead atom
 At high energies, pair production is the dominant process: $\sigma_{\text{pair}} = \frac{7}{9} n_a L_R$, and number of photons travelled distance x in the matter is

$$I(x) = I_0 e^{-7x/9L_R}$$

Particle detectors

Main types of particle detectors:

- 1) Tracking devices – coordinate measurements
- 2) Calorimeters – momentum measurements
- 3) Time resolution counters
- 4) Particle identification devices
- 5) Spectrometers

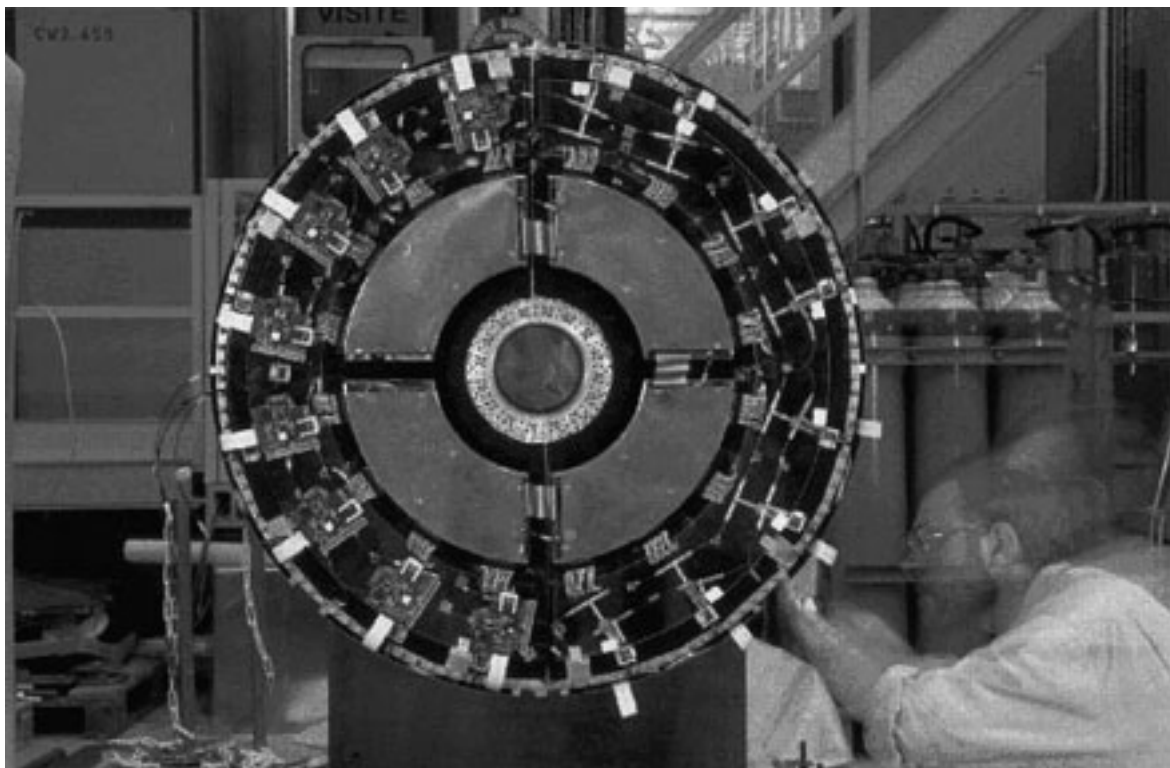


Figure 30: STIC detector for the DELPHI experiment

Position measurement

- ▣ Main principle: ionization products are either visualized (as in photoemulsions) or collected on electrodes to produce a computer-readable signal

Basic requirements of high-energy experiments:

- High spacial resolution ($\propto 10^2 \mu\text{m}$)
- Possibilities to register particles at the proper moment of time and with the high enough rate (good *triggering*)

To fulfil the latter, electronic signal pick-up is necessary, therefore photoemulsions and bubble chambers were abandoned...

❖ Modern tracking detectors fall in two major categories:

a) Gaseous detectors (“*gas chambers*”), resolution $\sim 100\text{-}500 \mu\text{m}$

b) Semiconductor detectors, resolution $\sim 5\mu\text{m}$

Proportional and drift chambers

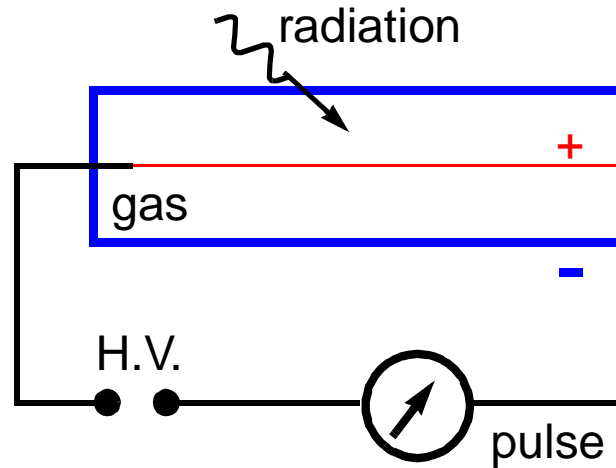


Figure 31: Basic scheme of a wire chamber

A simplest proportional chamber:

- A conducting chamber, filled with a gas mixture and serving as a cathode
- A wire inside serves as an anode
- Gas mixture adjustment: number of secondary electrons caused by the primary ionization electrons is proportional to the number of primary ion pairs ($\propto 10^5$ per pair for voltage of 10^4 - 10^5 V/cm)

➡ **Several anode wires \Rightarrow coordinate measurement (Multi-Wire Proportional Chamber, MWPC)**

❖ Alternative to MWPC : *drift chambers*

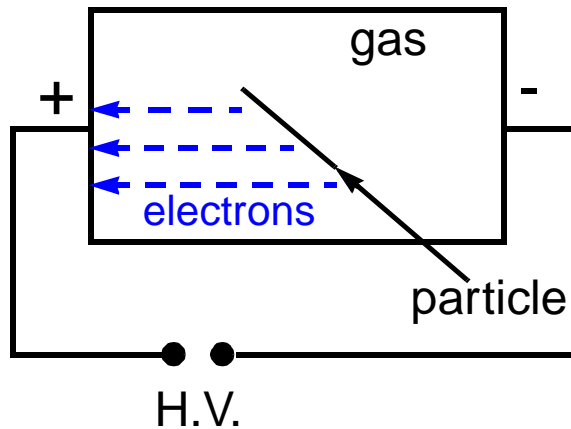


Figure 32: Basic scheme of a drift chamber

- Ionization electrons produced along the particle passage arrive to the pick-up anode at different times
- Knowing (from other detectors) the moment of particle's arrival and field in the chamber, one can calculate coordinates of the track

- ❖ *Streamer detectors* are wire chambers in which secondary ionization is not limited and develops into moving plasmas – streamers
- ❖ If H.V. pulse in a wire chamber is long enough, a spark will occur, which is achieved in *spark chambers*

Semiconductor detectors

- ▶▶▶ In semiconducting materials, ionizing particles produce electron-hole pair, and number of these pairs is proportional to energy loss by particles

Equipping a slice of silicon with narrow pick-up conducting strips, and subjecting it to a high voltage, one gets a detector , analogous to MWPC, with far better resolution.

- ❖ However, semiconductor detectors have rather limited lifetimes due to radiation damages.

Calorimeters

- ▶▶▶ To measure energy (and position) of the particle, calorimeters use absorbing material, which occasionally can change the nature of the particle

Signals produced by calorimeters are proportional to the energy deposited by a particle (eventually, all the energy it had)

- ▶▶▶▶ During the absorption process, particle interacts with the material of the calorimeter and produces a secondary shower
- ▶▶▶▶ Since electromagnetic and hadronic showers are somewhat different, there are two corresponding types of calorimeters

Electromagnetic calorimeters

- The dominant energy loss for electrons (or positrons) is bremsstrahlung
- Produced via the bremsstrahlung photons are absorbed producing e^+e^- pairs
- Hence, an initial electron in an absorber produces a cascade of photons and e^+e^- pairs, until its energy falls under the bremsstrahlung threshold of $E_C \approx 600 \text{ Mev}/Z$
 - ❖ To construct a proper calorimeter, one has to estimate its size, which has to be enough to absorb all the possible energy

Main assumptions for electromagnetic showers:

- a) Each electron with $E > E_C$ travels one radiation length and radiates a photon with $E_\gamma = E/2$
- b) Each photon with $E_\gamma > E_C$ travels one radiation length and creates a e^+e^- pair, which shares equally E_γ
- c) Electrons with $E < E_C$ cease to radiate; for $E > E_C$ ionization losses are negligible

These considerations lead to the expression:

$$t_{max} = \frac{\ln(E_0/E_C)}{\ln 2} \quad (24)$$

where t_{max} is number of radiation lengths needed to stop the electron of energy E_0 .

Electromagnetic calorimeters can be, for example, lead glass blocks collecting the light emitted by showers, or a sort of a drift chamber, interlayered with absorber.

Hadron calorimeters

- ❖ Hadronic showers are similar to the electromagnetic ones, but absorption length is larger than the radiation length of electromagnetic showers.
- ❖ Also, some contributions to the total absorption may not lead to a signal in the detector (e.g., nuclear excitations or neutrinos)

Main characteristics of an hadron calorimeters are:

- a) It has to be thicker than electromagnetic one
- b) Often, layers of ^{238}U are introduced to compensate for energy losses (low-energy neutrinos cause fission)
- c) energy resolution of hadron calorimeters is generally rather poor

Hadron calorimeter is usually a set of MWPC's or streamer tubes, interlayed with thick iron absorber

Scintillation counters

- ▣▣▣▣▶ To signal passage of particles through an experimental setup and to measure the “*time-of-flight*” (TOF), scintillation counters are widely used.
- ❖ Scintillators are materials (crystals or organic) in which ionizing particles produce visible light without losing much of its energy
- ❖ The light is guided down to photomultipliers and is being converted to a short electronic pulse

Particle identification

- Knowing momentum of particle is not enough to identify it, hence complementary information is needed
- For low-energy particles, TOF counters can provide this complementary data
- Energy loss rate dE/dx depends on particle mass for energies below ≈ 2 GeV

➡ **The most reliable particle identification device :**
Cherenkov counters

- In certain media, energetic charged particles move with velocities higher than the speed of light in these media
- Excited atoms along the path of the particle emit coherent photons at a characteristic angle θ_C to the direction of motion

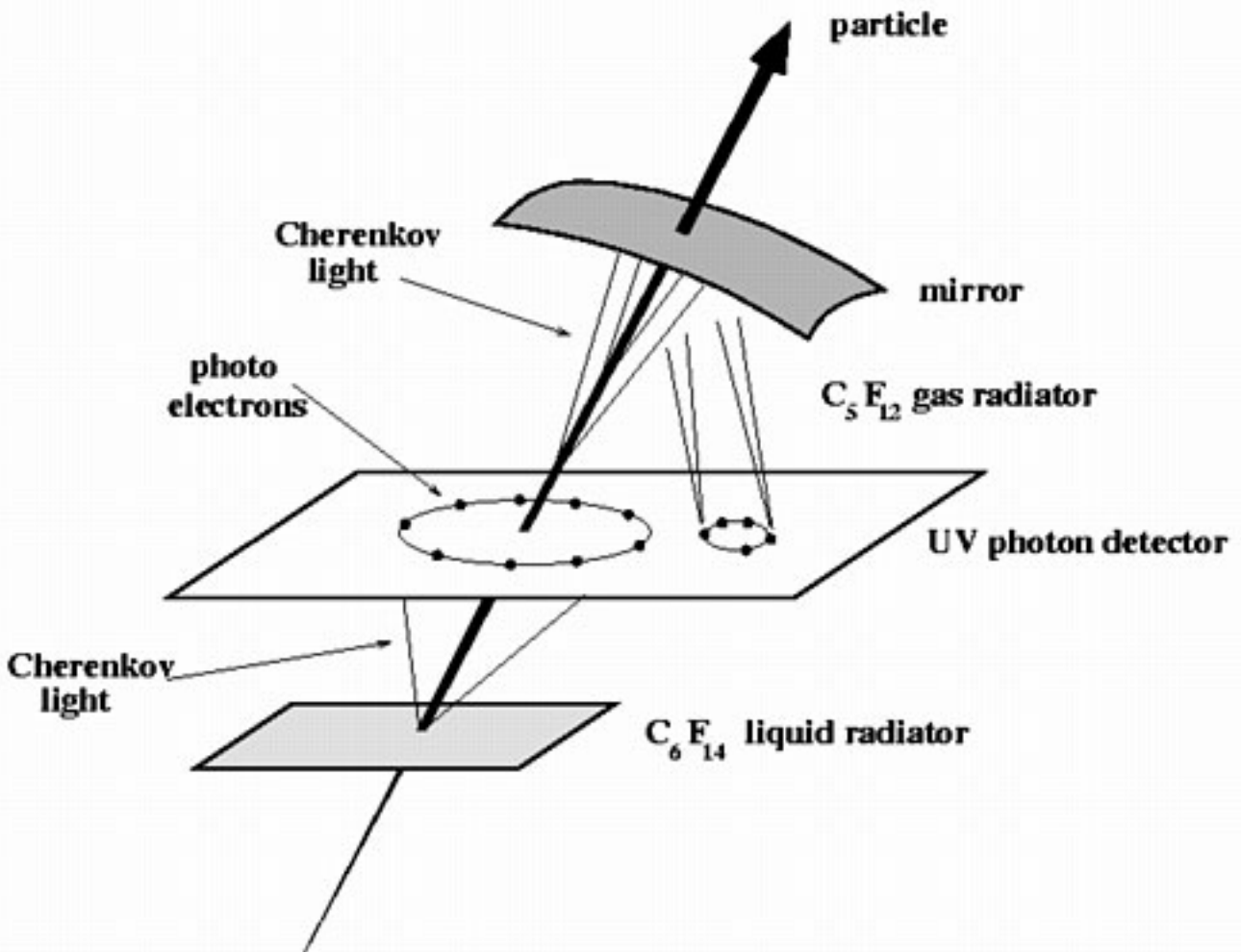


Figure 33: Cherenkov effect in the DELPHI RICH detector

The angle θ_C depends on the refractive index of the medium n and on the particle's velocity v :

$$\cos\theta_C = c / vn \quad (25)$$

Hence, measuring θ_C , the velocity of the particle can be easily derived, and the identification performed

Transition radiation measurements

- In ultra-high energy region, particles velocities do not differ very much
- Whenever a charged particle traverses a border between two media with different dielectric properties, a *transition radiation* occurs
- Intensity of emitted radiation is sensitive to the particle's energy $E = \gamma mc^2$.

Transition radiation measurements are particularly useful for separating electrons from other particles

Spectrometers

- ▶ Momenta of particles are measured by the curvature of the track in a magnetic field

Spectrometers are tracking detectors placed inside a magnet, providing momentum information.

In collider experiments, no special spectrometers are arranged, but all the tracking setup is contained inside a solenoidal magnet.

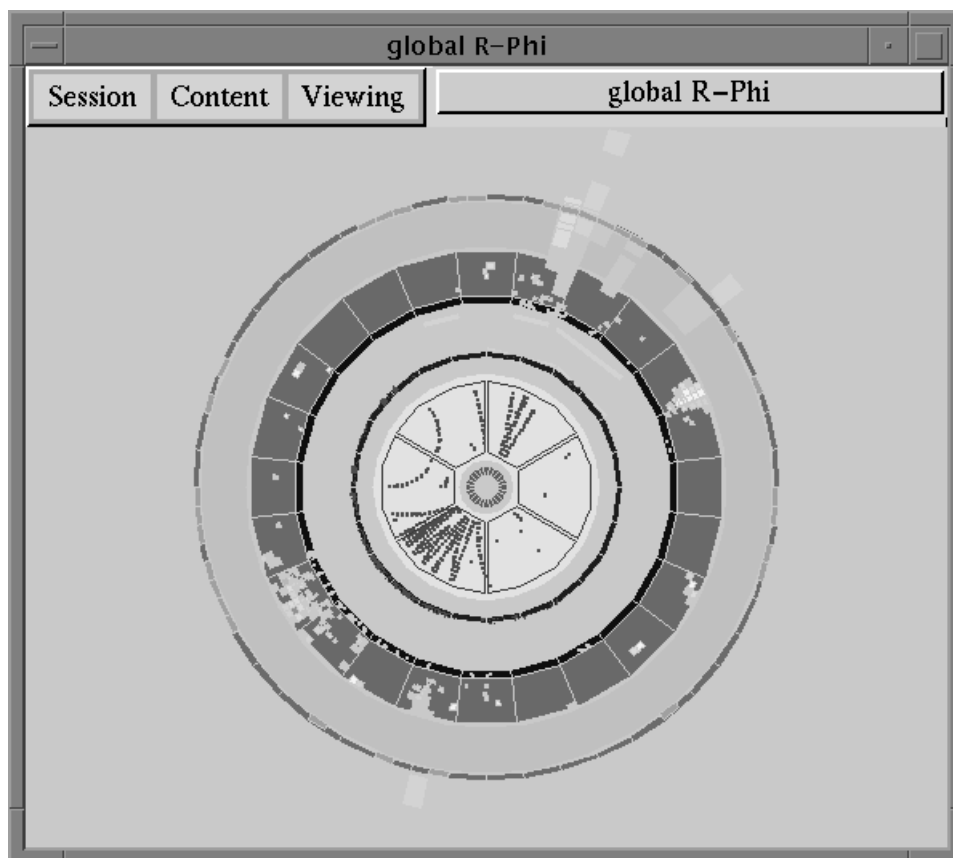


Figure 34: A hadronic event as seen by the DELPHI detector

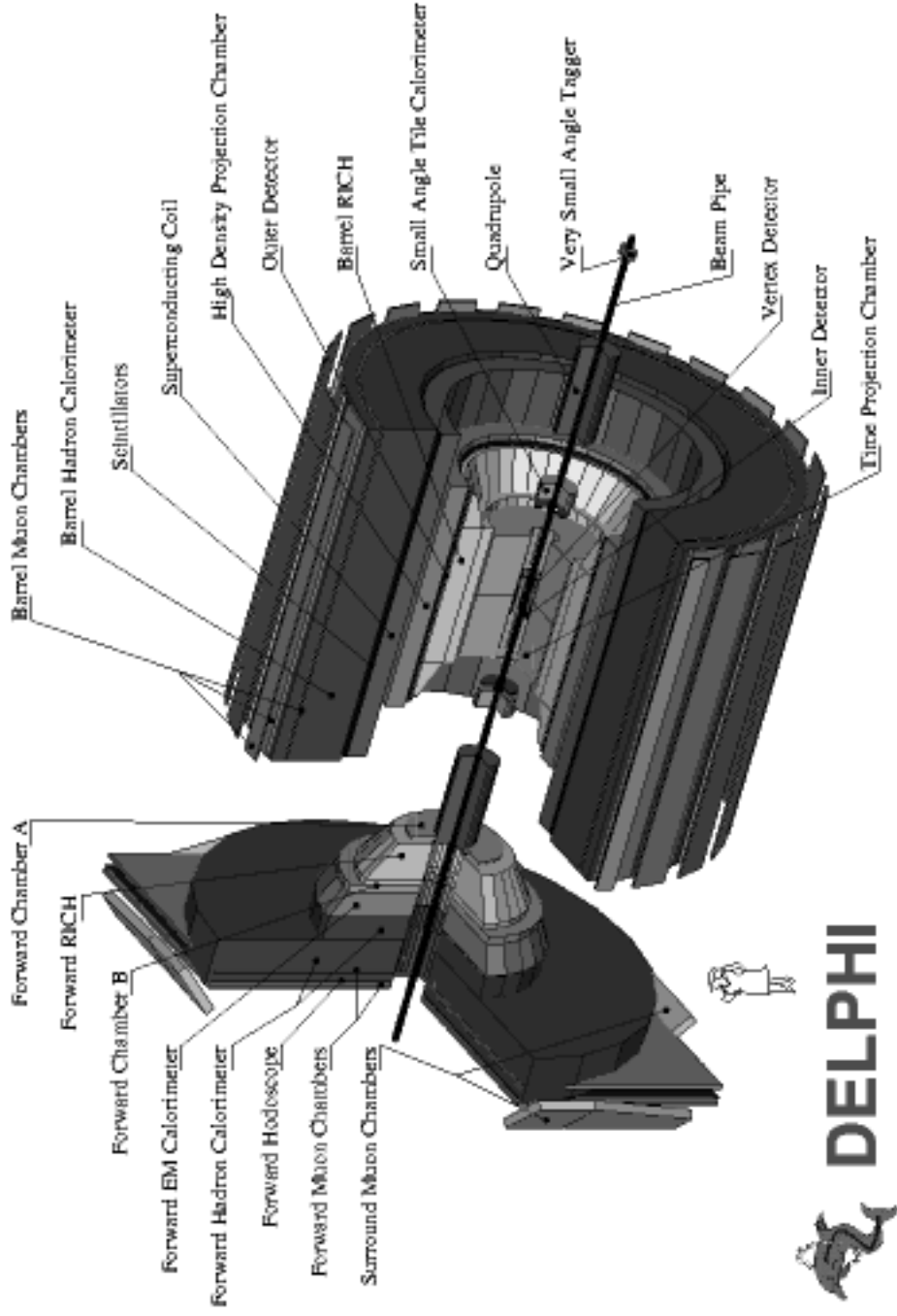


Figure 35: The DELPHI detector at LEP

IV. Space-time symmetries

- ⇒ Many conservation laws have their origin in the symmetries and invariance properties of the underlying interactions

Translational invariance

- ❖ When a closed system of particles is moved from from one position in space to another, its physical properties do not change

Considering an infinitesimal translation:

$$\vec{x}_i \rightarrow \vec{x}'_i = \vec{x}_i + \delta\vec{x}$$

the Hamiltonian of the system transforms as

$$H(\vec{x}_1, \vec{x}_2, \dots, \vec{x}_n) \rightarrow H(\vec{x}_1 + \delta\vec{x}, \vec{x}_2 + \delta\vec{x}, \dots, \vec{x}_n + \delta\vec{x})$$

In the simplest case of a free particle,

$$H = -\frac{1}{2m} \nabla^2 = -\frac{1}{2m} \left(\frac{\partial^2}{\partial x^2} + \frac{\partial^2}{\partial y^2} + \frac{\partial^2}{\partial z^2} \right) \quad (26)$$

From Equation (26) it is clear that

$$H(\vec{x}'_1, \vec{x}'_2, \dots, \vec{x}'_n) = H(\vec{x}_1, \vec{x}_2, \dots, \vec{x}_n) \quad (27)$$

which is true for any general closed system: the Hamiltonian is invariant under the translation operator \hat{D} , which is defined as an action onto an arbitrary wavefunction $\psi(\vec{x})$ such as

$$\hat{D}\psi(\vec{x}) \equiv \psi(\vec{x} + \delta\vec{x}) \quad (28)$$

For a single-particle state $\psi'(\vec{x}) = H(\vec{x})\psi(\vec{x})$, by definition (28) one obtains:

$$\hat{D}\psi'(\vec{x}) = \psi'(\vec{x} + \delta\vec{x}) = H(\vec{x} + \delta\vec{x})\psi(\vec{x} + \delta\vec{x})$$

further, since the Hamiltonian is invariant under translation, $\hat{D}\psi'(\vec{x}) = H(\vec{x})\psi(\vec{x} + \delta\vec{x})$ and using definitions once again,

$$\hat{D}H(\vec{x})\psi(\vec{x}) = H(\vec{x})\hat{D}\psi(\vec{x}) \quad (29)$$

This means that \hat{D} *commutes* with Hamiltonian (a standard notation for this is $[\hat{D}, H] = 0$)

Since $\delta\vec{x}$ is an infinitely small quantity, translation (28) can be expanded as

$$\psi(\vec{x} + \delta\vec{x}) = \psi(\vec{x}) + \delta\vec{x} \cdot \nabla\psi(\vec{x}) \quad (30)$$

Form (30) includes explicitly the momentum operator $\hat{p} = -i\nabla$, hence the translation operator \hat{D} can be rewritten as

$$\hat{D} = 1 + i\delta\vec{x} \cdot \hat{p} \quad (31)$$

Substituting (31) to (29), one obtains

$$[\hat{p}, H] = 0 \quad (32)$$

which is nothing but the *momentum conservation law* for a single-particle state whose Hamiltonian is invariant under translation.

Generalization of (31) and (32) for the case of multiparticle state leads to the general momentum

conservation law for the total momentum $\vec{p} = \sum_{i=1}^n \vec{p}_i$

Rotational invariance

❖ When a closed system of particles is rotated about its centre-of-mass, its physical properties remain unchanged

Under the rotation about, for example, z-axis through an angle θ , coordinates x_i, y_i, z_i transform to new coordinates x'_i, y'_i, z'_i as following:

$$\begin{aligned}x'_i &= x_i \cos \theta - y_i \sin \theta \\y'_i &= x_i \sin \theta + y_i \cos \theta \\z'_i &= z\end{aligned}\tag{33}$$

Correspondingly, the new Hamiltonian of the rotated system will be the same as the initial one,

$$H(\vec{x}_1, \vec{x}_2, \dots, \vec{x}_n) = H(\vec{x}'_1, \vec{x}'_2, \dots, \vec{x}'_n)$$

Considering rotation through an infinitesimal angle $\delta\theta$, equations (33) transforms to

$$x' = x - y\delta\theta, \quad y' = y + x\delta\theta, \quad z' = z$$

A rotational operator is introduced by analogy with the translation operator \hat{D} :

$$\hat{R}_z \psi(\vec{x}) \equiv \psi(\vec{x}') = \psi(x - y\delta\theta, y + x\delta\theta, z) \quad (34)$$

Expansion to first order in $\delta\theta$ gives

$$\psi(\vec{x}') = \psi(\vec{x}) - \delta\theta \left(y \frac{\partial}{\partial x} - x \frac{\partial}{\partial y} \right) \psi(\vec{x}) = (1 + i\delta\theta \hat{L}_z) \psi(\vec{x})$$

where \hat{L}_z is the z-component of the orbital angular momentum operator \hat{L} :

$$\hat{L}_z = -i \left(x \frac{\partial}{\partial y} - y \frac{\partial}{\partial x} \right)$$

►►► For the general case of the rotation about an arbitrary direction specified by a unit vector \vec{n} , \hat{L}_z has to be replaced by the corresponding projection of \hat{L} : $\hat{L} \cdot \vec{n}$, hence

$$\hat{R}_n = 1 + i\delta\theta (\hat{L} \cdot \vec{n}) \quad (35)$$

Considering \hat{R}_n acting on a single-particle state $\psi'(\vec{x}) = H(\vec{x})\psi(\vec{x})$ and repeating same steps as for the translation case, one gets:

$$[\hat{R}_n, H] = 0 \quad (36)$$

$$[\hat{L}, H] = 0 \quad (37)$$

This applies for a spin-0 particle moving in a central potential, i.e., in a field which does not depend on a direction, but only on the absolute distance.

▣▣▣▣ If a particle possesses a non-zero spin, the total angular momentum is the sum of the orbital and spin angular momenta:

$$\hat{J} = \hat{L} + \hat{S} \quad (38)$$

and the wavefunction is the product of [independent] space wavefunction $\psi(\vec{x})$ and spin wavefunction χ :

$$\Psi = \psi(\vec{x})\chi$$

For the case of spin-1/2 particles, the spin operator is represented in terms of Pauli matrices σ :

$$\hat{S} = \frac{1}{2}\sigma \quad (39)$$

where σ has components :
(recall page 10 of these notes)

$$\sigma_1 = \begin{pmatrix} 0 & 1 \\ 1 & 0 \end{pmatrix}, \sigma_2 = \begin{pmatrix} 0 & -i \\ i & 0 \end{pmatrix}, \sigma_3 = \begin{pmatrix} 1 & 0 \\ 0 & -1 \end{pmatrix} \quad (40)$$

Let us denote now spin wavefunction for spin “up” state as $\chi = \alpha$ ($S_z = 1/2$) and for spin “down” state as $\chi = \beta$ ($S_z = -1/2$), so that

$$\alpha = \begin{pmatrix} 1 \\ 0 \end{pmatrix}, \beta = \begin{pmatrix} 0 \\ 1 \end{pmatrix} \quad (41)$$

Both α and β satisfy the eigenvalue equations for operator (39):

$$\hat{S}_z \alpha = \frac{1}{2}\alpha, \hat{S}_z \beta = -\frac{1}{2}\beta$$

Analogously to (35), the rotation operator for the spin-1/2 particle generalizes to

$$\hat{R}_n = 1 + i\delta\theta(\hat{J} \cdot \vec{n}) \quad (42)$$

When the rotation operator \hat{R}_n acts onto the wave function $\Psi = \psi(\vec{x})\chi$, components \hat{L} and \hat{S} of \hat{J} act independently on the corresponding wavefunctions:

$$\hat{J}\Psi = (\hat{L} + \hat{S})\psi(\vec{x})\chi = [\hat{L}\psi(\vec{x})]\chi + \psi(\vec{x})[\hat{S}\chi]$$

That means that although the total angular momentum has to be conserved,

$$[\hat{J}, H] = 0$$

but the rotational invariance does not in general lead to the conservation of \hat{L} and \hat{S} separately:

$$[\hat{L}, H] = -[\hat{S}, H] \neq 0$$

However, presuming that the forces can change only orientation of the spin, but not its absolute value \Rightarrow

$$[H, \hat{L}^2] = [H, \hat{S}^2] = 0$$

▣▣▣▣ Good quantum numbers are those which are associated with conserved observables (operators commute with the Hamiltonian)

Spin is one of the quantum numbers which characterize any particle - elementary or composite.

❖ Spin \vec{S}_P of the particle is the total angular momentum \vec{J} of its constituents in their centre-of-mass frame

- Quarks are spin-1/2 particles \Rightarrow the spin quantum number $S_P=J$ can be either integer or half-integer
- Its projections on the z-axis – J_z – can take any of $2J+1$ values, from $-J$ to J with the “step” of 1, depending on the particle’s spin orientation

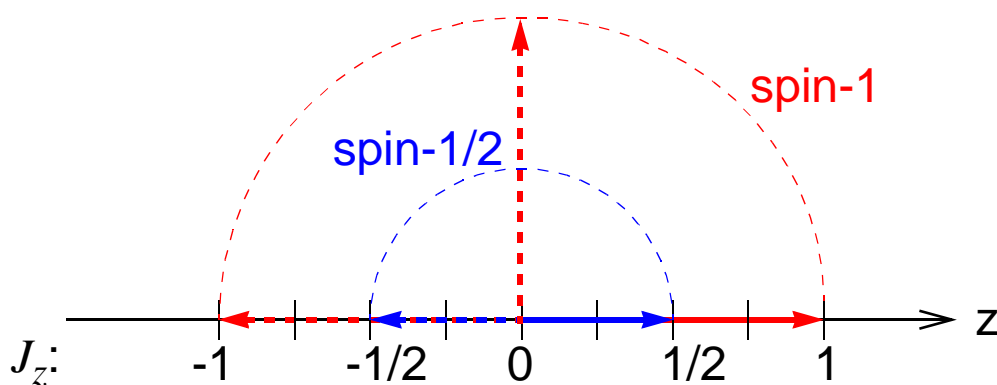


Figure 36: A naive illustration of possible J_z values for spin-1/2 and spin-1 particles

❖ Usually, it is assumed that L and S are “good” quantum numbers together with $J=S_P$, while J_z depends on the spin orientation.

Using “good” quantum numbers, one can refer to a particle via *spectroscopic notation*, like

$${}^{2S+1}L_J \quad (43)$$

– Following chemistry traditions, instead of numerical values of $L=0,1,2,3\dots$, letters S,P,D,F... are used correspondingly

– In this notation, the lowest-lying ($L=0$) bound state of two particles of spin-1/2 will be 1S_0 or 3S_1

$$\begin{array}{cc}
 L=0 & {}^1S_0 & & {}^3S_1 \\
 & \uparrow \downarrow & & \uparrow \uparrow \\
 & S=1/2-1/2=0 & & S=1/2+1/2=1 \\
 & J=L+S=0 & & J=L+S=1
 \end{array}$$

Figure 37: Quark-antiquark states for $L=0$

For mesons with $L \geq 1$, possible states are:

$${}^1L_L, {}^3L_{L+1}, {}^3L_L, {}^3L_{L-1}$$

⇒ Baryons are bound states of 3 quarks ⇒ there are two orbital angular momenta connected to the relative motion of quarks.

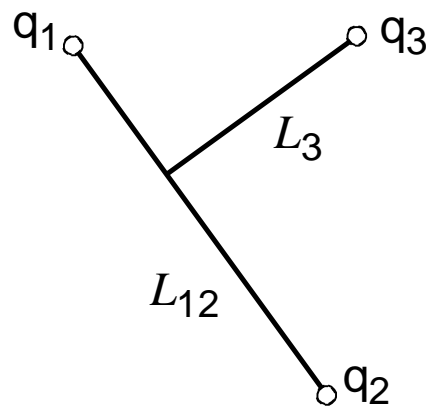


Figure 38: Internal orbital angular momenta of a three-quark state

- total orbital angular momentum is $L=L_{12}+L_3$.
- spin of a baryon $S=S_1+S_2+S_3 \Rightarrow S=1/2$ or $S=3/2$

Possible baryon states:

$$\begin{array}{ll}
 {}^2S_{1/2}, {}^4S_{3/2} & (L=0) \\
 {}^2P_{1/2}, {}^2P_{3/2}, {}^4P_{1/2}, {}^4P_{3/2}, {}^4P_{5/2} & (L=1) \\
 {}^2L_{L+1/2}, {}^2L_{L-1/2}, {}^4L_{L-3/2}, {}^4L_{L-1/2}, {}^4L_{L+1/2}, {}^4L_{L+3/2} & (L \geq 2)
 \end{array}$$

Parity

❖ Parity transformation is the transformation by reflection:

$$\vec{x}_i \rightarrow \vec{x}'_i = -\vec{x}_i \quad (44)$$

A system is invariant under parity transformation if

$$H(-\vec{x}_1, -\vec{x}_2, \dots, -\vec{x}_n) = H(\vec{x}_1, \vec{x}_2, \dots, \vec{x}_n)$$

➡ Parity is not an exact symmetry: it is violated in weak interaction!

A parity operator \hat{P} is defined as

$$\hat{P}\psi(\vec{x}, t) \equiv P_a \psi(-\vec{x}, t) \quad (45)$$

Since two consecutive reflections must result in the identical to initial system,

$$\hat{P}^2\psi(\vec{x}, t) = \psi(\vec{x}, t) \quad (46)$$

From equations (45) and (46), $P_a = +1, -1$

Considering then an eigenfunction of momentum:

$\psi_{\vec{p}}(\vec{x}, t) = e^{i(\vec{p}\vec{x} - Et)}$, it is straightforward that

$$\hat{P}\psi_{\vec{p}}(\vec{x}, t) = P_a\psi_{\vec{p}}(-\vec{x}, t) = P_a\psi_{-\vec{p}}(\vec{x}, t)$$

The latter is always true for $\vec{p} = 0$, i.e., a particle at rest is an eigenstate of the parity operator with eigenvalue P_a .

Different particles have different values of parity P_a . For a system of particles,

$$\hat{P}\psi(\vec{x}_1, \vec{x}_2, \dots, \vec{x}_n, t) \equiv P_1P_2\dots P_n\psi(-\vec{x}_1, -\vec{x}_2, \dots, -\vec{x}_n, t)$$

In polar coordinates, the parity transformation is:

$$r \rightarrow r' = r, \theta \rightarrow \theta' = \pi - \theta, \varphi \rightarrow \varphi' = \pi + \varphi$$

and a wavefunction can be written as

$$\psi_{nlm}(\vec{x}) = R_{nl}(r)Y_l^m(\theta, \varphi) \quad (47)$$

In Equation (47), R_{nl} is a function of the radius only, and Y_l^m are *spherical harmonics*, which describe angular dependence.

Under the parity transformation, R_{nl} does not change, while spherical harmonics change as

$$Y_l^m(\theta, \varphi) \rightarrow Y_l^m(\pi - \theta, \pi + \varphi) = (-1)^l Y_l^m(\theta, \varphi)$$

↓

$$\hat{P}\psi_{nlm}(\vec{x}) = P_a \psi_{nlm}(-\vec{x}) = P_a (-1)^l \psi_{nlm}(\vec{x})$$

⇒ which means that a particle with a definite orbital angular momentum is also an eigenstate of parity with an eigenvalue $P_a (-1)^l$.

Considering only electromagnetic and strong interactions, and using the usual argumentation, one can prove that parity is conserved:

$$[\hat{P}, H] = 0$$

❖ Recall: the Dirac equation (4) suggests a four-component wavefunction to describe both electrons and positrons

⇒ Intrinsic parities of e^- and e^+ are related, namely:

$$P_{e^+} P_{e^-} = -1$$

This is true for all fermions (spin-1/2 particles), i.e.,

$$P_f P_{\bar{f}} = -1 \quad (48)$$

Experimentally this can be confirmed by studying the reaction $e^+e^- \rightarrow \gamma\gamma$ where initial state has zero orbital momentum and parity of $P_{e^-} P_{e^+}$.

If the final state has relative orbital angular momentum l_γ , its parity is $P_\gamma^2 (-1)^{l_\gamma}$. Since, $P_\gamma^2 = 1$ from the parity conservation law stems that

$$P_{e^-} P_{e^+} = (-1)^{l_\gamma}$$

Experimental measurements of l_γ confirm (48)

While (48) can be proved in experiments, it is impossible to determine P_{e^-} or P_{e^+} , since these particles are created or destroyed only in pairs.

– Conventionally defined parities of leptons are:

$$P_{e^-} = P_{\mu^-} = P_{\tau^-} \equiv 1 \quad (49)$$

And consequently, parities of antileptons have opposite sign.

– Since quarks and antiquarks are also produced only in pairs, their parities are defined also by convention:

$$P_u = P_d = P_s = P_c = P_b = P_t = 1 \quad (50)$$

with parities of antiquarks being -1.

For a meson $M=(a\bar{b})$, parity is then calculated as

$$P_M = P_a P_{\bar{b}} (-1)^L = (-1)^{L+1} \quad (51)$$

For the low-lying mesons ($L=0$) that means parity of -1, which is confirmed by observations

For a baryon $B=(abc)$, parity is given as

$$P_B = P_a P_b P_c (-1)^{L_{12}} (-1)^{L_3} = (-1)^{L_{12} + L_3} \quad (52)$$

and for antibaryon $P_{\bar{B}} = -P_B$, similarly to the case of leptons.

For the low-lying baryons (52) predicts positive parities, which is also confirmed by experiment.

Parity of the photon can be deduced from the classical field theory, considering Poisson's equation:

$$\nabla \cdot \vec{E}(\vec{x}, t) = \frac{1}{\epsilon_0} \rho(\vec{x}, t)$$

Under a parity transformation, charge density changes as $\rho(\vec{x}, t) \rightarrow \rho(-\vec{x}, t)$ and ∇ changes its sign, so that to keep the equation invariant, the electric field must transform as

$$\vec{E}(\vec{x}, t) \rightarrow -\vec{E}(-\vec{x}, t) \quad (53)$$

On the other hand, the electromagnetic field is described by the vector and scalar potentials:

$$\vec{E} = -\nabla\phi - \frac{\partial\vec{A}}{\partial t} \quad (54)$$

For the photon, only the vector part corresponds to the wavefunction:

$$\vec{A}(\vec{x}, t) = N\vec{\epsilon}(\vec{k})e^{i(\vec{k}\vec{x} - Et)}$$

Under the parity transformation,

$$\vec{A}(\vec{x}, t) \rightarrow P_{\gamma}\vec{A}(-\vec{x}, t)$$

and from (54) stems that

$$\vec{E}(\vec{x}, t) \rightarrow P_{\gamma}\vec{E}(-\vec{x}, t). \quad (55)$$

Comparing (55) and (53), one concludes that parity of photon is

$$P_{\gamma} = -1$$

Charge conjugation

❖ Charge conjugation replaces particles by their antiparticles, reversing charges and magnetic moments

➡ Charge conjugation is violated by the weak interaction

For the strong and electromagnetic interactions, charge conjugation is a symmetry:

$$[\hat{C}, H] = 0$$

– It is convenient now to denote a state in a compact notation, using Dirac’s “ket” representation: $|\pi^+, \vec{p}\rangle$ denotes a pion having momentum \vec{p} , or, in general case,

$$|\pi^+ \Psi_1; \pi^- \Psi_2\rangle \equiv |\pi^+ \Psi_1\rangle |\pi^- \Psi_2\rangle \quad (56)$$

Next, we denote particles which have distinct antiparticles by “ a ”, and otherwise - by “ α ”

In these notation, we describe the action of the charge conjugation operator as:

$$\hat{C}|\alpha, \Psi\rangle = C_\alpha|\alpha, \Psi\rangle \quad (57)$$

meaning that the final state acquires a phase factor C_α , and otherwise

$$\hat{C}|a, \Psi\rangle = |\bar{a}, \Psi\rangle \quad (58)$$

meaning that the from the particle in the initial state we came to the antiparticle in the final state.

Since the second transformation turns antiparticles back to particles, $\hat{C}^2 = 1$ and hence

$$C_\alpha = \pm 1 \quad (59)$$

For multiparticle states the transformation is:

$$\begin{aligned} \hat{C}|\alpha_1, \alpha_2, \dots, a_1, a_2, \dots; \Psi\rangle &= \\ &= C_{\alpha_1} C_{\alpha_2} \dots |\alpha_1, \alpha_2, \dots, \bar{a}_1, \bar{a}_2, \dots; \Psi\rangle \end{aligned} \quad (60)$$

- From (57) it is clear that particles $\alpha=\gamma,\pi^0,\dots$ etc., are eigenstates of \hat{C} with eigenvalues $C_\alpha=\pm 1$.
- Other eigenstates can be constructed from particle-antiparticle pairs:

$$\hat{C}|a, \Psi_1; \bar{a}, \Psi_2\rangle = |\bar{a}, \Psi_1; a, \Psi_2\rangle = \pm |a, \Psi_1; \bar{a}, \Psi_2\rangle$$

For a state of definite orbital angular momentum, interchanging between particle and antiparticle reverses their relative position vector, for example:

$$\hat{C}|\pi^+ \pi^-; L\rangle = (-1)^L |\pi^+ \pi^-; L\rangle \quad (61)$$

For fermion-antifermion pairs theory predicts

$$\hat{C}|f\bar{f}; J, L, S\rangle = (-1)^{L+S} |f\bar{f}; J, L, S\rangle \quad (62)$$

This implies that π^0 , being a 1S_0 state of $u\bar{u}$ and $d\bar{d}$, must have C-parity of 1.

Tests of C-invariance

Prediction of $C_{\pi^0} = 1$ can be confirmed experimentally by studying the decay $\pi^0 \rightarrow \gamma\gamma$. The final state has $C=1$, and from the relations

$$\begin{aligned}\hat{C}|\pi^0\rangle &= C_{\pi^0}|\pi^0\rangle \\ \hat{C}|\gamma\gamma\rangle &= C_\gamma C_\gamma|\gamma\gamma\rangle = |\gamma\gamma\rangle\end{aligned}$$

it stems that $C_{\pi^0} = 1$.

C_γ can be inferred from the classical field theory:

$$\vec{A}(\vec{x}, t) \rightarrow C_\gamma \vec{A}(\vec{x}, t)$$

under the charge conjugation, and since all electric charges swap, electric field and scalar potential also change sign:

$$\vec{E}(\vec{x}, t) \rightarrow -\vec{E}(\vec{x}, t), \quad \phi(\vec{x}, t) \rightarrow -\phi(\vec{x}, t),$$

which upon substitution into (54) gives $C_\gamma = -1$.

To check predictions of the C-invariance and of the value of C_γ , one can try to look for the decay

$$\pi^0 \rightarrow \gamma + \gamma + \gamma$$

If both predictions are true, this mode should be forbidden:

$$\hat{C}|\gamma\gamma\gamma\rangle = (C_\gamma)^3|\gamma\gamma\gamma\rangle = -|\gamma\gamma\gamma\rangle$$

which contradicts all previous observations. Experimentally, this 3γ mode have never been observed.

Another confirmation of C-invariance comes from observation of η -meson decays:

$$\begin{aligned}\eta &\rightarrow \gamma + \gamma \\ \eta &\rightarrow \pi^0 + \pi^0 + \pi^0 \\ \eta &\rightarrow \pi^+ + \pi^- + \pi^0\end{aligned}$$

They are electromagnetic decays, and first two clearly indicate that $C_\eta=1$. Identical charged pions momenta distribution in third confirm C-invariance.

V. Hadron quantum numbers

Characteristics of a hadron:

1) Mass

2) Quantum numbers arising from space symmetries : J, P, C . Common notation:

– J^P (e.g. for proton: $\frac{1}{2}^+$), or

– J^{PC} if a particle is also an eigenstate of C -parity (e.g. for π^0 : 0^{-+})

3) Internal quantum numbers: Q and B (always conserved), S, C, \tilde{B}, T (conserved in e.m. and strong interactions)

How do we know what are quantum numbers of a newly discovered hadron?

How do we know that mesons consist of a quark-antiquark pair, and baryons - of three quarks?

Some *a priori* knowledge is needed:

| Particle | Mass (Gev/c ²) | Quark composition | Q | B | S | C | \tilde{B} |
|----------------|----------------------------|-------------------|----|---|----|----|-------------|
| p | 0.938 | uud | 1 | 1 | 0 | 0 | 0 |
| n | 0.940 | udd | 0 | 1 | 0 | 0 | 0 |
| K ⁻ | 0.494 | s \bar{u} | -1 | 0 | -1 | 0 | 0 |
| D ⁻ | 1.869 | d \bar{c} | -1 | 0 | 0 | -1 | 0 |
| B ⁻ | 5.279 | b \bar{u} | -1 | 0 | 0 | 0 | -1 |

Considering the lightest 3 quarks (u, d, s), possible 3-quark and 2-quark states will be (q_{i,j,k} are u- or d-quarks):

| | sss | ssq _i | sq _i q _j | q _i q _j q _k |
|---|-----|------------------|--------------------------------|--|
| S | -3 | -2 | -1 | 0 |
| Q | -1 | 0; -1 | 1; 0; -1 | 2; 1; 0; -1 |

| | s \bar{s} | s \bar{q}_i | $\bar{s}q_i$ | q _i \bar{q}_i | q _i \bar{q}_j |
|---|-------------|---------------|--------------|----------------------------|----------------------------|
| S | 0 | -1 | 1 | 0 | 0 |
| Q | 0 | 0; -1 | 1; 0 | 0 | -1; 1 |

❖ Hence restrictions arise: for example, mesons with S=-1 and Q=1 are forbidden

►►► Particles which fall out of above restrictions are called *exotic* particles (like $dd\bar{u}s$, $uu\bar{d}s$ etc.)

From observations of strong interaction processes, quantum numbers of many particles can be deduced:

$$\begin{array}{r}
 p + p \rightarrow p + n + \pi^+ \\
 \hline
 Q= \quad 2 \qquad \qquad 1 \qquad 1 \\
 S= \quad 0 \qquad \qquad 0 \qquad 0 \\
 B= \quad 2 \qquad \qquad 2 \qquad 0
 \end{array}$$

$$\begin{array}{r}
 p + p \rightarrow p + p + \pi^0 \\
 \hline
 Q= \quad 2 \qquad \qquad 2 \qquad 0 \\
 S= \quad 0 \qquad \qquad 0 \qquad 0 \\
 B= \quad 2 \qquad \qquad 2 \qquad 0
 \end{array}$$

$$\begin{array}{r}
 p + \pi^- \rightarrow \pi^0 + n \\
 \hline
 Q= \quad 1 \quad -1 \qquad \qquad 0 \\
 S= \quad 0 \quad 0 \qquad \qquad 0 \\
 B= \quad 1 \quad 0 \qquad \qquad 1
 \end{array}$$

Observations of pions confirm these predictions, ensuring that pions are non-exotic particles.

Assuming that K^- is a strange meson, one can predict quantum numbers of Λ -baryon:

$$\begin{array}{r}
 K^- + p \rightarrow \pi^0 + \Lambda \\
 \hline
 Q= \quad 0 \quad \quad 0 \quad 0 \\
 S= \quad -1 \quad \quad 0 \quad -1 \\
 B= \quad 1 \quad \quad 0 \quad 1
 \end{array}$$

And further, for K^+ -meson:

$$\begin{array}{r}
 \pi^- + p \rightarrow K^+ + \pi^- + \Lambda \\
 \hline
 Q= \quad 0 \quad \quad 1 \quad -1 \\
 S= \quad 0 \quad \quad 1 \quad -1 \\
 B= \quad 1 \quad \quad 0 \quad 1
 \end{array}$$

- ▣▣▣▣➔ All of the more than 200 observed hadrons satisfy this kind of predictions , and no exotic particles have been found so far
- ▣▣▣▣➔ It confirms validity of the quark model, which suggests that only quark-antiquark and 3-quark (or 3-antiquark) states can exist

Even more quantum numbers...

It is convenient to introduce some more quantum numbers, which are conserved in strong and e.m. interactions:

- Sum of all internal quantum numbers, except of Q,

$$\text{hypercharge } Y \equiv B + S + C + \tilde{B} + T$$

- Instead of Q:

$$I_3 \equiv Q - Y/2$$

which is to be treated as a projection of a new vector:

- *Isospin*

$$I \equiv (I_3)_{\max}$$

so that I_3 takes $2I+1$ values from $-I$ to I

- ❖ It appears that I_3 is a good quantum number to denote up- and down- quarks, and it is convenient to use notations for particles as $I(J^P)$ or $I(J^{PC})$

| | B | S | C | \tilde{B} | T | Y | Q | I_3 |
|---|-----|----|---|-------------|---|------|------|-------|
| u | 1/3 | 0 | 0 | 0 | 0 | 1/3 | 2/3 | 1/2 |
| d | 1/3 | 0 | 0 | 0 | 0 | 1/3 | -1/3 | -1/2 |
| s | 1/3 | -1 | 0 | 0 | 0 | -2/3 | -1/3 | 0 |
| c | 1/3 | 0 | 1 | 0 | 0 | 4/3 | 2/3 | 0 |
| b | 1/3 | 0 | 0 | -1 | 0 | -2/3 | -1/3 | 0 |
| t | 1/3 | 0 | 0 | 0 | 1 | 4/3 | 2/3 | 0 |

Hypercharge Y, isospin I and its projection I_3 are additive quantum numbers, so that corresponding quantum numbers for hadrons can be deduced from those of quarks:

$$Y^{a+b} = Y^a + Y^b ; I_3^{a+b} = I_3^a + I_3^b$$

$$I^{a+b} = I^a + I^b, I^a + I^b - 1, \dots, |I^a - I^b|$$

❖ Proton and neutron both have isospin of 1/2, and also very close masses:

$$p(938) = uud ; n(940) = udd : I(J)^P = \frac{1}{2} \left(\frac{1}{2} \right)^+$$

proton and neutron are said to belong to the
isospin doublet

Other examples of *isospin multiplets*:

$$K^+(494) = u\bar{s} ; K^0(498) = d\bar{s} : I(J)^P = \frac{1}{2}(0)^-$$

$$\pi^+(140) = u\bar{d} ; \pi^-(140) = d\bar{u} : I(J)^P = 1(0)^-$$

$$\pi^0(135) = (u\bar{u}-d\bar{d})/\sqrt{2} : I(J)^{PC} = 1(0)^{-+}$$

⇒ Principle of *isospin symmetry*: it is a good approximation to treat u- and d-quarks as having same masses

Particles with $I=0$ are *isosinglets* :

$$\Lambda(1116) = uds, I(J)^P = 0\left(\frac{1}{2}\right)^+$$

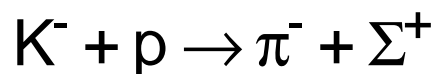
❖ By introducing isospin, we imply new criteria for non-exotic particles:

| | sss | ssq _i | sq _i q _j | q _i q _j q _k |
|----------|-----|------------------|--------------------------------|--|
| <i>S</i> | -3 | -2 | -1 | 0 |
| <i>Q</i> | -1 | 0; -1 | 1; 0; -1 | 2; 1; 0; -1 |
| <i>I</i> | 0 | 1/2 | 0; 1 | 3/2; 1/2 |

| | $s\bar{s}$ | $s\bar{q}_i$ | $\bar{s}q_i$ | $q_i\bar{q}_i$ | $q_i\bar{q}_j$ |
|-----|------------|--------------|--------------|----------------|----------------|
| S | 0 | -1 | 1 | 0 | 0 |
| Q | 0 | 0; -1 | 1; 0 | 0 | -1; 1 |
| I | 0 | 1/2 | 1/2 | 0; 1 | 0; 1 |

In all observed interactions these criteria are satisfied as well, confirming once again the quark model.

❖ This allows predictions of possible multiplet members: suppose we observe production of the Σ^+ baryon in a strong interaction:



which then decays weakly :

$$\Sigma^+ \rightarrow \pi^+ + n$$

$$\Sigma^+ \rightarrow \pi^0 + p$$

It follows that Σ^+ baryon quantum numbers are: $B=1$, $Q=1$, $S=-1$ and hence $Y=0$ and $I_3=1$.

⇒ Since $I_3 > 0 \Rightarrow I \neq 0$ and there are more multiplet members!

The simplest attempt to calculate mass difference of up and down quarks:

$$M(\Sigma^-) = M_0 + m_s + 2m_d + \delta/3$$

$$M(\Sigma^0) = M_0 + m_s + m_d + m_u - \delta/3$$

$$M(\Sigma^+) = M_0 + m_s + 2m_u$$

⇓

$$m_d - m_u = [M(\Sigma^-) + M(\Sigma^0) - 2M(\Sigma^+)] / 3 = 3.7 \text{ MeV}/c^2$$

⇒ NB : this is a very simplistic model, because under these assumptions $M(\Sigma^0) = M(\Lambda)$, however, their mass difference $M(\Sigma^0) - M(\Lambda) \approx 77 \text{ MeV}/c^2$.

Generally, combining other methods:

$$2 \leq m_d - m_u \leq 4 \text{ (MeV}/c^2 \text{)}$$

which is negligible comparing to hadron masses (but not if compared to estimated u and d masses themselves)

Resonances

- Resonances are highly unstable particles which decay by the strong interaction (lifetimes about 10^{-23} s)

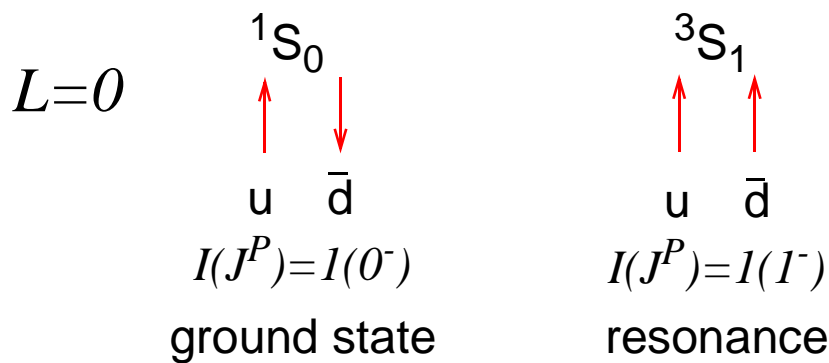
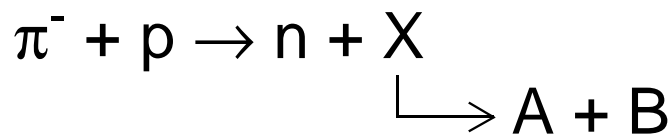


Figure 39: Example of a $q\bar{q}$ system in ground and first excited states

- If a ground state is a member of an isospin multiplet, then resonant states will form a corresponding multiplet too

Since resonances have very short lifetimes, they can only be detected by registering their decay products:



- Invariant mass of the particle is measured via masses of its decay products:

$$W^2 \equiv (E_A + E_B)^2 - (\vec{p}_A + \vec{p}_B)^2 = E^2 - \vec{p}^2 = M^2 \quad (63)$$

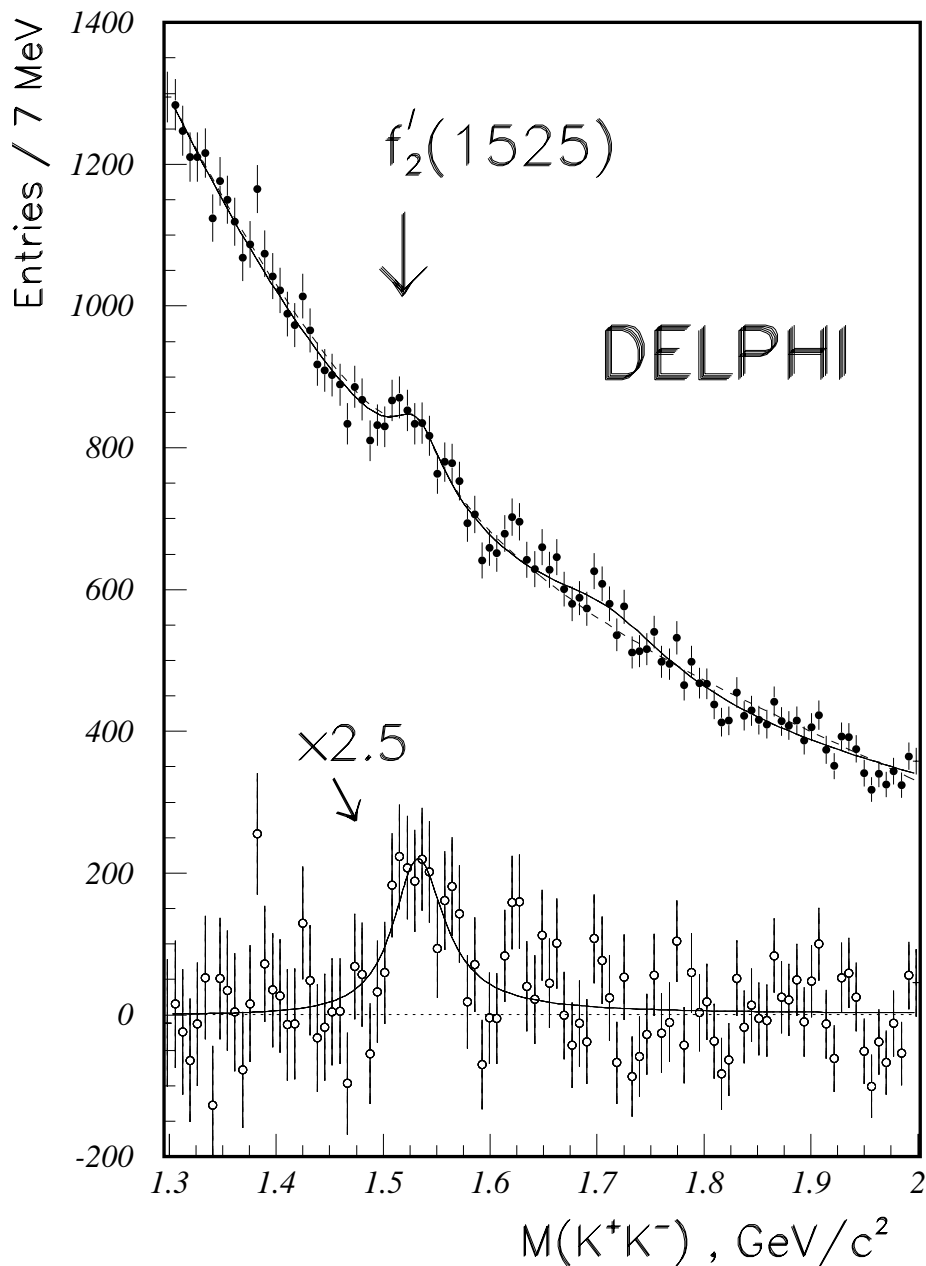


Figure 40: A typical resonance peak in K^+K^- invariant mass distribution

➡ Resonance peak shapes are approximated by the Breit-Wigner formula:

$$N(W) = \frac{K}{(W - W_0)^2 + \Gamma^2/4} \quad (64)$$

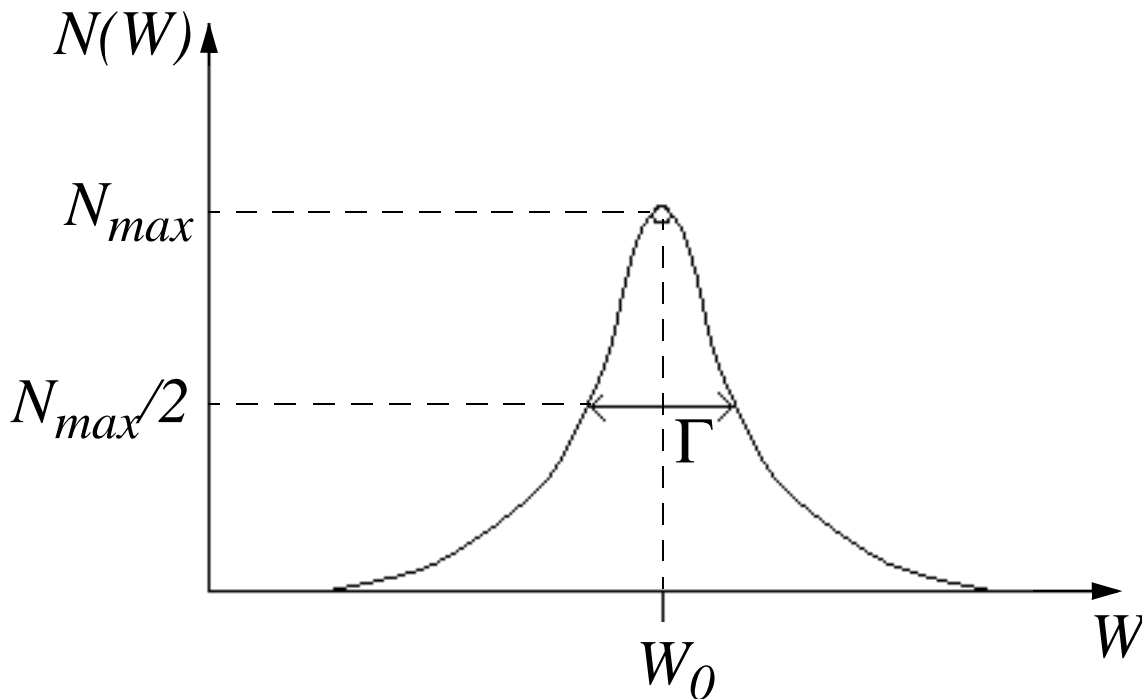


Figure 41: Breit-Wigner shape

- ❖ Mean value of the Breit-Wigner shape is the mass of a resonance: $M=W_0$
- ❖ Γ is the width of a resonance, and is inverse mean lifetime of a particle at rest: $\Gamma \equiv 1/\tau$

Some excited states of pion:

| <i>resonance</i> | $I(J^{PC})$ |
|------------------|-------------|
| $\rho^0(769)$ | $1(1^{--})$ |
| $f_2^0(1275)$ | $0(2^{++})$ |
| $\rho^0(1700)$ | $1(3^{--})$ |

❖ Resonances with $B=0$ are meson resonances, and with $B=1$ – baryon resonances.

Many baryon resonances can be produced in pion-nucleon scattering:

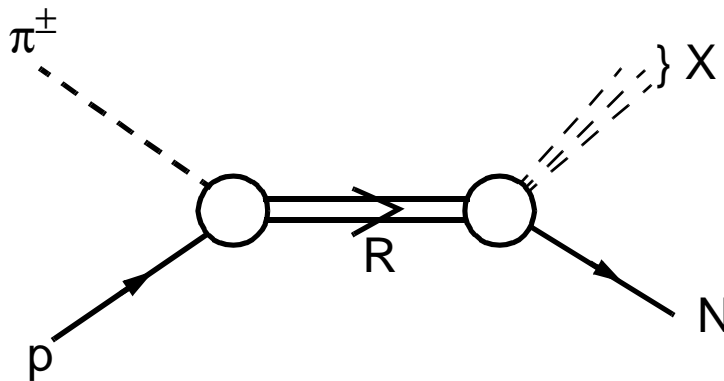
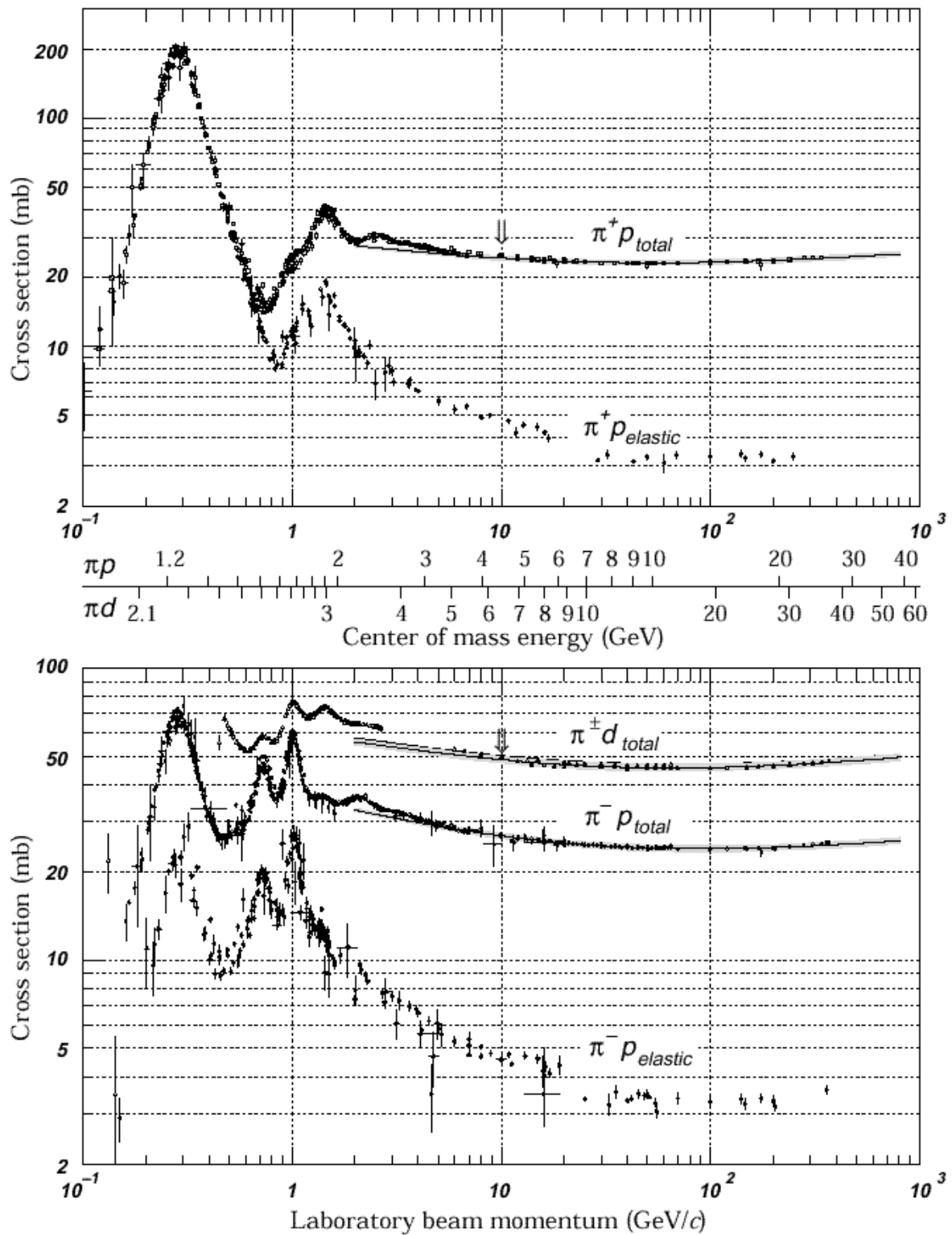


Figure 42: Formation of a resonance R and its subsequent inclusive decay into a nucleon N

❖ Peaks in the observed total cross-section of the π^+p -reaction correspond to resonances formation

Figure 43: Scattering of p^+ and p^- on proton

- ❖ Fits by the Breit-Wigner formula show that both Δ^{++} and Δ^0 have approximately same mass of $\approx 1232 \text{ MeV}/c^2$ and width $\approx 120 \text{ MeV}/c^2$.
 - ❖ Studies of angular distributions of decay products show that $I(J^P) = \frac{3}{2} \left(\frac{3}{2}\right)^+$
 - ❖ Remaining members of the multiplet are also observed: Δ^+ and Δ^-
- ➡ There is no lighter state with these quantum numbers $\Rightarrow \Delta$ is a ground state, although a resonance.

Quark diagrams

- ➡ Quark diagrams are convenient way of illustrating strong interaction processes

Consider an example:

$$\Delta^{++} \rightarrow p + \pi^+$$

The only 3-quark state consistent with Δ^{++} quantum numbers is (uuu), while $p=(uud)$ and $\pi^+=(u\bar{d})$

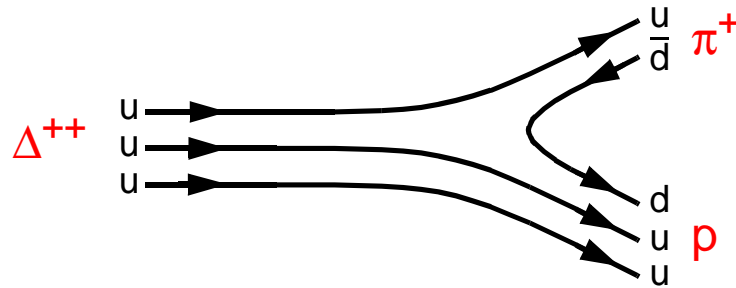


Figure 44: Quark diagram of the reaction $\Delta^{++} \rightarrow p + \pi^+$

Analogously to Feinman diagrams:

- ❖ arrow pointing to the right denotes a particle, and to the left – antiparticle
- ❖ time flows from left to right

Allowed resonance formation process:

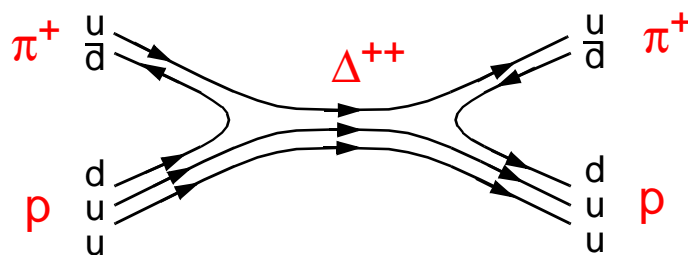


Figure 45: Formation and decay of Δ^{++} resonance in π^+p elastic scattering

Hypothetical exotic resonance:

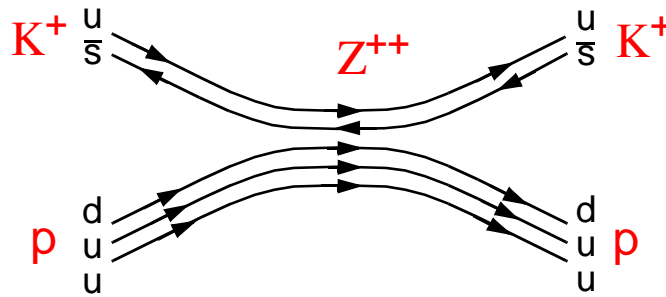


Figure 46: Formation and decay of an exotic resonance Z^{++} in K^+p elastic scattering

❖ Quantum numbers of such a particle Z^{++} are exotic, moreover, there are no resonance peaks in the corresponding cross-section:

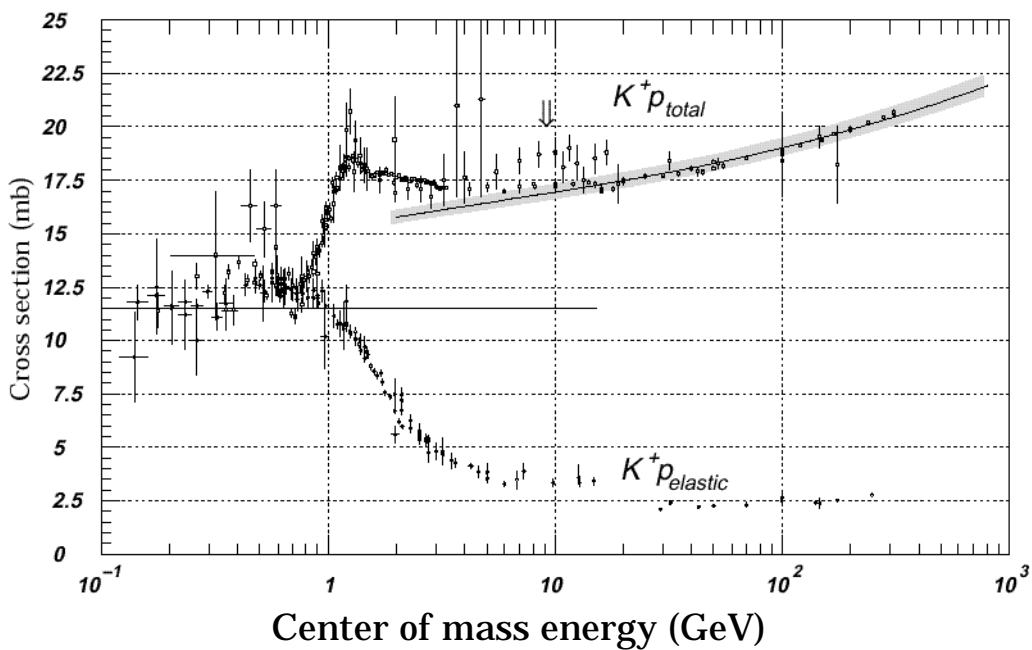
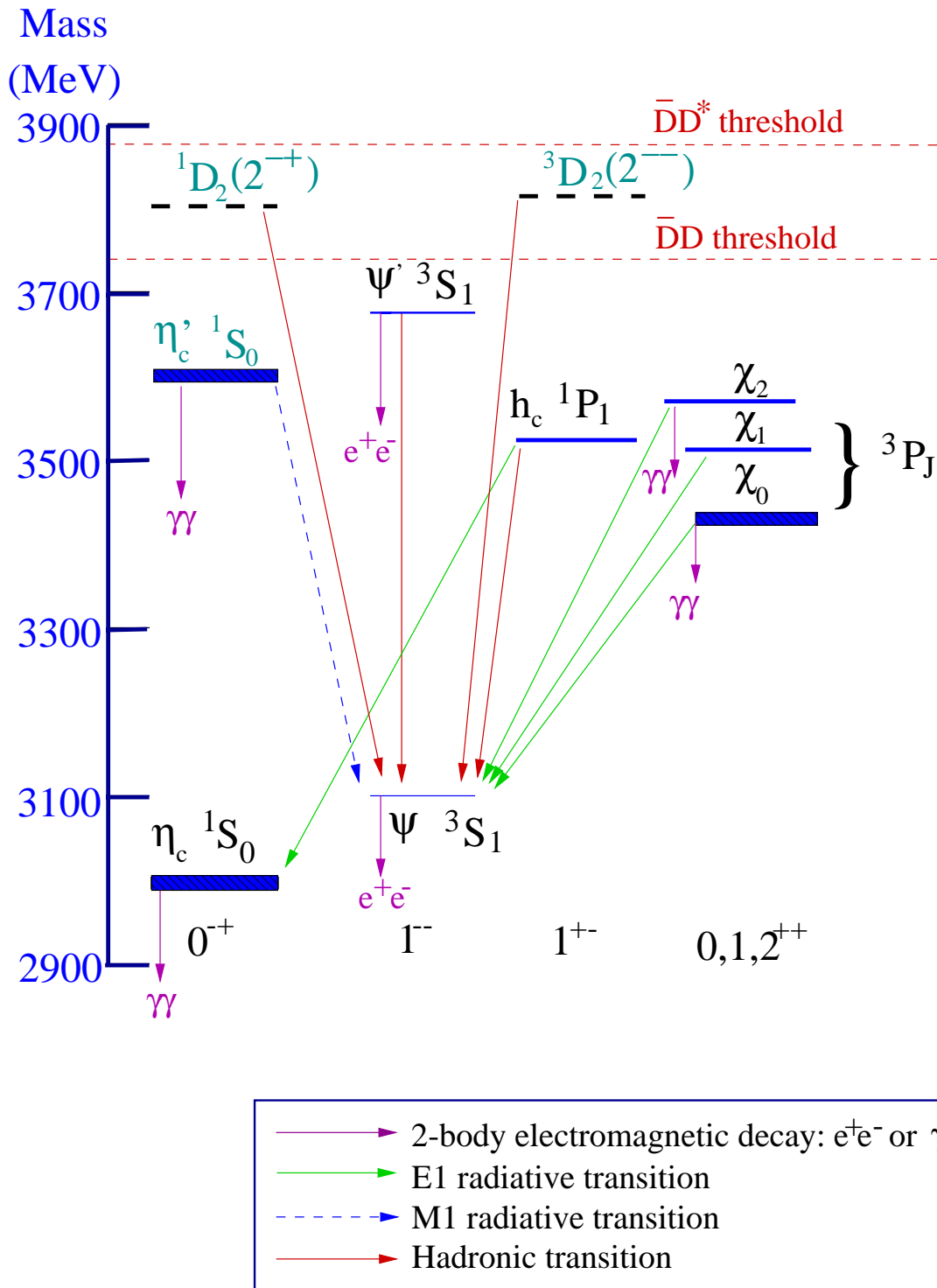


Figure 47: Cross-section for K^+p scattering

VI. Quark states and colours

- ▣▣▣▣ Forces acting between quarks in hadrons can be investigated by studying a simple quark-antiquark system
- ▣▣▣▣ Systems of heavy quarks, like $c\bar{c}$ (*charmonium*) and $b\bar{b}$ (*bottomium* or *bottomonium*), are essentially non-relativistic (masses of quarks are much bigger than their kinetic energies)
 - ❖ Charmonium and bottomium are analogous to a hydrogen atom in a sense that they consist of many energy levels
 - ❖ While the hydrogen atom is governed by the electromagnetic force, the charmonium system is dominated by the strong force

Like in hydrogen atom, energy states of a quarkonium can be labelled by their principal quantum number n , and J, L, S , where $L \leq n-1$ and S can be either 0 or 1.



Note: The thickness of the line representing each charmonium state is roughly proportional to the state's observed total width.

Figure 48: The charmonium spectrum

From Equations (51) and (62), parity and C-parity of a quarkonium are:

$$P = P_q P_{\bar{q}} (-1)^L = (-1)^{L+1} \quad ; \quad C = (-1)^{L+S}$$

Predicted and observed charmonium and bottomium states for $n=1$ and $n=2$:

| | | J^{PC} | $c\bar{c}$ state | $b\bar{b}$ state |
|-------|---------|----------|-------------------|-------------------|
| $n=1$ | 1S_0 | 0^{-+} | $\eta_c(2980)$ | – |
| $n=1$ | 3S_1 | 1^{--} | $J/\psi(3097)$ | $Y(9460)$ |
| $n=2$ | 1S_0 | 0^{-+} | – | – |
| $n=2$ | 3S_1 | 1^{--} | $\psi(3686)$ | $Y(10023)$ |
| $n=2$ | 3P_0 | 0^{++} | $\chi_{c0}(3415)$ | $\chi_{b0}(9860)$ |
| $n=2$ | 3P_1 | 1^{++} | $\chi_{c1}(3511)$ | $\chi_{b1}(9892)$ |
| $n=2$ | 3P_2 | 2^{++} | $\chi_{c2}(3556)$ | $\chi_{b2}(9913)$ |
| $n=2$ | 1P_1 | 1^{+-} | – | |

❖ States J/ψ and ψ have the same J^{PC} quantum numbers as a photon: 1^{--} , and the most common way to form them is through e^+e^- -annihilation, where virtual photon converts to a charmonium state

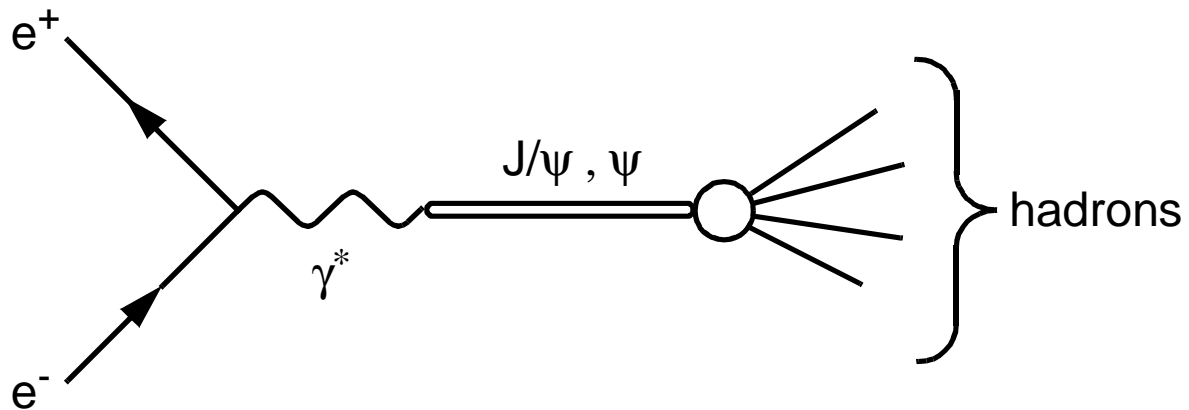


Figure 49: Formation and decay of J/ψ (ψ) mesons in e^+e^- annihilation

- ❖ If centre-of-mass energy of incident e^+ and e^- is equal to the quarkonium mass, formation of the latter is highly probable, which leads to the peak in the cross-section $\sigma(e^+e^- \rightarrow \text{hadrons})$.
- ❖ Still, a $\mu^+\mu^-$ pair can be produced as a final state too:

$$\sigma(e^+e^- \rightarrow \mu^+\mu^-) = \frac{4\pi\alpha^2}{3E_{CM}^2} \quad (65)$$

(σ is calculated theoretically within the field theory)

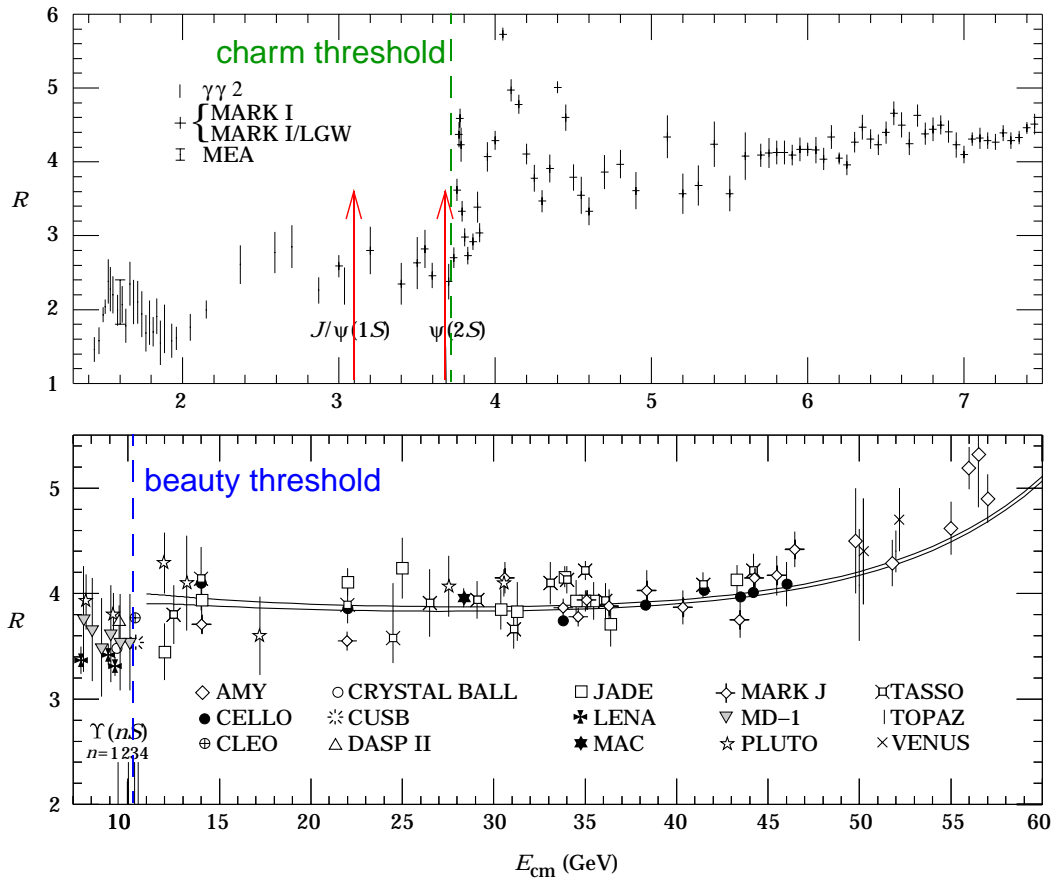


Figure 50: Cross-section ratio R in e^+e^- collision

Convenient way to represent cross-sections in e^+e^- annihilation:

$$R \equiv \frac{\sigma(e^+e^- \rightarrow hadrons)}{\sigma(e^+e^- \rightarrow \mu^+\mu^-)} \tag{66}$$

❖ Charm threshold (3730 MeV): twice mass of the lightest charmed meson, D

Wide peaks above charm threshold: short-living resonances

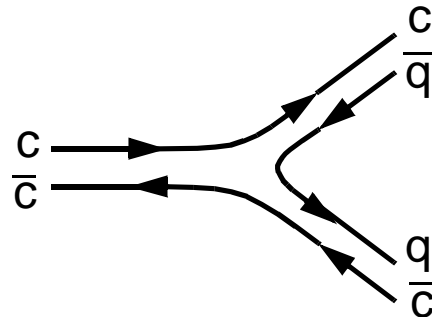


Figure 51: Charmonium resonance decay to charmed mesons

Narrow J/ψ and ψ peaks below charm threshold: can not decay by the mechanism on Fig.51 due to the energy conservation, hence have very long lifetimes (annihilation of a heavy quark-antiquark is *suppressed* as opposed to light ones)

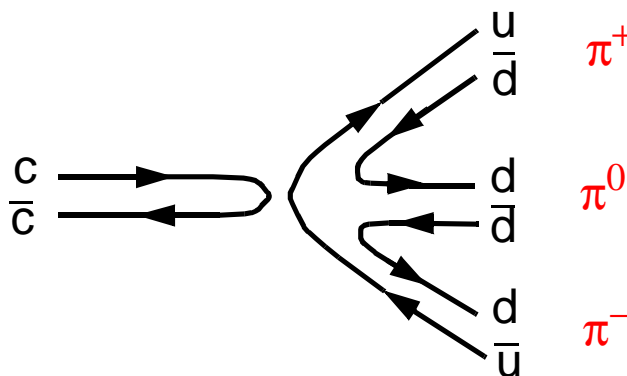


Figure 52: Charmonium decay to light non-charmed mesons

⇒ Charmonium states with quantum numbers different of those of photon can not be produced as in Fig.49, but can be found in radiative decays of J/ψ or ψ :

$$\psi(3686) \rightarrow \chi_{ci} + \gamma \quad (i=0,1,2) \quad (67)$$

$$\psi(3686) \rightarrow \eta_c(2980) + \gamma \quad (68)$$

$$J/\psi(3097) \rightarrow \eta_c(2980) + \gamma \quad (69)$$

❖ Bottomium spectrum is observed in much the same way as the charmonium one

❖ Beauty threshold is at $10560 \text{ MeV}/c^2$ (twice mass of the B meson)

⇒ Similarities between spectra of bottomium and charmonium suggest similarity of forces acting in the two systems

The quark-antiquark potential

- ❖ Assume the $q\bar{q}$ potential being a central one, $V(r)$, and the system to be non-relativistic

In the centre-of-mass frame of a $q\bar{q}$ pair, the Schrödinger equation will be

$$-\frac{1}{2\mu}\nabla^2\psi(\vec{x}) + V(r)\psi(\vec{x}) = E\psi(\vec{x}) \quad (70)$$

Here $\mu = m_q/2$ is the *reduced mass* of a quark, and $r = |\vec{x}|$ is the distance between quarks.

Mass of a quarkonium state in this framework is

$$M(q\bar{q}) = 2m_q + E \quad (71)$$

In the case of a Coulomb-like potential $V(r) \propto r^{-1}$, energy levels depend only on the principal quantum number n :

$$E_n = -\frac{\mu\alpha^2}{2n^2}$$

In the case of a harmonic oscillator potential $V(r) \propto r^2$, the degeneracy of energy levels is broken:

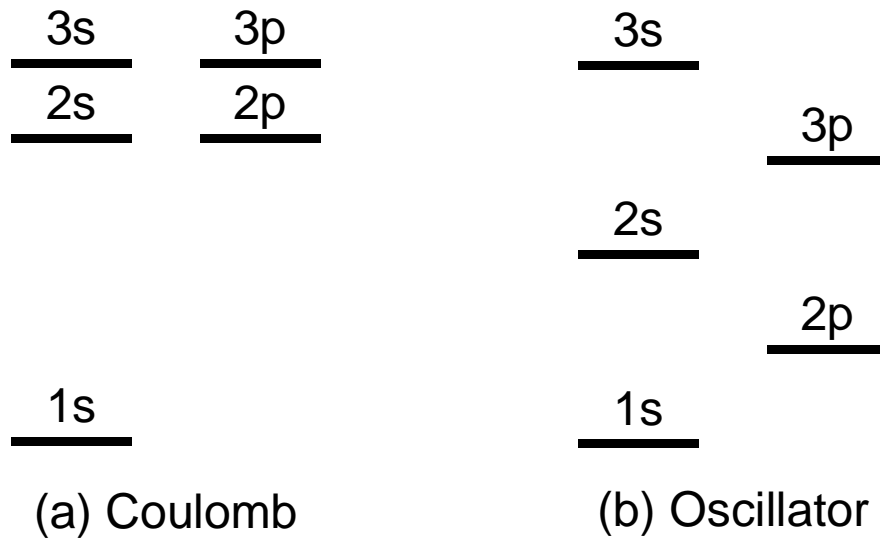


Figure 53: Energy levels arising from Coulomb and harmonic oscillator potentials for $n=1,2,3$

Comparing with Fig.48, one can see that heavy quarkonia spectra are intermediate between two possibilities; it can be fitted by:

$$V(r) = -\frac{a}{r} + br \tag{72}$$

Coefficients a and b are determined by solving Equation (70) and fitting results to data

$$a=0.48 \qquad b=0.18 \text{ GeV}^2$$

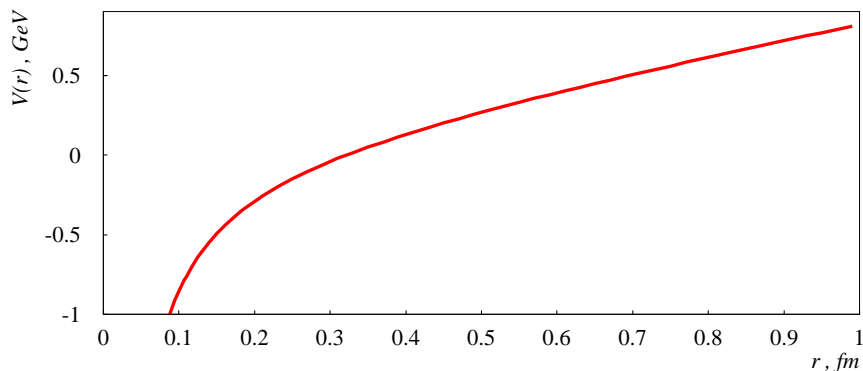


Figure 54: Modified Coulomb potential (72)

Other forms of the potential can give equally good fits, for example

$$V(r) = a \ln(br) \tag{73}$$

where parameters appear to be

$$a=0.7 \text{ GeV}$$

$$b=0.5 \text{ GeV}$$

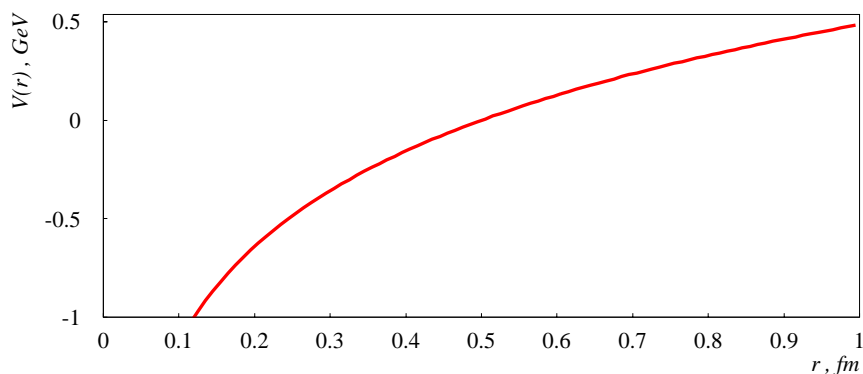


Figure 55: Logarithmic potential (73)

- ❖ In the range of $0.2 \leq r \leq 0.8$ fm potentials like (72) and (73) are in good agreement \Rightarrow in this region the quark-antiquark potential can be considered as well-defined
- ▣ Simple non-relativistic approach using the Schrödinger equation explains existence of several energy states for a given quark-antiquark system

Light mesons; nonets

- ❖ Mesons with spin $J=0$ are called “*pseudoscalar mesons*” (spins of quarks are counter-directed)
- ❖ Mesons with spin $J=1$ are “*vector mesons*” (co-directed spins of quarks)

There is nine possible $q\bar{q}$ combinations containing lightest quarks (u,d,s).

- *Pseudoscalar meson nonet*: 9 mesons with $J^P=0^-$
- *Vector meson nonet*: 9 mesons with $J^P=1^-$

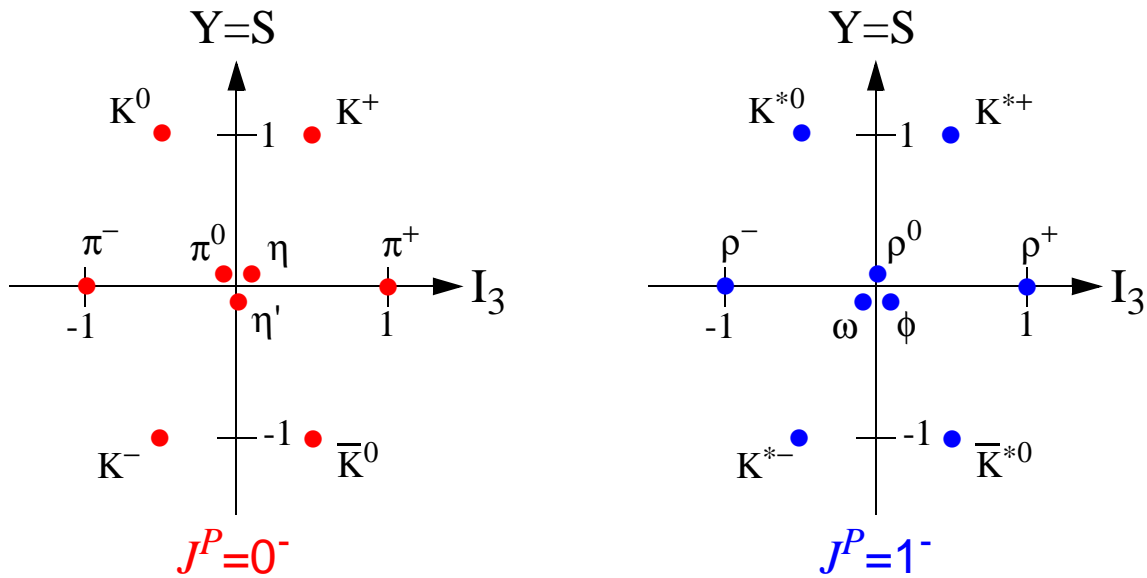


Figure 56: Light meson nonets in (I_3, Y) space (“weight diagrams”)

❖ In each nonet, there are three particles with equal quantum numbers $Y=S=I_3=0$

They correspond to a $q\bar{q}$ pair like $u\bar{u}$, $d\bar{d}$, $s\bar{s}$, or they can be a *linear combination* of these states (it follows from the isospin operator analysis):

$$\frac{1}{\sqrt{2}}(u\bar{u} - d\bar{d}) \quad I = 1, I_3 = 0 \quad (74)$$

$$\frac{1}{\sqrt{2}}(u\bar{u} + d\bar{d}) \quad I = 0, I_3 = 0 \quad (75)$$

⇒ π^0 and ρ^0 mesons are linear combinations of $u\bar{u}$ and $d\bar{d}$ states (74): $(u\bar{u} - d\bar{d})/(\sqrt{2})$

⇒ ω meson is assigned linear combination (75):
 $(u\bar{u} + d\bar{d})/(\sqrt{2})$

Inclusion of $s\bar{s}$ pair leads to some more possible combinations:

$$\eta(547) = \frac{(d\bar{d} + u\bar{u} - 2s\bar{s})}{\sqrt{6}} \quad I = 0, I_3 = 0 \quad (76)$$

$$\eta'(958) = \frac{(d\bar{d} + u\bar{u} + s\bar{s})}{\sqrt{3}} \quad I = 0, I_3 = 0 \quad (77)$$

⇒ Meson $\phi(1019)$ is a quarkonium $s\bar{s}$, having $I=0$ and $I_3=0$

Light baryons

❖ Three-quark states of the lightest quarks (u,d,s) form baryons, which can be arranged in *supermultiplets* (*singlets*, *octets* and *decuplets*).

►►► The lightest baryon supermultiplets are octet of

$J^P = \frac{1}{2}^+$ particles and decuplet of $J^P = \frac{3}{2}^+$ particles

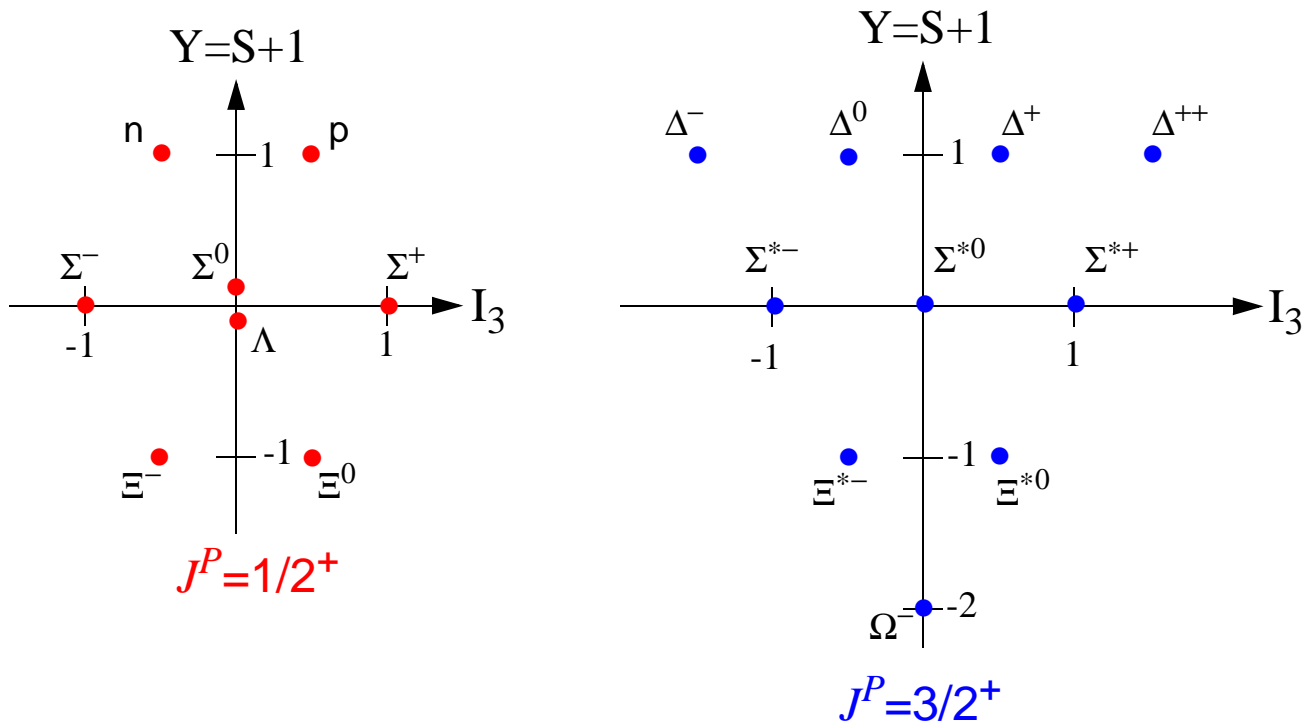


Figure 57: Weight diagrams for light baryons

❖ Weight diagrams of baryons can be deduced from the quark model under assumption that the **combined** space-spin wavefunctions are *symmetric* under interchange of **like** quarks

- Parity of a 3-quark state $q_i q_j q_k$ is $P = P_i P_j P_k = 1$
- Spin of such a state is sum of quark spins
- From presumption of symmetry under exchange of like quarks, any pair of like quarks qq must have spin-1



⇒ there are six distinct combination of the form $q_i q_j q_k$:

uud, uus, ddu, dds, ssu, ssd

each of them can have spin $J=1/2$ or $J=3/2$

⇒ three combinations of the form $q_i q_i q_i$ are possible:

uuu, ddd, sss

spins of all like-quarks have to be parallel (symmetry presumption), hence $J=3/2$ only

⇒ the remaining combination is **uds**, with two distinct states having spin values $J=1/2$ and one state with $J=3/2$

▣▣▣▣➔ By adding up numbers, one gets 8 states with $J^P=1/2^+$ and 10 states with $J^P=3/2^+$, exactly what is shown by weight diagrams

❖ Measured masses of baryons show that the mass difference between members of same isospin multiplets is much smaller than that between members of different isospin multiplets

In what follows, equal masses of isospin multiplet members are assumed, e.g.,

$$m_p = m_n \equiv m_N$$

Experimentally, more s-quarks contains a particle, heavier it is:

$$\Xi^0(1315)=(uss); \Sigma^+(1189)=(uus); p(938)=(uud)$$

$$\Omega^-(1672)=(sss); \Xi^{*0}(1532)=(uss);$$

$$\Sigma^{*+}(1383)=(uus); \Delta^{++}(1232)=(uuu)$$

▣▣▣▣➔ There is evidence that main contribution to big mass differences comes from the s-quark

Knowing masses of baryons, one can calculate 6 estimates of the mass difference between s-quark and light quarks (u,d):

For the $3/2^+$ decuplet:

$$M_{\Omega} - M_{\Xi} = M_{\Xi} - M_{\Sigma} = M_{\Sigma} - M_{\Delta} = m_s - m_{u,d}$$

and for the $1/2^+$ octet:

$$M_{\Xi} - M_{\Sigma} = M_{\Xi} - M_{\Lambda} = M_{\Lambda} - M_N = m_s - m_{u,d}$$

Average value of those differences gives

$$m_s - m_{u,d} \approx 160 \text{ MeV}/c^2 \quad (78)$$

▣▣▣▣➔ BUT quarks are spin-1/2 particles \Rightarrow fermions \Rightarrow their wavefunctions are *antisymmetric* and all the discussion above **contradicts Pauli principle!**

COLOUR

❖ Experimental data confirm predictions based on the assumption of symmetric wave functions

➡ That means that apart of space and spin degrees of freedom, quarks have yet another attribute

In 1964-1965, Greenberg and Nambu with colleagues proposed the new property – the *colour* – with THREE possible states, and associated with the corresponding wavefunction χ^C :

$$\Psi = \psi(\vec{x})\chi\chi^C \quad (79)$$

❖ Conserved quantum numbers associated with χ^C are *colour charges* – in strong interaction they play analogous role to the electric charge in e.m. interaction

❖ Hadrons can exist only in *colour singlet* states, with total colour charge of zero

❖ Quarks have to be *confined* within the hadrons, since non-zero colour states are forbidden

❖ Three independent colour wavefunctions are represented by “*colour spinors*”:

$$r = \begin{pmatrix} 1 \\ 0 \\ 0 \end{pmatrix}, \quad g = \begin{pmatrix} 0 \\ 1 \\ 0 \end{pmatrix}, \quad b = \begin{pmatrix} 0 \\ 0 \\ 1 \end{pmatrix} \quad (80)$$

❖ They are acted on by eight independent “*colour operators*” which are represented by a set of 3-dimensional matrices (analogues of Pauli matrices)

❖ Colour charges I_3^C and Y^C are eigenvalues of corresponding operators

Values of I_3^C and Y^C for the colour states of quarks and antiquarks:

| | Quarks | | Antiquarks | | |
|--------------------|---------|-------|------------|-------|------|
| | I_3^C | Y^C | I_3^C | Y^C | |
| r (“red”) | 1/2 | 1/3 | \bar{r} | -1/2 | -1/3 |
| g (“green”) | -1/2 | 1/3 | \bar{g} | 1/2 | -1/3 |
| b (“blue”) | 0 | -2/3 | \bar{b} | 0 | 2/3 |

❖ *Colour hypercharge* Y^C and *colour isospin charge* I_3^C are additive quantum numbers, having opposite sign for quark and antiquark

Confinement condition for the total colour charges of a hadron:

$$I_3^C = Y^C = 0 \quad (81)$$

The most general colour wavefunction for a baryon is a linear superposition of six possible combinations:

$$\begin{aligned} \chi_B^C = & \alpha_1 r_1 g_2 b_3 + \alpha_2 g_1 r_2 b_3 + \alpha_3 b_1 r_2 g_3 \\ & + \alpha_4 b_1 g_2 r_3 + \alpha_5 g_1 b_2 r_3 + \alpha_6 r_1 b_2 g_3 \end{aligned} \quad (82)$$

where α_i are constants. Apparently, the color confinement demands the totally antisymmetric combination:

$$\begin{aligned} \chi_B^C = & \frac{1}{\sqrt{6}} (r_1 g_2 b_3 - g_1 r_2 b_3 + b_1 r_2 g_3 \\ & - b_1 g_2 r_3 + g_1 b_2 r_3 - r_1 b_2 g_3) \end{aligned} \quad (83)$$

Colour confinement principle (81) implies certain requirements for states containing both quarks and antiquarks:

- consider combination $q^m \bar{q}^n$ of m quarks and n antiquarks, $m \geq n$
- for a particle with α quarks in r-state, β quarks in g-state, γ quarks in b-state ($\alpha + \beta + \gamma = m$) and $\bar{\alpha}$, $\bar{\beta}$, $\bar{\gamma}$ antiquarks in corresponding antistates ($\bar{\alpha} + \bar{\beta} + \bar{\gamma} = n$), the colour wavefunction is

$$r^\alpha g^\beta b^\gamma \bar{r}^{\bar{\alpha}} \bar{g}^{\bar{\beta}} \bar{b}^{\bar{\gamma}} \quad (84)$$

Adding up colour charges and applying the confinement requirement,

$$I_3^C = (\alpha - \bar{\alpha})/2 - (\beta - \bar{\beta})/2 = 0$$

$$Y^C = (\alpha - \bar{\alpha})/3 + (\beta - \bar{\beta})/3 - 2(\gamma - \bar{\gamma})/3 = 0$$

$$\Downarrow$$

$$\alpha - \bar{\alpha} = \beta - \bar{\beta} = \gamma - \bar{\gamma} \equiv p$$

Here p is a non-negative integer, and hence $m - n = 3p$

⇒ The only combination $q^m \bar{q}^n$ allowed by the colour confinement principle is

$$(3q)^p (q\bar{q})^n \quad p, n \geq 0 \quad (85)$$

❖ Form (85) forbids states with fractional electric charges

❖ However, it allows exotic combinations like $qqq\bar{q}$, $qqq\bar{q}\bar{q}$. Existence of such is not confirmed experimentally though.

VII. QCD, jets and gluons

- **Quantum Chromodynamics (QCD):** the theory of strong interactions
 - ❖ Interactions are carried out by a massless spin-1 particle – *gauge boson*
 - ❖ In quantum electrodynamics (QED) gauge bosons are photons, in QCD – *gluons*
 - ❖ Gauge bosons couple to conserved charges: photons in QED – to electric charges, and gluons in QCD – to colour charges
- Gluons have electric charge of 0 and couple to colour charges \Rightarrow strong interactions are **flavour-independent**

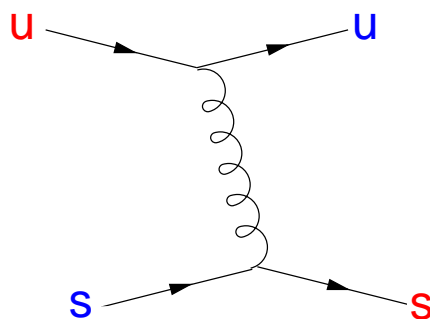


Figure 58: Gluon exchange between quarks

⇒ **Gluons carry colour charges themselves!**

Colour quantum numbers of the gluon on Fig.58 are:

$$I_3^C = I_3^C(r) - I_3^C(b) = \frac{1}{2} \quad (86)$$

$$Y^C = Y^C(r) - Y^C(b) = 1 \quad (87)$$

In general, gluons exist in 8 different colour states

⇒ **Gluons can couple to other gluons!**

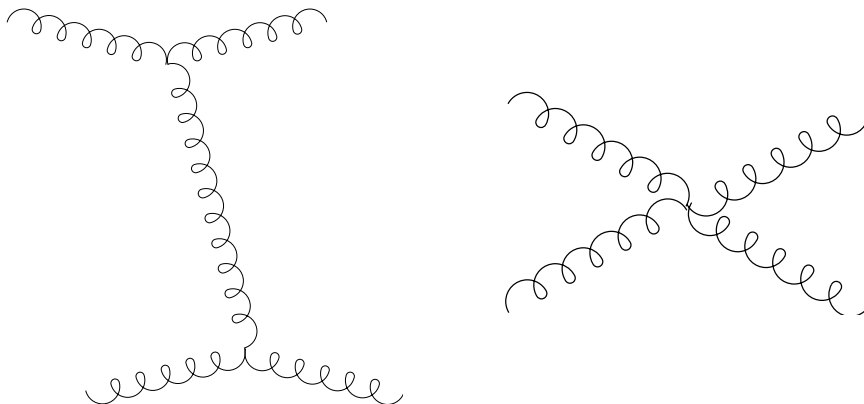


Figure 59: Lowest-order contributions to gluon-gluon scattering

❖ Bound colourless states of gluons are called *glueballs* (not detected experimentally yet)

❖ Gluons are massless \Rightarrow long-range interaction

Principle of *asymptotic freedom*:

- ▣▣▣▣▣ At short distances, strong interactions are sufficiently weak (lowest order diagrams) \Rightarrow quarks and gluons are essentially free particles
- ▣▣▣▣▣ At large distances, high-order diagrams dominate \Rightarrow “anti-screening” of colour charge \Rightarrow interaction is very strong

Asymptotic freedom thus implies the requirement of colour confinement

❖ Due to the complexity of high-order diagrams, the very process of confinement can not be calculated analytically \Rightarrow only numerical models are available

At short distances, the quark-antiquark potential is:

$$V(r) = -\frac{4}{3} \frac{\alpha_s}{r} \quad (r < 0.1 \text{ fm}) \quad (88)$$

Strong coupling constant α_s

❖ Constant α_s in Equation (88) is QCD analogue of α_{em} and is a measure of the interaction strength

However, α_s is a “running constant”, and increases with increase of r , becoming divergent at very big distances.

➡ At large distances, quarks are subject to the “confining potential” which grows with r :

$$V(r) \approx \lambda r \quad (r > 1fm) \quad (89)$$

Short distance interactions are associated with the **large** momentum transfer:

$$|\vec{q}| = O(r^{-1}) \quad (90)$$

Lorentz-invariant momentum transfer Q is defined as

$$Q^2 = \vec{q}^2 - E_q^2 \quad (91)$$

In the leading order of QCD, α_s is given by

$$\alpha_s = \frac{12\pi}{(33 - 2N_f) \ln(Q^2 / \Lambda^2)} \quad (92)$$

Here N_f is the number of allowed quark flavours, and $\Lambda \approx 0.2$ GeV is the QCD scale parameter which has to be defined experimentally.

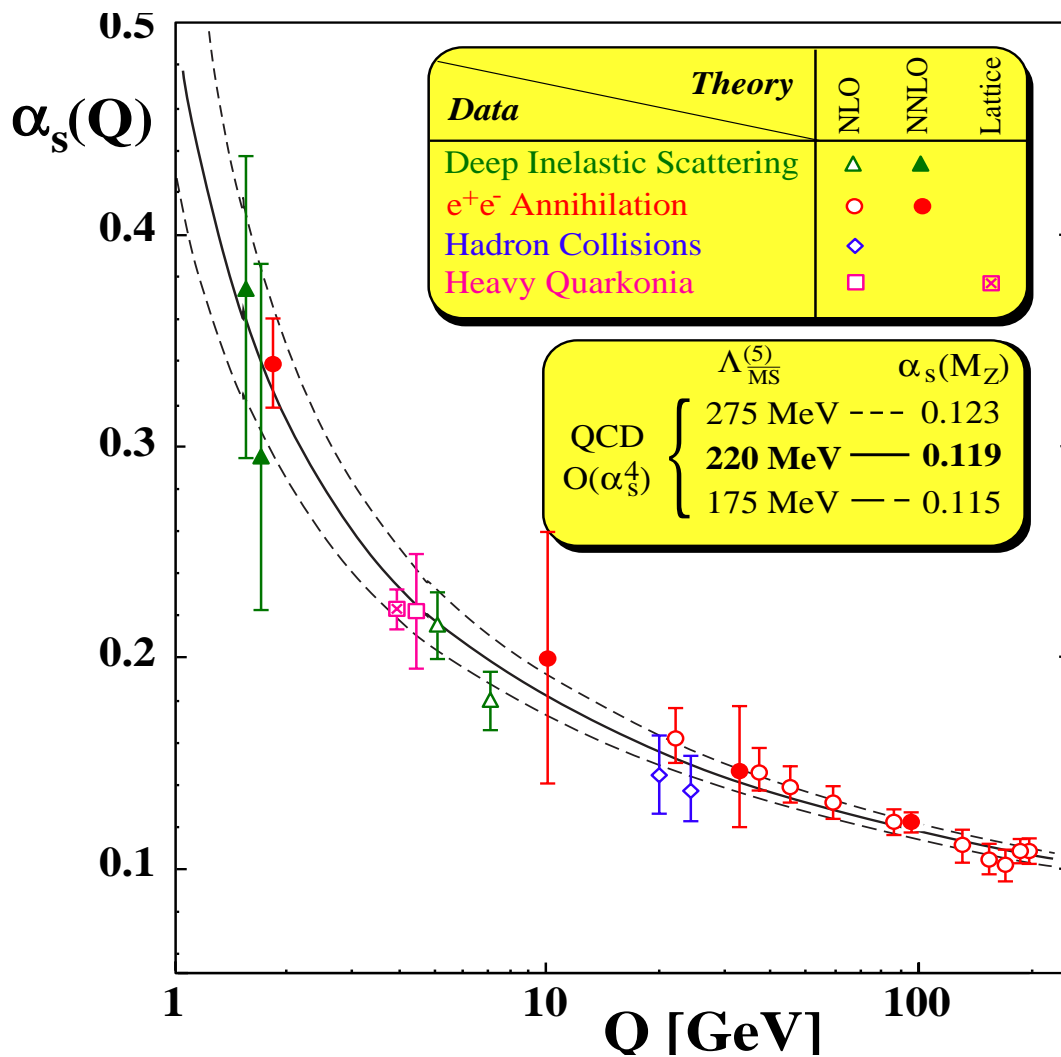


Figure 60: Running of α_s

Electron-positron annihilation

A clean laboratory to study QCD:

$$e^+ + e^- \rightarrow \gamma^* \rightarrow \text{hadrons} \quad (93)$$

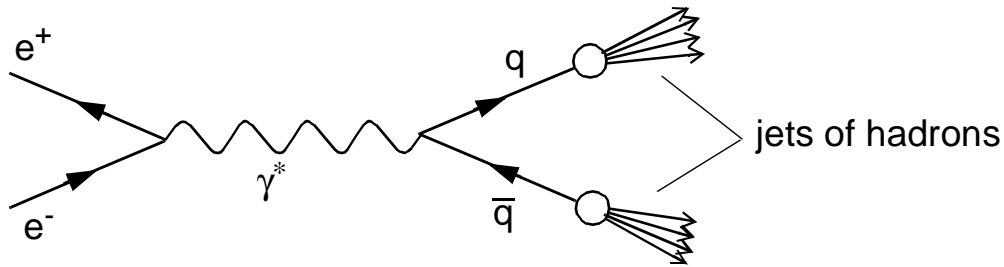


Figure 61: e^+e^- annihilation into hadrons

- At energies between 15 GeV and 40 GeV, e^+e^- annihilation produces a photon which converts into a quark-antiquark pair
- Quark and antiquark *fragment* into observable hadrons
- Since quark and antiquark momenta are equal and counterparallel, hadrons are produced in two opposing *jets* of equal energies
- Direction of a jet reflects direction of a corresponding quark

Comparison of the process (93) with the reaction

$$e^+ + e^- \rightarrow \gamma^* \rightarrow \mu^+ + \mu^- \quad (94)$$

must show the same angular distribution both for muons and jets:

$$\frac{d\sigma}{d\cos\theta}(e^+e^- \rightarrow \mu^+\mu^-) = \frac{\pi\alpha^2}{2Q^2}(1 + \cos^2\theta) \quad (95)$$

where θ is the production angle with respect to the initial electron direction in CM frame.

For a quark-antiquark pair,

$$\frac{d\sigma}{d\cos\theta}(e^+e^- \rightarrow q\bar{q}) = 3e_q^2 \frac{d\sigma}{d\cos\theta}(e^+e^- \rightarrow \mu^+\mu^-) \quad (96)$$

where the fractional charge of a quark e_q is taken into account and factor 3 arises from number of colours.

▮▮▮▮ If quarks have spin 1/2, angular distribution of jets goes like $(1+\cos^2\theta)$; if quarks have spin 0 – like $(1-\cos^2\theta)$

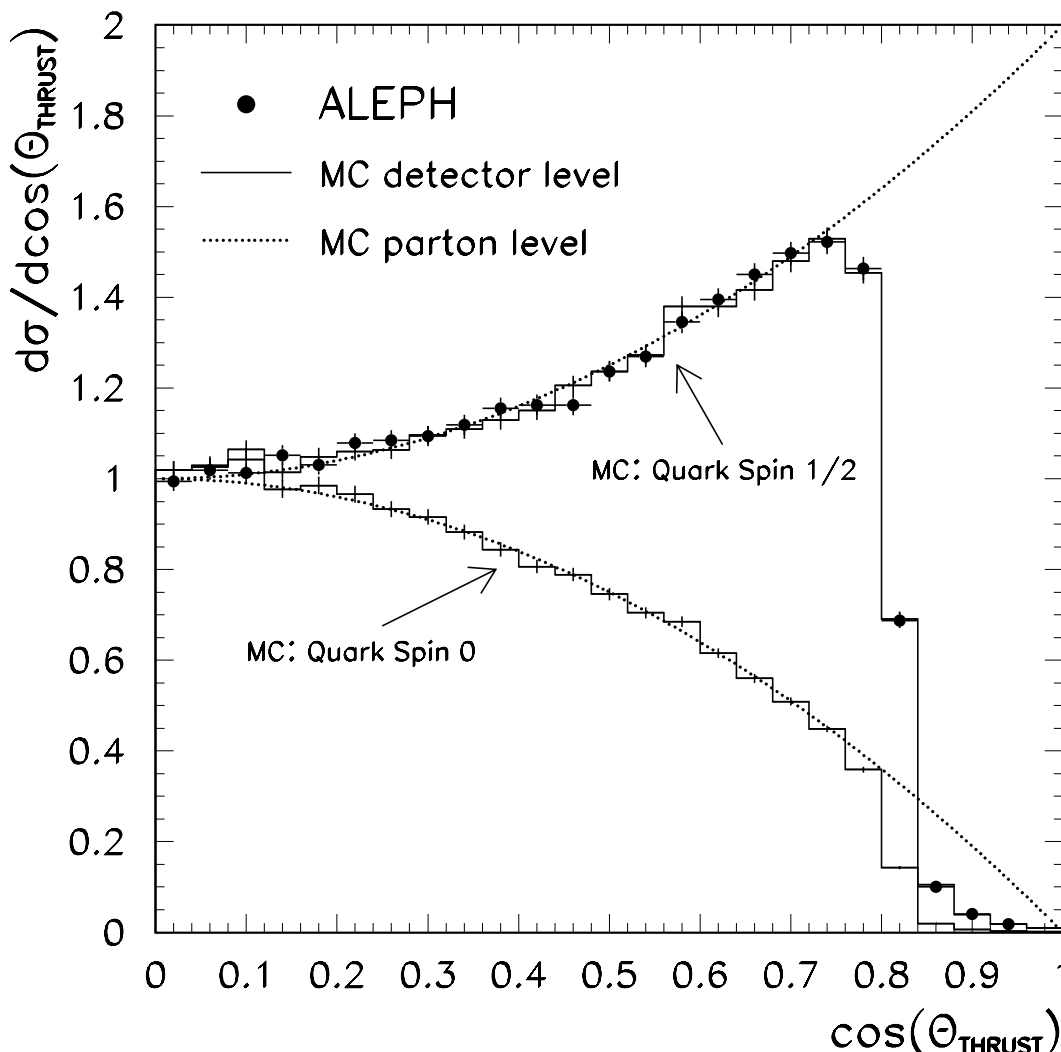


Figure 62: Angular distribution of the quark jet in e^+e^- annihilation, compared with models

Experimental angular dependence is clearly proportional to $(1+\cos^2\theta) \Rightarrow$ jets are aligned with spin-1/2 quarks

►►► If a high-momentum (hard) gluon is emitted by a quark or antiquark, it fragments to a jet of its own, which leads to a three-jet event:

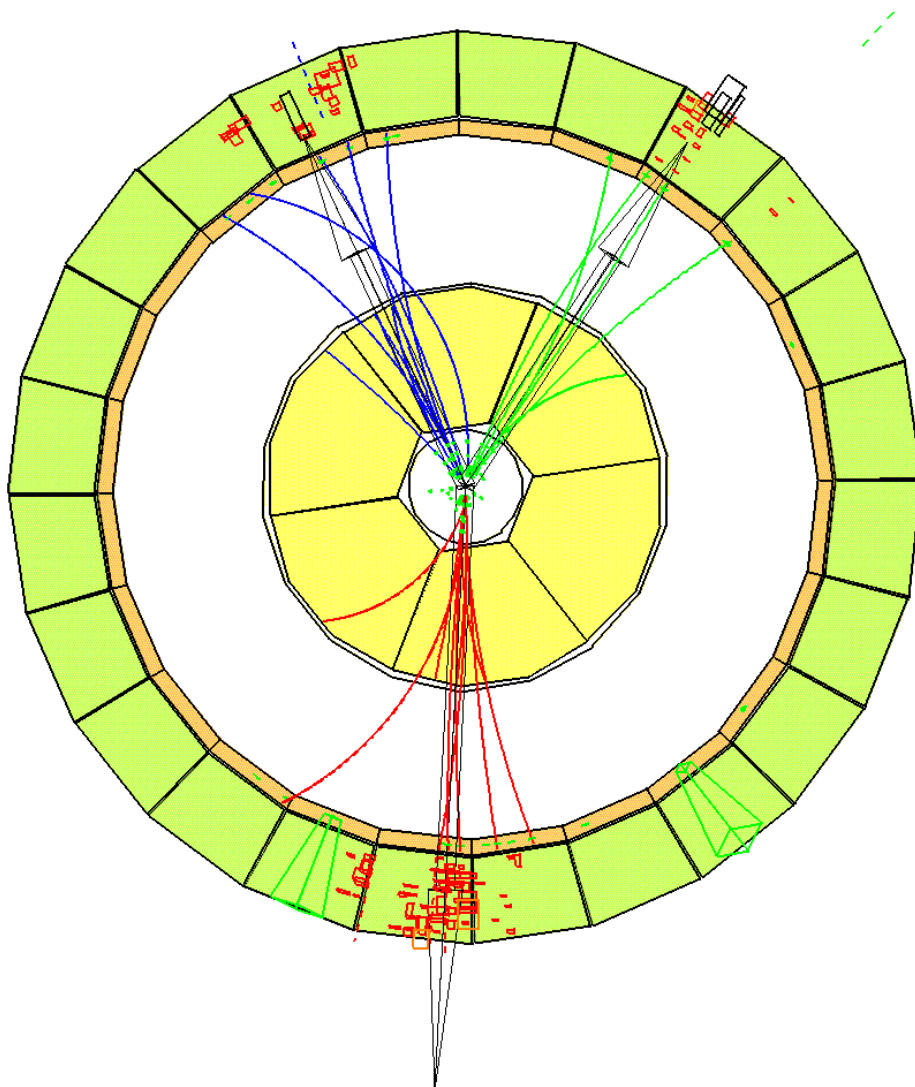


Figure 63: A three-jet event in e^+e^- annihilation as seen by the DELPHI detector

❖ In three-jet events, it is difficult to distinguish which jet belongs to the gluon, hence a specific sensitive variable has to be chosen

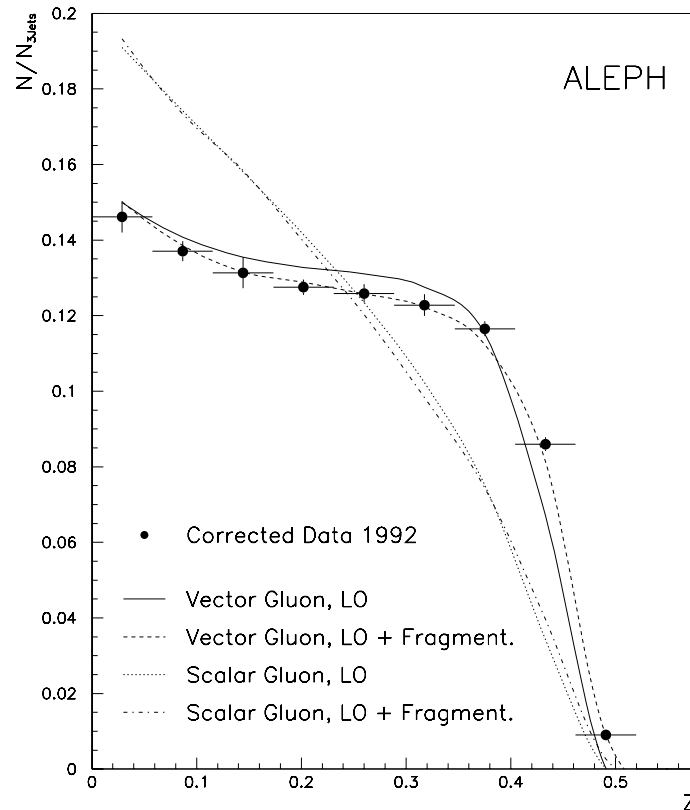


Figure 64: Distribution of Z (as in Eq.(97)) in 3-jet e^+e^- annihilation events, compared with models

A standard procedure is to measure relative jet energies $E_1 > E_2 > E_3$, and define

$$Z = \frac{1}{\sqrt{3}}(E_2 - E_3) \quad (97)$$

since the most energetic jet has to belong to a quark

Angular distributions of jets confirm models where quarks are spin-1/2 fermions and gluons are spin-1 bosons

Observed rate of three-jet and two-jet events can be used to determine value of α_s (probability for a quark to emit a gluon is determined by α_s):

$$\alpha_s = 0.15 \pm 0.03 \quad \text{for } E_{CM} = 30 \text{ to } 40 \text{ GeV}$$

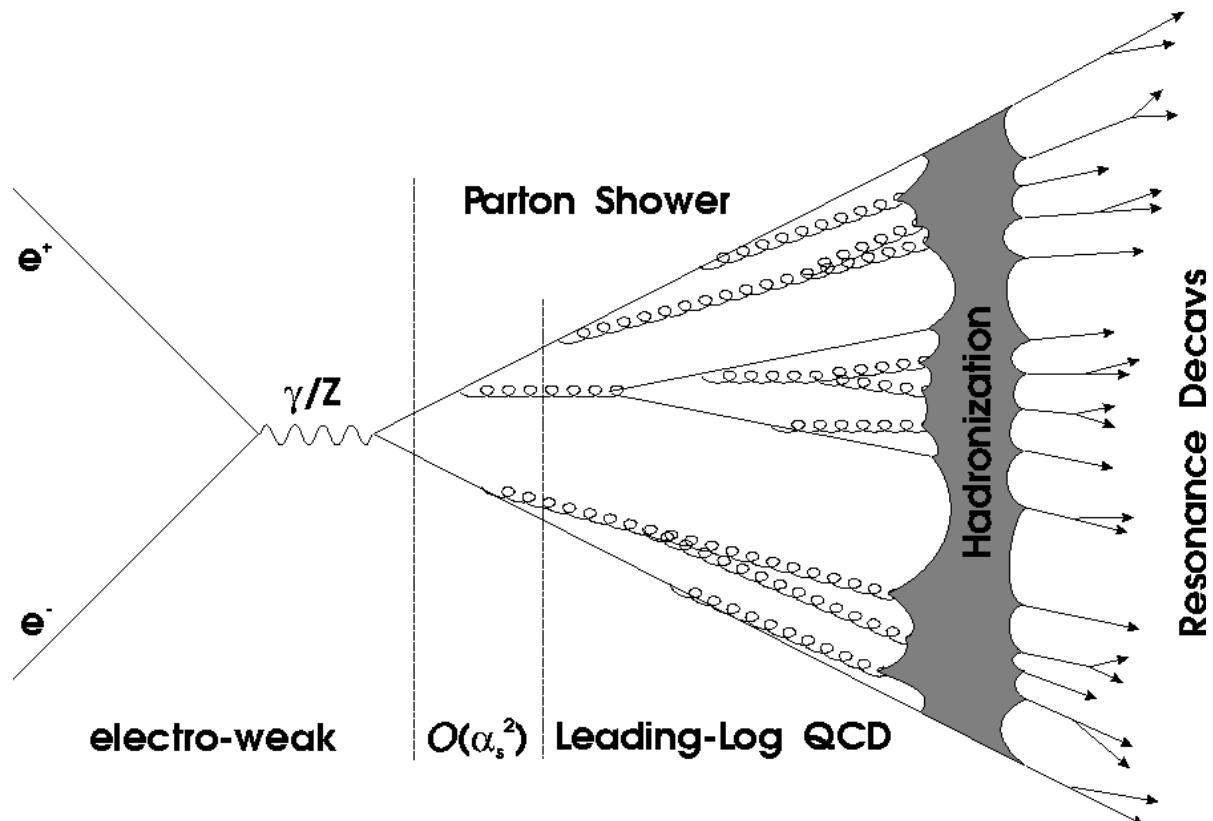


Figure 65: Principal scheme of hadroproduction in e^+e^- annihilation. Hadronization (=fragmentation) begins at distances of order 1 fm between partons

The total cross-section of $e^+e^- \rightarrow \text{hadrons}$ is often expressed as in Eq.(66):

$$R \equiv \frac{\sigma(e^+e^- \rightarrow \text{hadrons})}{\sigma(e^+e^- \rightarrow \mu^+\mu^-)} \quad (98)$$

where the denominator is (see also Eq.(65))

$$\sigma(e^+e^- \rightarrow \mu^+\mu^-) = \frac{4\pi\alpha^2}{3Q^2} \quad (99)$$

Using the same argumentation as in Eq.(96), and assuming that the main contribution comes from quark-antiquark two-jet events,

$$\begin{aligned} \sigma(e^+e^- \rightarrow \text{hadrons}) &= \sum_q \sigma(e^+e^- \rightarrow q\bar{q}) = \\ &= 3 \sum_q e_q^2 \sigma(e^+e^- \rightarrow \mu^+\mu^-) \end{aligned} \quad (100)$$

and hence

$$R = 3 \sum_q e_q^2 \quad (101)$$

❖ R is a good probe for both number of colours in QCD and number of quark flavours allowed to be produced at a given Q : from Eq.(101) it follows that:

$$R(u,d,s)=2 ; R(u,d,s,c)=10/3 ; R(u,d,s,c,b)=11/3$$

If the radiation of hard gluons is taken into account, the extra factor proportional to α_s arises:

$$R = 3 \sum_q e_q^2 \left(1 + \frac{\alpha_s(Q^2)}{\pi} \right) \tag{102}$$

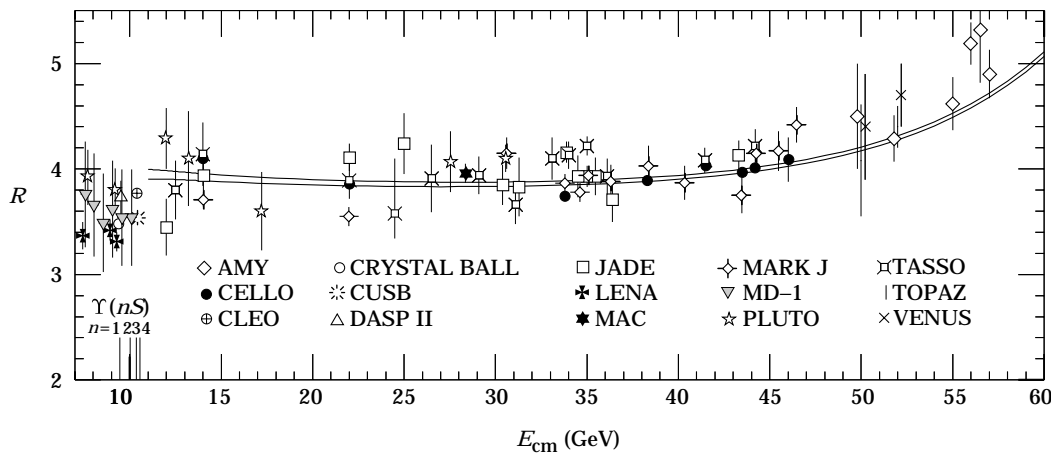


Figure 66: Measured R (Eq.(98)) with theoretical predictions for five available flavours (u,d,s,c,b), using two different α_s calculations

Elastic electron scattering

- ▣▣▣▣ Beams of structureless leptons are a good tool for investigating properties of hadrons
- ▣▣▣▣ Elastic lepton-hadron scattering can be used to measure sizes of hadrons

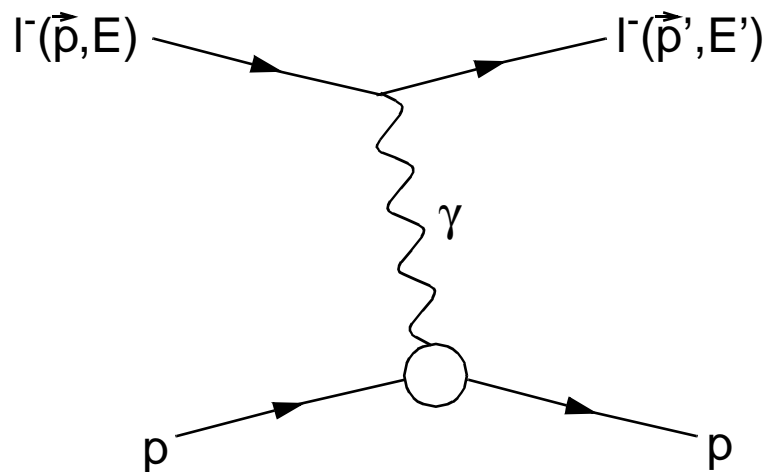


Figure 67: Dominant one-photon exchange mechanism for elastic lepton-proton scattering

Angular distribution of an electron of momentum p scattered by a static electric charge e is described by the Rutherford formula:

$$\left(\frac{d\sigma}{d\Omega}\right)_R = \frac{m^2 \alpha^2}{4p^2 \sin^4(\theta/2)} \quad (103)$$

If the electric charge is not point-like, but is spread with a spherically symmetric density distribution, i.e., $e \rightarrow e\rho(r)$, where $\rho(r)$ is normalized:

$$\int \rho(r) d^3\vec{x} = 1$$

then the differential cross-section (103) is replaced by

$$\frac{d\sigma}{d\Omega} = \left(\frac{d\sigma}{d\Omega} \right)_R G_E^2(q^2) \quad (104)$$

where the *electric form factor*

$$G_E(q^2) = \int \rho(r) e^{i\vec{q} \cdot \vec{x}} d^3\vec{x} \quad (105)$$

is the Fourier-transform of $\rho(r)$ with respect to the momentum transfer $\vec{q} = \vec{p} - \vec{p}'$.

– For $q = 0$, $G_E(0) = 1$ (low momentum transfer)

– For $q^2 \rightarrow \infty$, $G_E(q^2) \rightarrow 0$ (large momentum transfer)

❖ Measurements of cross-section (104) determine the form-factor and hence the charge distribution of the proton

The RMS charge radius is given by

$$r_E^2 \equiv \overline{r^2} = \int r^2 \rho(r) d^3\vec{x} = -6 \left. \frac{dG_E(q^2)}{dq^2} \right|_{q^2=0} \quad (106)$$

⇒ In addition to G_E , there is also G_M – the *magnetic form factor*, associated with the magnetic moment distribution within the proton

⇒ At high momentum transfers, the recoil energy of the proton is not negligible, and \vec{q} is replaced by the Lorentz-invariant Q , given by

$$Q^2 = (\vec{p} - \vec{p}')^2 - (E - E')^2 \quad (107)$$

⇒ at high Q , static interpretation of charge and magnetic moment distribution breaks down

⇒ Eq.(106) is valid only for low $Q^2 = q^2$.

Taking into account magnetic moment of the electron itself, and neglecting its mass as compared with energy, one obtains

$$\frac{d\sigma}{d\Omega} = \frac{\alpha^2}{4E^2 \sin^4(\theta/2)} \left(\frac{E'}{E}\right) [G_1(Q^2) \cos^2(\theta/2) + 2\tau G_2(Q^2) \sin^2(\theta/2)] \quad (108)$$

Here

$$G_1(Q^2) = \frac{G_E^2 + \tau G_M^2}{1 + \tau}; \quad G_2(Q^2) = G_M^2; \quad \tau = \frac{Q^2}{4M_p^2}$$

and form factors are normalized so that

$$G_E(0) = 1 \quad \text{and} \quad G_M(0) = \mu_p = 2.79$$

⇒ Experimentally, it is sufficient to measure E' and θ of outgoing electrons in order to derive G_E and G_M using Eq.(108)

Results of proton size measurements are conveniently divided into three Q^2 regions:

- 1) low $Q^2 \Rightarrow \tau$ is very small $\Rightarrow G_E$ dominates the cross-section and r_E can be precisely measured:

$$r_E = 0.85 \pm 0.02 \text{ fm} \quad (109)$$

- 2) intermediate range: $0.02 \leq Q^2 \leq 3 \text{ GeV}^2 \Rightarrow$ both G_E and G_M give sizeable contribution \Rightarrow they can be defined through parameterization:

$$G_E(Q^2) \approx \frac{G_M(Q^2)}{\mu_p} \approx \left(\frac{\beta^2}{\beta^2 + Q^2} \right)^2 \quad (110)$$

with $\beta^2 = 0.84 \text{ GeV}^2$

- 3) high $Q^2 > 3 \text{ GeV}^2 \Rightarrow$ only G_M can be measured accurately

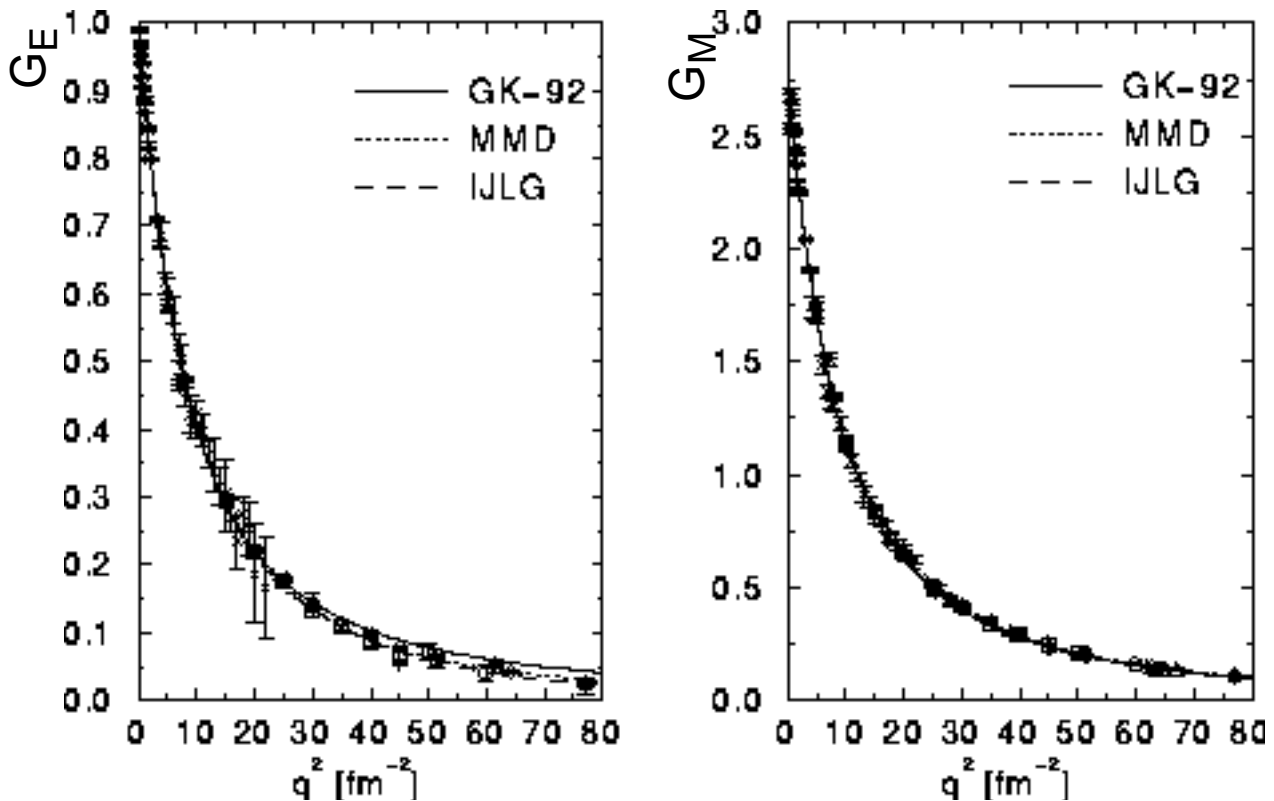


Figure 68: Electric and magnetic proton form-factors, compared with different parameterizations

Inelastic lepton scattering

- ▣ Historically, was first to give evidence of quark constituents of the proton
- ❖ In what follows, only one-photon exchange is considered

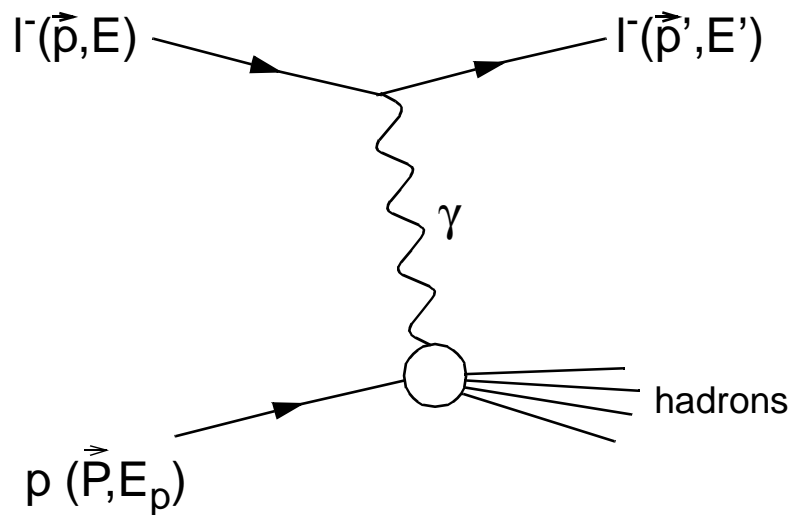


Figure 69: One-photon exchange in inelastic lepton-proton scattering

- The exchanged photon acts as a probe of the proton structure
- The momentum transfer $\vec{p} - \vec{p}'$ corresponds to the photon wavelength which must be **small** enough to probe a proton \Rightarrow **big** momentum transfer is needed
- ❖ When a photon resolves a quark within a proton, the total lepton-proton scattering is a two-step process:

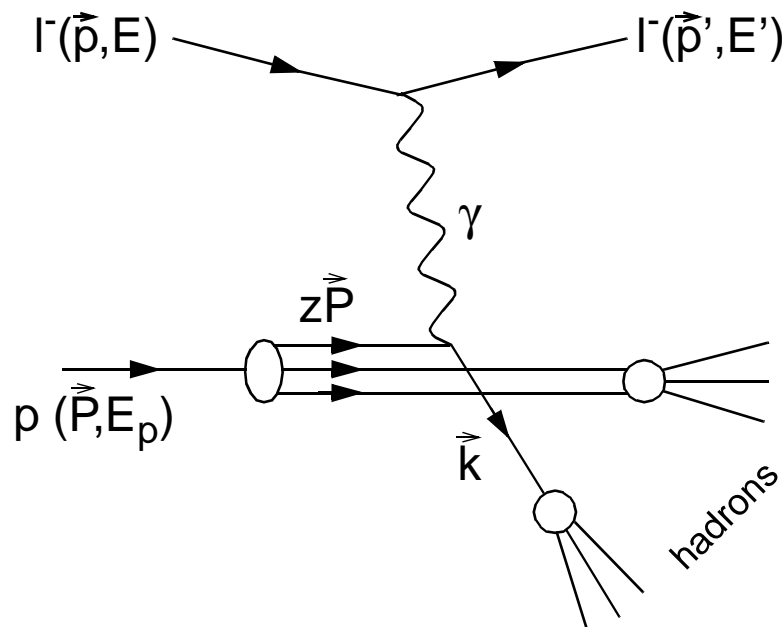


Figure 70: Detailed picture of deep-inelastic lepton-proton scattering

- 1) First step: elastic scattering of the lepton from one of the quarks:

$$l + q \rightarrow l + q \quad (l = e, \mu)$$

- 2) Second step: fragmentation of the recoil quark and the proton remnant into observable hadrons

➡ Angular distributions of recoil leptons reflect properties of quarks from which they scattered

For further studies, some new variables have to be defined:

– Lorentz-invariant generalization for the transferred energy ν , defined by:

$$2M_p \nu \equiv W^2 + Q^2 - M_p^2 \quad (111)$$

where W is the invariant mass of the final hadron state; in the rest frame of the proton $\nu = E - E'$

– Dimensionless scaling variable x :

$$x \equiv \frac{Q^2}{2M_p \nu} \quad (112)$$

For $Q \gg M_p$ and a very large proton momentum $\vec{P} \gg M_p$, x is the fraction of the proton momentum carried by the struck quark; $0 \leq x \leq 1$

⇒ Energy E' and angle θ of scattered lepton are independent variables, describing inelastic process

$$\frac{d\sigma}{dE' d\Omega'} = \frac{\alpha^2}{4E^2 \sin^4(\theta/2)} \frac{1}{v} [\cos^2(\theta/2) F_2(x, Q^2) + \sin^2(\theta/2) \frac{Q^2}{xM_p^2} F_1(x, Q^2)] \quad (113)$$

❖ Form (113) is a generalization of the elastic scattering formula (108)

❖ *Structure functions* F_1 and F_2 parameterize the interaction at the quark-photon vertex (just like G_1 and G_2 parameterized the elastic scattering)

⇒ Bjorken scaling:

$$F_{1,2}(x, Q^2) \approx F_{1,2}(x) \quad (114)$$

At $Q \gg M_p$, structure functions are approximately independent on Q^2 .

❖ If all particle masses, energies and momenta are multiplied by a scale factor, structure functions at any given x remain unchanged

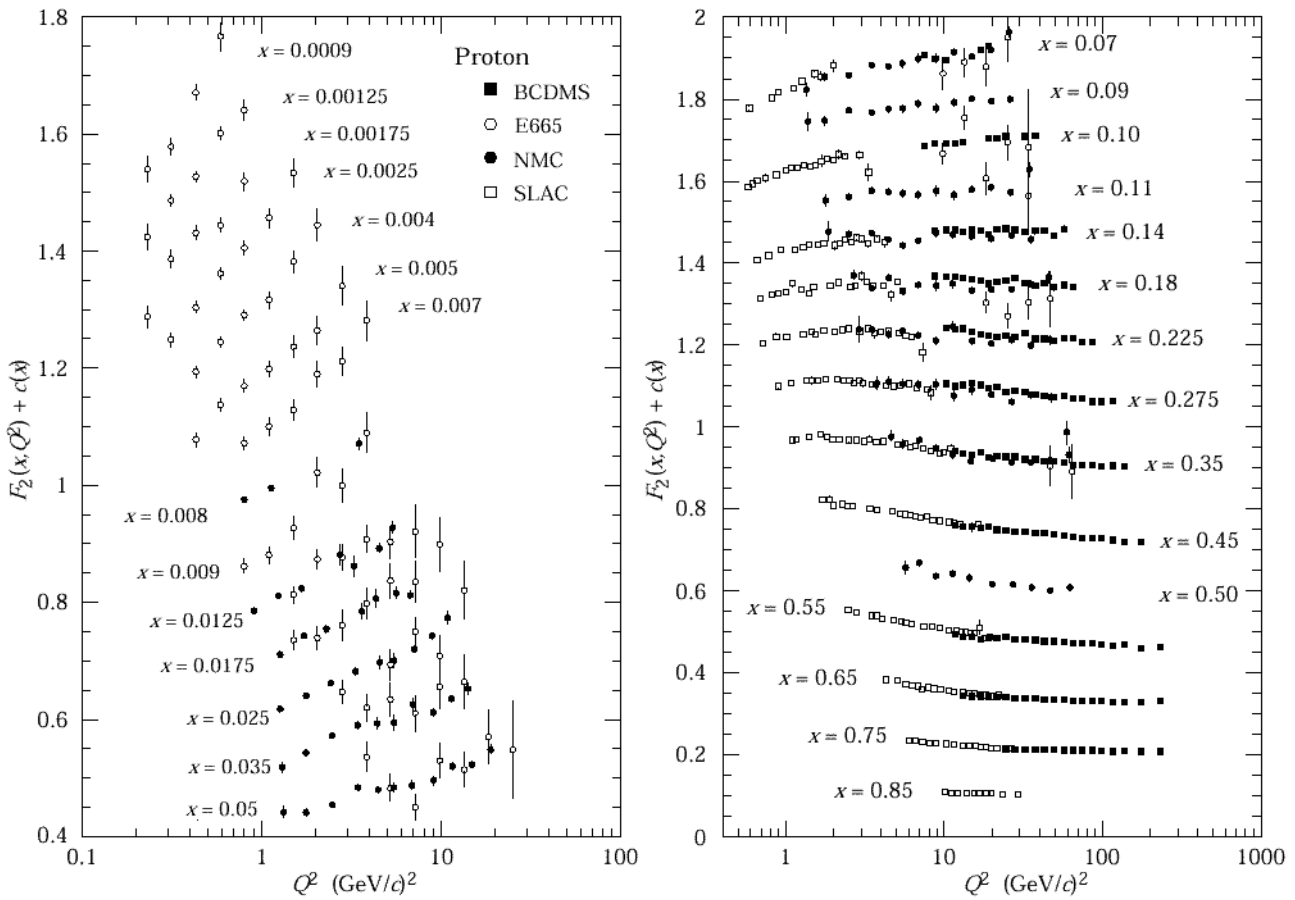


Figure 71: Structure functions F_2 of proton from different experiments

- ▣▣▣▣▣ SLAC data from '69 were first evidence of quarks
- ▣▣▣▣▣ Scaling violation is observed at very small and very big x

- ▣▣▣▣➔ The approximate scaling behaviour can be explained if protons are considered as composite objects
- ▣▣▣▣➔ The trivial *parton model*: proton consists of some partons; interactions between partons are not taken into account.

The parton model can be valid if the target proton has a sufficiently big momentum, so that

$$z = x$$

- ❖ Measured cross-section at any given x is proportional to the probability of finding a parton with a fraction $z=x$ of the proton momentum

If there are several partons,

$$F_2(x, Q^2) = \sum_a e_a^2 x f_a(x) \quad (115)$$

where $f_a(x)dx$ is the probability of finding parton a with fractional momentum between x and $x+dx$.

❖ Parton distributions $f_a(x)$ are not known theoretically $\Rightarrow F_2(x)$ has to be measured experimentally

While form (115) does not depend on the spin of a parton, predictions for F_1 do:

$$\begin{aligned}
 F_1(x, Q^2) &= 0 && (\text{spin-0}) \\
 2xF_1(x, Q^2) &= F_2(x, Q^2) && (\text{spin-1/2})
 \end{aligned}
 \tag{116}$$

❖ The expression for spin-1/2 is called *Callan-Gross relation* and is very well confirmed by experiments \Rightarrow most evidently partons are quarks.

❖ Comparing proton and neutron structure functions and those from neutrino scattering, squared charge e_a^2 of Eq.(115) can be evaluated; it appears to be consistent with square charges of quarks.

VIII. Weak Interactions: W and Z bosons

- ▣▣▣▣ Like in QED and QCD, the force carriers are spin-1 bosons that couple to quarks and leptons
- ▣▣▣▣ Force carriers of weak interactions are three *intermediate vector bosons*: W^+ and W^- (mass 80.4 GeV), and Z^0 (91.2 GeV)
- ▣▣▣▣ W^+ , W^- and Z^0 bosons are **very massive** particles, hence weak interactions have very short range (order of 2×10^{-3} fm)
 - ❖ Before the Electroweak Theory was developed, all observed weak processes were *charged current* reactions (e.g. β -decay) mediated by W^+ or W^- bosons
 - ❖ Electroweak theory predicted a *neutral current* caused by the Z^0 boson

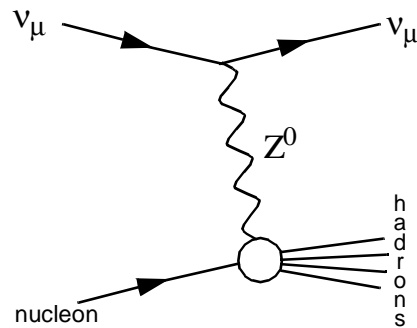


Figure 72: Predicted neutral current reaction: no muon in final state

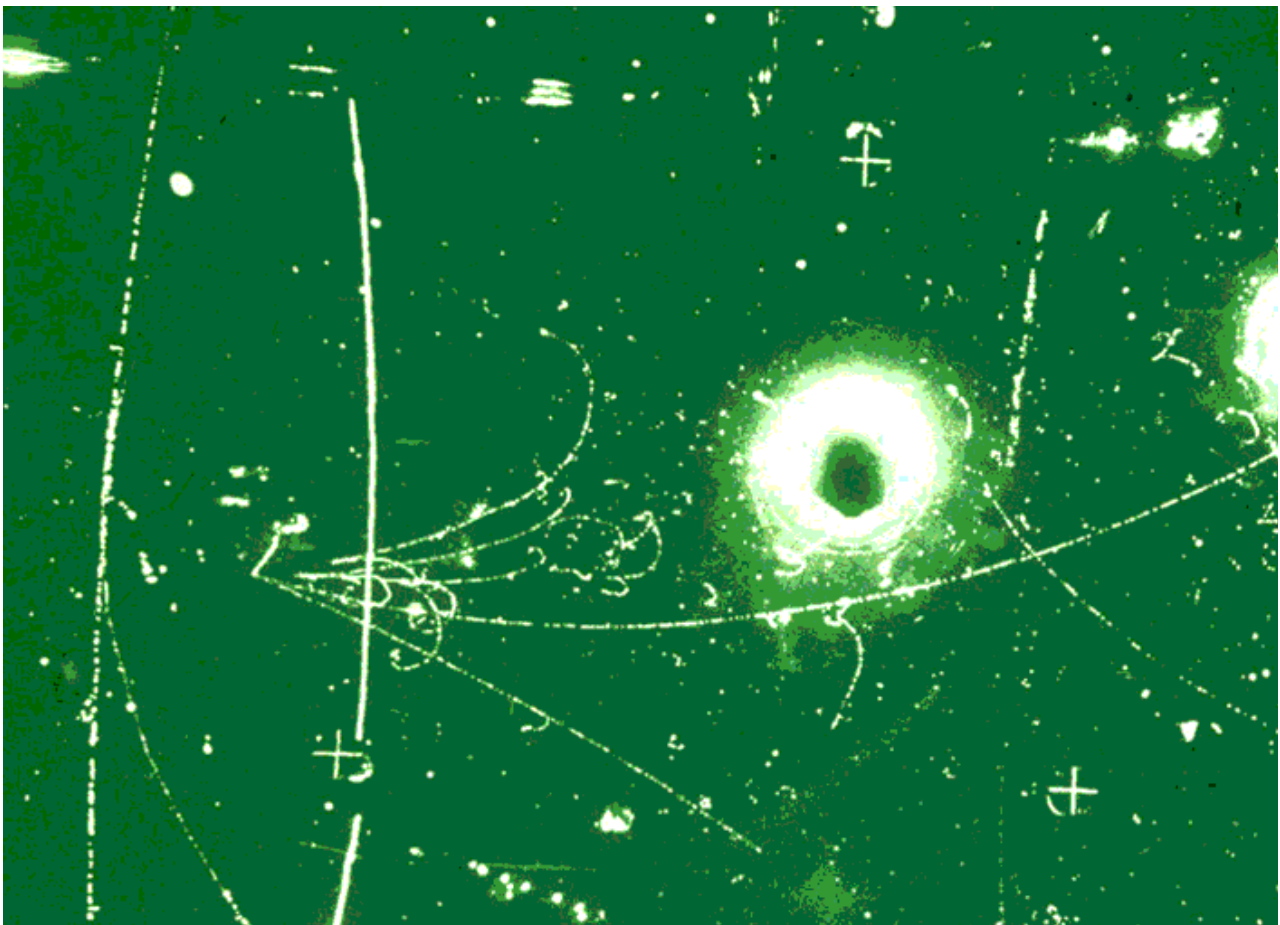


Figure 73: One of the first neutral current reactions as seen by the Gargamelle bubble chamber in 1973

First dedicated experiment to study vector bosons:
SPS proton-antiproton collider at CERN (detectors
UA1 and UA2):

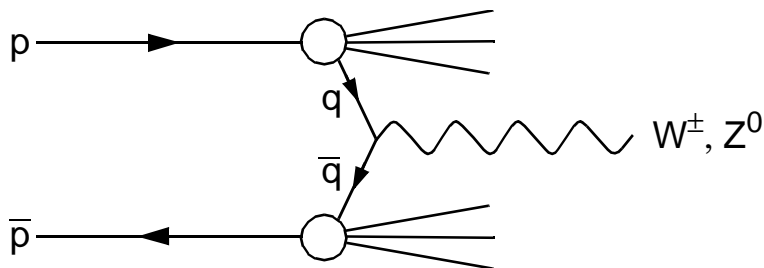
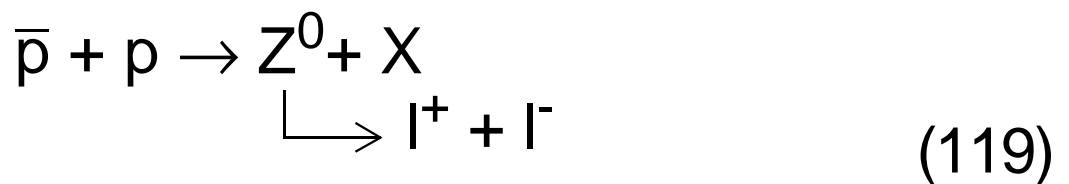
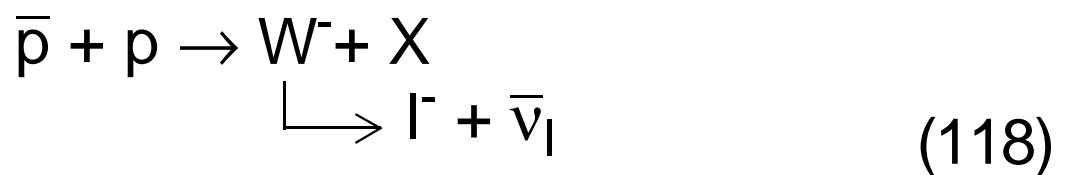
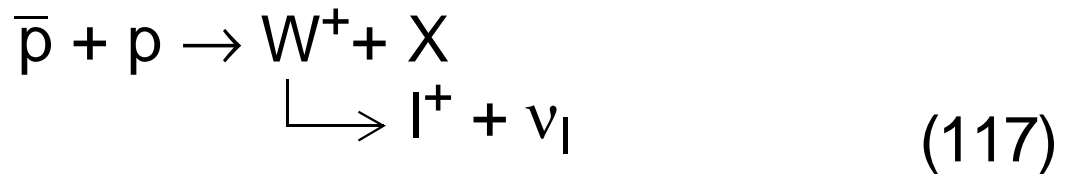


Figure 74: Mechanism of W^\pm and Z production in $p\bar{p}$ annihilation

From the quark point of view, processes (117)-(119) are quark-antiquark annihilations:

$$u + \bar{d} \rightarrow W^+ , \quad d + \bar{u} \rightarrow W^- \quad (120)$$

$$u + \bar{u} \rightarrow Z^0 , \quad d + \bar{d} \rightarrow Z^0 \quad (121)$$

To obtain sufficient centre-of-mass energies, proton and antiproton beams at SPS had energy of 270 GeV each.

W bosons

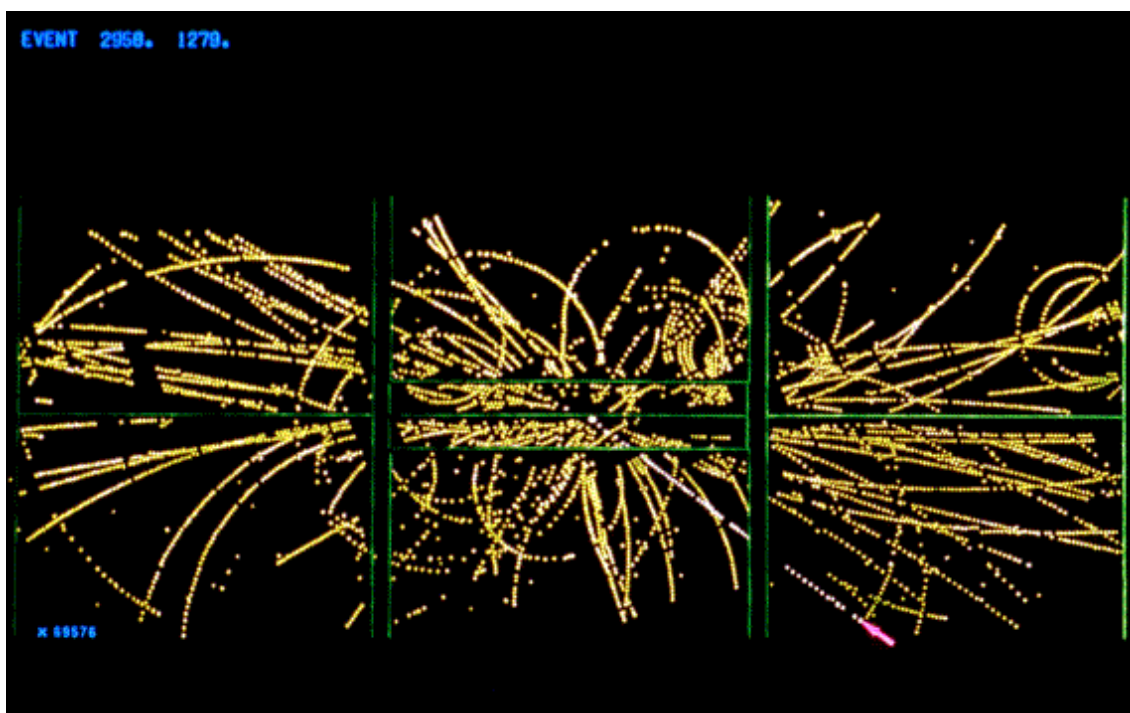


Figure 75: A W boson observed by UA1 detector in 1982; high transverse momentum electron is arrowed

▣▣▣▣➔ Signature of a W boson:

- a lepton with large momentum ($>10 \text{ GeV}/c$)
- emitted at a wide angle to the beam ($>5^\circ$)
- large “*missing transverse momentum*” carried out by neutrino

If $p_T(W)=0 \Rightarrow \cancel{p}_T = p_T(l)$: the missing transverse momentum is equal to the transverse momentum of the detected lepton

From 43 events observed by UA1, the mass of W^+ and W^- was defined as

$$M_W = 80.33 \pm 0.15 \text{ GeV}/c^2 \quad (122)$$

and the decay width as

$$\Gamma_W = 2.07 \pm 0.06 \text{ GeV} \quad (123)$$

which corresponds to a lifetime of $3.2 \times 10^{-25} \text{ s}$

Branching ratios of leptonic decay modes of W^\pm are about 11% for each lepton generation

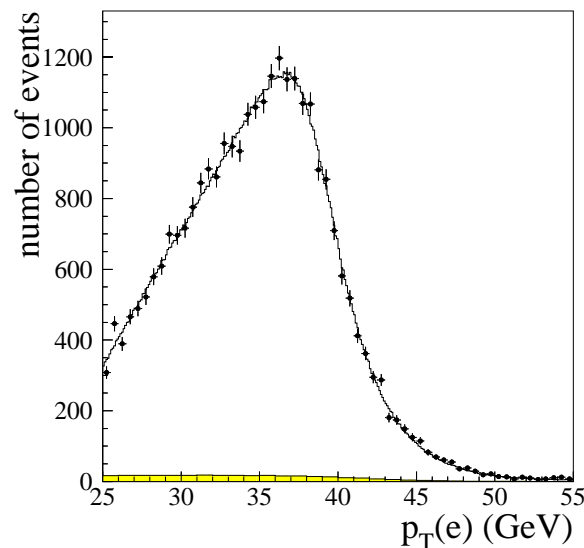


Figure 76: Recent result from the D0 experiment at the Tevatron; fit gives $M_W = 80.48 \pm 0.09$ GeV

W bosons can be pair-produced in e^+e^- annihilation, and the up-to-date world average for the W mass is

$$M_W = 80.39 \pm 0.06 \text{ GeV}/c^2 \quad (124)$$

Z^0 boson

- ▣▣▣▣➔ Signature of a Z^0 boson in $p\bar{p}$ collision: pair of leptons (e^+e^-) with very large momenta.
- ▣▣▣▣➔ Mass of the Z^0 is then invariant mass of leptons

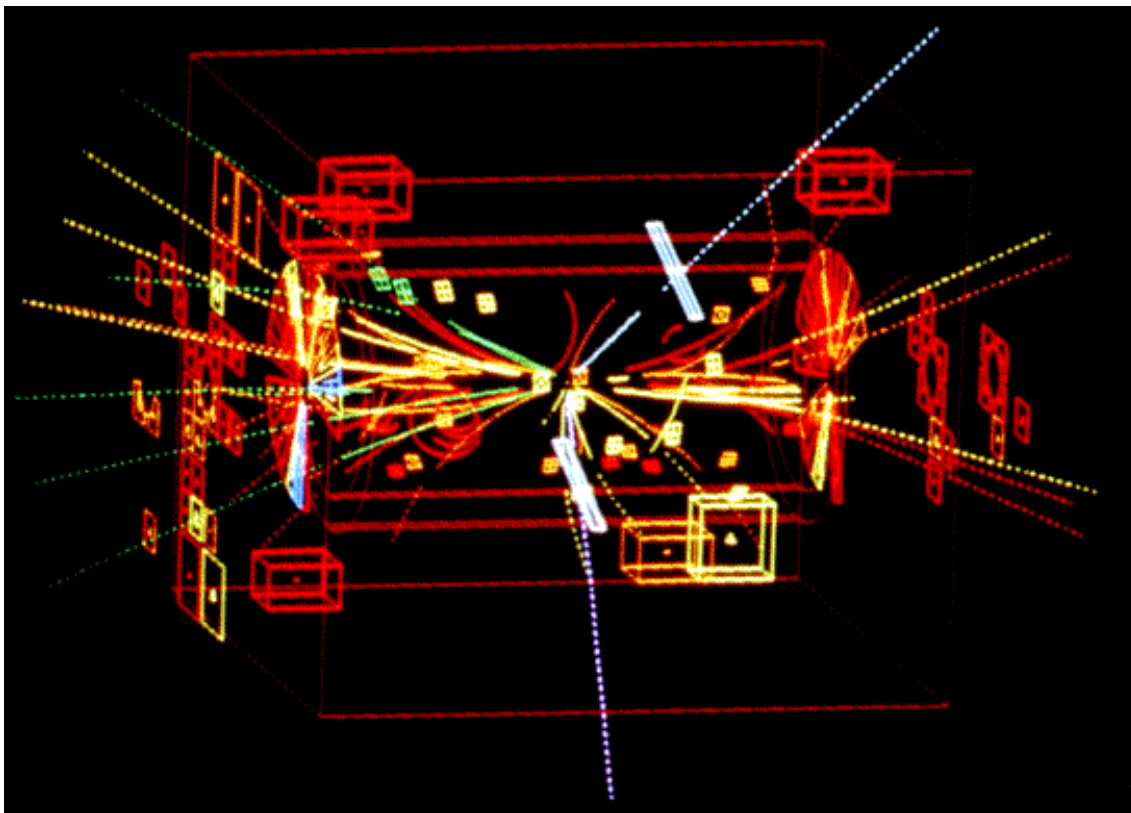


Figure 77: Z^0 production event in UA1 detector.

Knowing M_W , M_Z was predicted to be $\approx 90 \text{ GeV}/c^2$

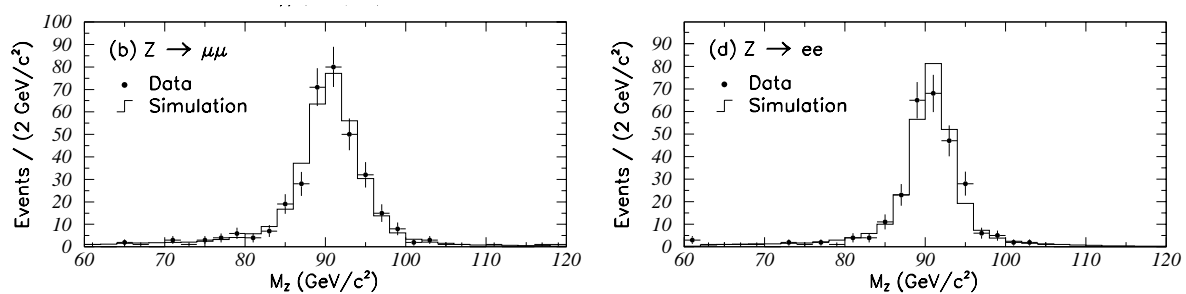


Figure 78: Dilepton mass spectra near the Z^0 peak as measured by the CDF collaboration

More precise methods give world average values of

$$M_Z = 91.187 \pm 0.007 \text{ GeV}/c^2 \quad (125)$$

$$\Gamma_Z = 2.490 \pm 0.007 \text{ GeV}/c^2 \quad (126)$$

which corresponds to a lifetime of 2.6×10^{-25} s.

Branching ratios of leptonic decay modes of Z^0 are around 3.4% for each lepton generation

Charged current reactions

1) purely *leptonic* processes:

$$\mu^- \rightarrow e^- + \bar{\nu}_e + \nu_\mu \quad (127)$$

2) purely hadronic processes:

$$\Lambda \rightarrow \pi^- + p \quad (128)$$

3) *semileptonic* reactions:

$$n \rightarrow p + e^- + \bar{\nu}_e \quad (129)$$

Recall: all the electromagnetic interactions can be built from eight basic interactions:

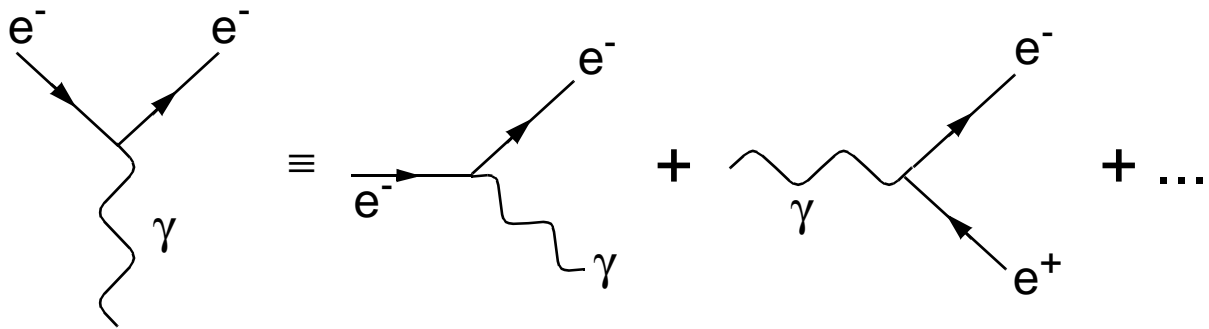


Figure 79: The basic vertex for electron-photon interactions

In a similar way, leptonic weak interaction processes can be built from a certain number of reactions corresponding to basic vertices:

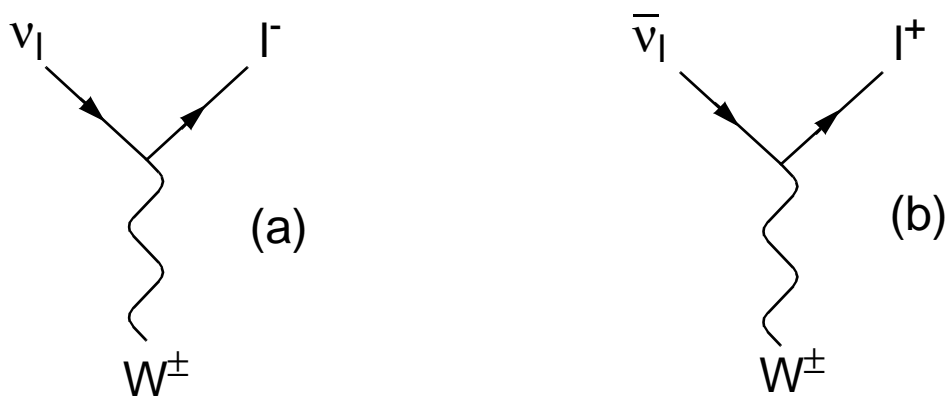


Figure 80: The two basic vertices for W^\pm -lepton interactions

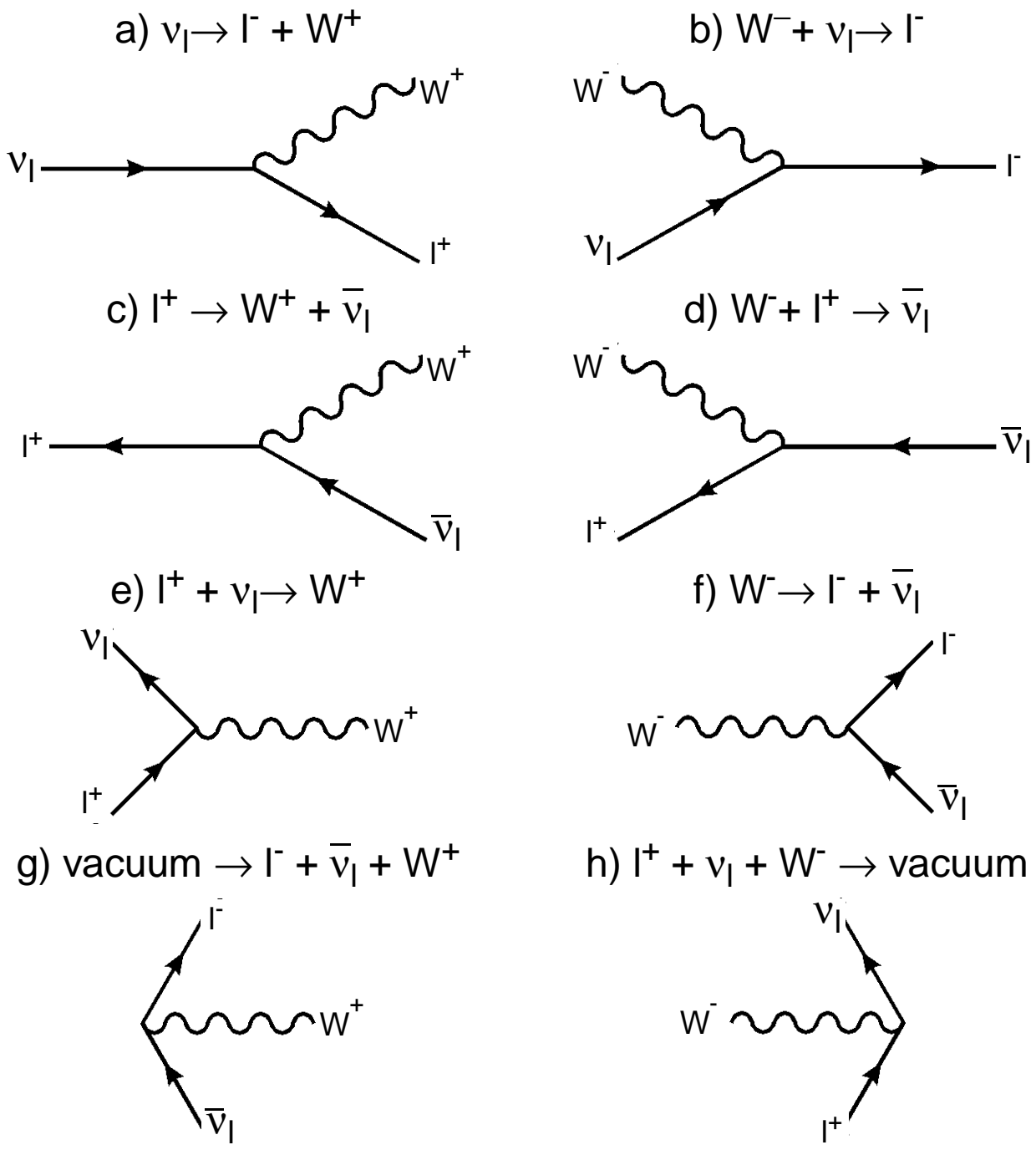


Figure 81: Eight basic reactions derived from the vertex of Fig.80(a)

Analogous diagrams can be plotted for Fig.80(b) simply replacing particles with antiparticles

Weak interactions always conserve lepton quantum numbers

Diagram-wise this conservation is guaranteed by:

- at each vertex, there is one arrow pointing in and one pointing out
- lepton indices “l” are the same on both lines

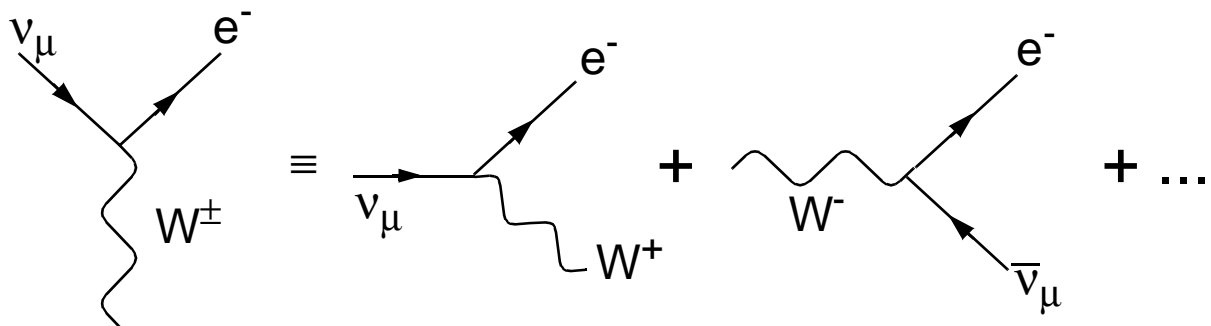


Figure 82: Vertices **violating** lepton number conservation

- ❖ Processes of Fig.81 are virtual, so that two or more have to be combined to conserve energy
- ❖ However, processes like 81(e) and 81(f) do not violate energy conservation if

$$M_W > M_l + M_{\nu_l} \quad (l = e, \mu, \tau)$$

❖ In particular, reactions (117) and (118), used to detect the W bosons, are dominated by mechanisms like of Fig.81(e) and (f).

▣▣▣▣ Leptonic vertices are characterized by the corresponding strength parameter α_W independently on lepton type involved

Knowing the decay rate of $W \rightarrow e\nu$, one can estimate α_W to the first order:

$$\Gamma(W \rightarrow e\nu) \approx 0.2 \text{ GeV} \quad (130)$$

Since the process involves only one vertex and lepton masses are negligible \Rightarrow

$$\Gamma(W \rightarrow e\nu) \approx \alpha_W M_W \approx 80\alpha_W \text{ GeV} \quad (131)$$

which gives

$$\alpha_W \approx 1/400 = O(\alpha) \quad (132)$$

hence the strength of the weak interaction is comparable with the e.m. one

Analogues of electron-electron scattering by photon exchange:

$$\nu_\mu + e^- \rightarrow \mu^- + \nu_e \tag{133}$$

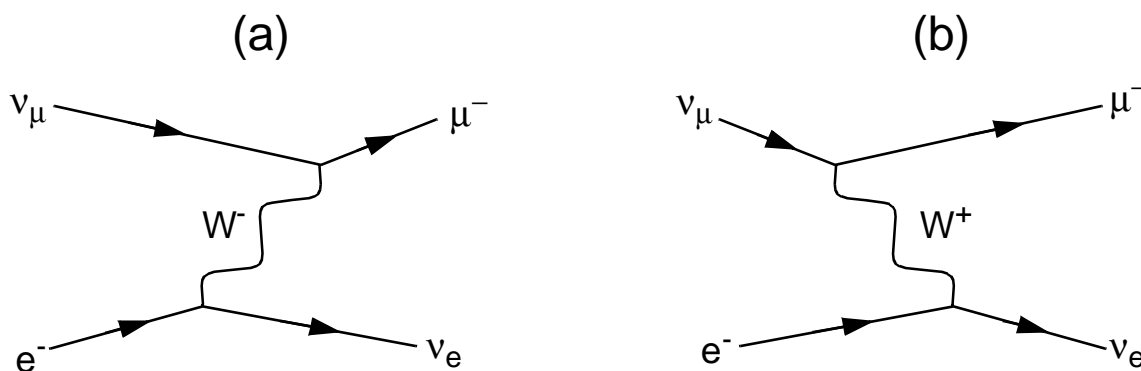


Figure 83: Time-ordered diagrams for inverse muon decay (133)

Time ordering implies changing the sign of the current!

A conventional muon decay is depicted like:

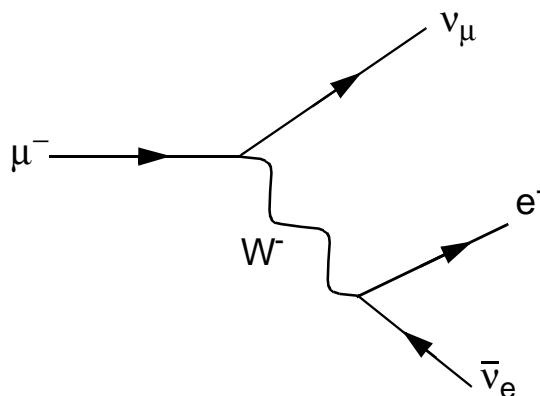


Figure 84: Dominant diagram for muon decay

Including higher order diagrams, inverse muon decay (133) can look like:

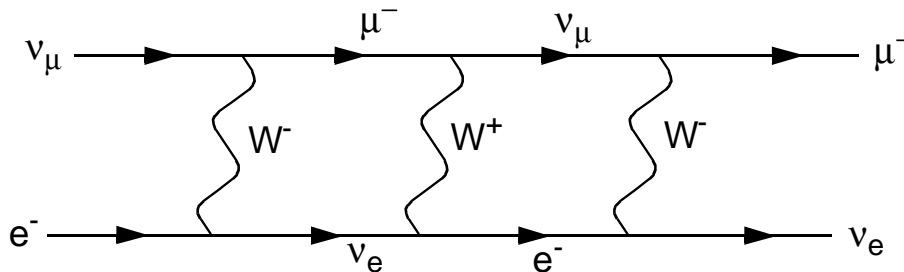


Figure 85: Some higher order contributions to inverse muon decay

❖ A diagram like Fig.86 gives a contribution of order α_W^6 to the total cross section, analogously to the e.m. case.

Since W bosons are very heavy, interactions like (133) can be approximated by a zero-range interaction:

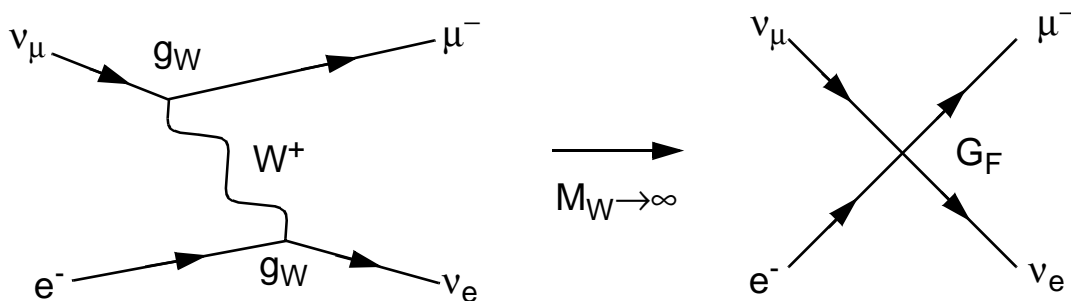


Figure 86: Low-energy zero-range interaction in muon decay

Taking into account spin effects, the relation between α_W and G_F in zero-range approximation is:

$$\frac{G_F}{\sqrt{2}} = \frac{g_W^2}{M_W^2} = \frac{4\pi\alpha_W}{M_W^2} \quad (134)$$

where g_W is the coupling constant in W-vertices, $\alpha_W \equiv g_W^2/4\pi$ by definition.

This gives the estimate of $\alpha_W = 4.2 \times 10^{-3} = 0.58\alpha$, which is perfectly compatible with estimate (132).

❖ Weak interactions of hadrons: constituent quarks emit or absorb W bosons

➡ **Lepton-quark symmetry**: corresponding generations of quarks and leptons have identical weak interactions:

$$\begin{pmatrix} \nu_e \\ e^- \end{pmatrix} \leftrightarrow \begin{pmatrix} u \\ d \end{pmatrix}, \quad \begin{pmatrix} \nu_\mu \\ \mu^- \end{pmatrix} \leftrightarrow \begin{pmatrix} c \\ s \end{pmatrix}, \quad \text{etc.}$$

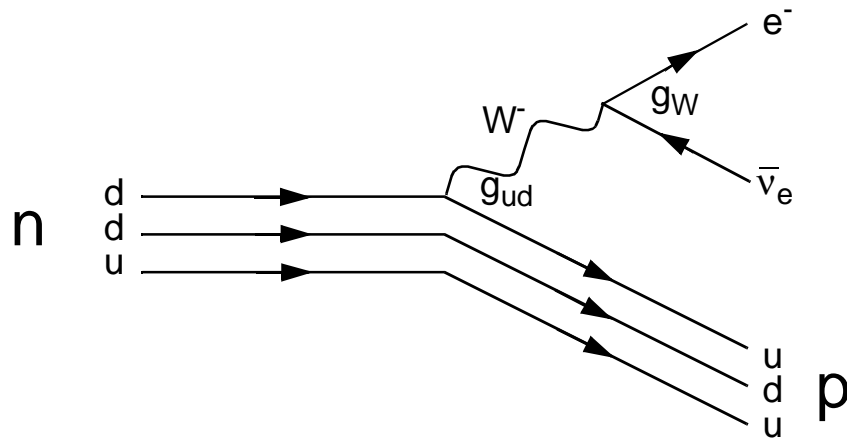


Figure 87: Neutron β -decay

The corresponding coupling constants do not change upon exchange of quarks/leptons:

$$g_{ud} = g_{cs} = g_W \tag{135}$$

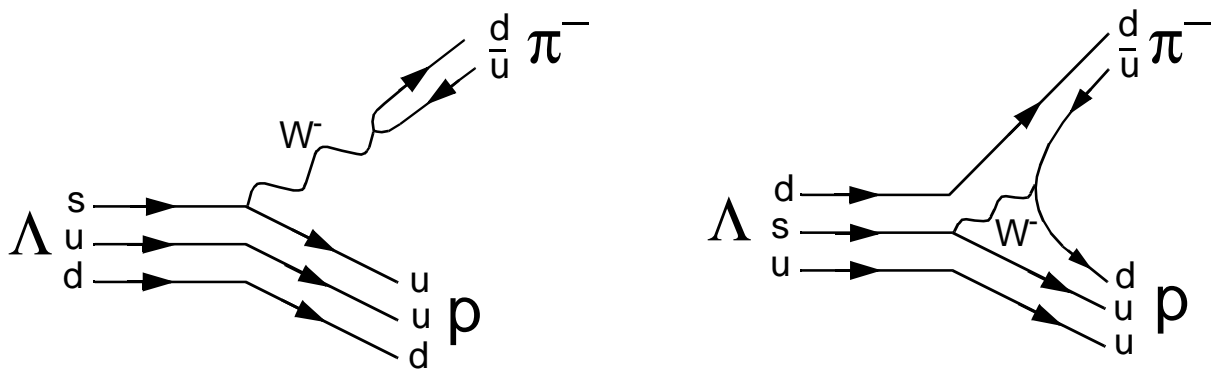


Figure 88: Dominant quark diagrams for Λ decay

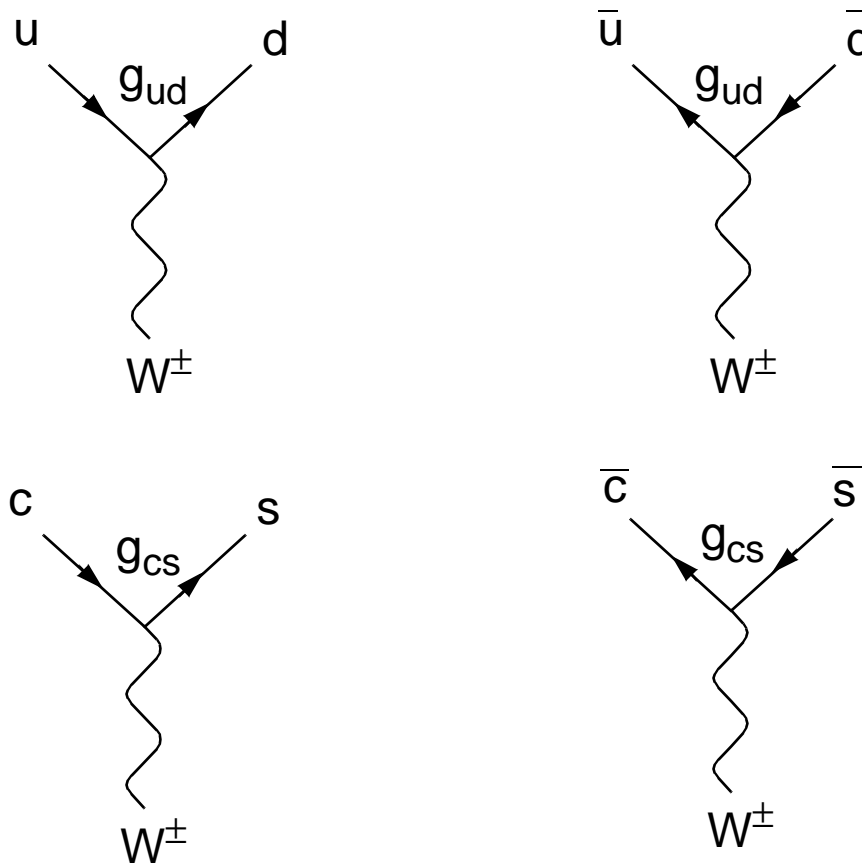


Figure 89: W-quark vertices assumed by lepton-quark symmetry

For example, allowed reaction is:

$$\pi^- \rightarrow \mu^- + \bar{\nu}_\mu \quad (d\bar{u} \rightarrow \mu^- + \bar{\nu}_\mu) \quad (136)$$

However, some reactions do not comply with the lepton-quark symmetry:

$$K^- \rightarrow \mu^- + \bar{\nu}_\mu \quad (s\bar{u} \rightarrow \mu^- + \bar{\nu}_\mu) \quad (137)$$

►►► To solve the contradiction, the “*quark mixing*” hypothesis was introduced by Cabibbo:

d- and s-quarks participate the weak interactions via the linear combinations:

$$\begin{aligned} d' &= d \cos \theta_C + s \sin \theta_C \\ s' &= -d \sin \theta_C + s \cos \theta_C \end{aligned} \tag{138}$$

Parameter θ_C is *Cabibbo angle*, and hence the quark-lepton symmetry applies to doublets like

$$\begin{pmatrix} u \\ d' \end{pmatrix} \text{ and } \begin{pmatrix} c \\ s' \end{pmatrix}$$

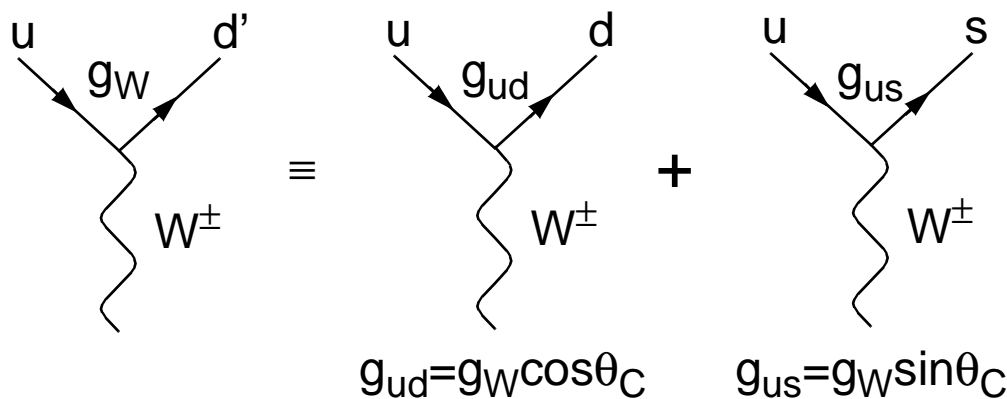


Figure 90: Interpretation of quark mixing

Quark mixing hypothesis allows some more W-quark vertices:

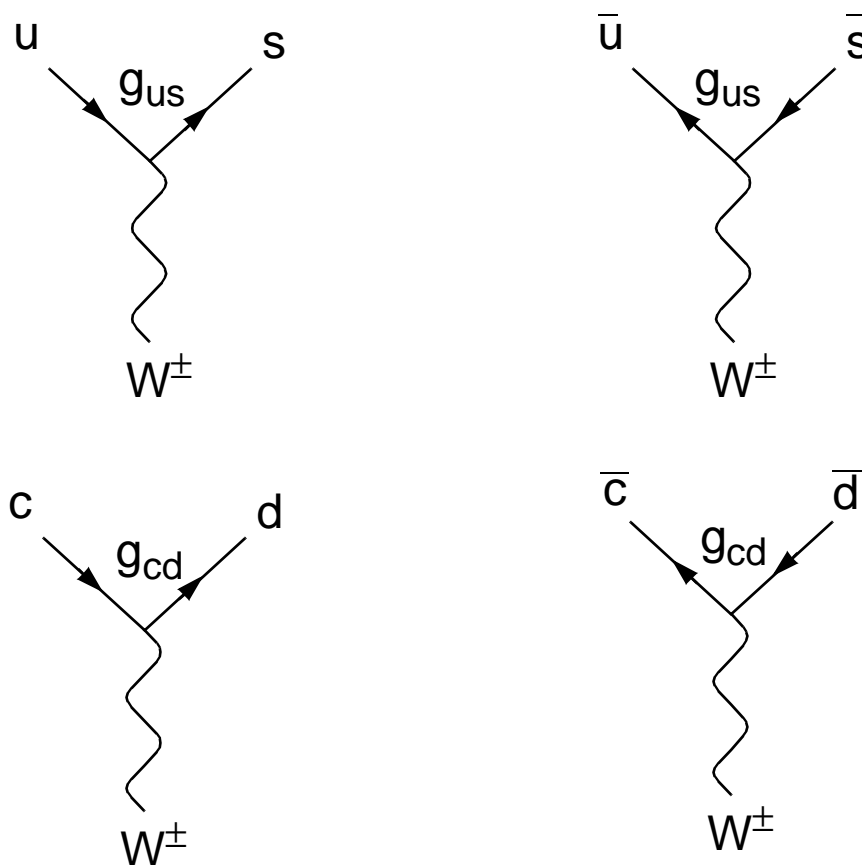


Figure 91: Additional W-quark vertices assumed by lepton-quark symmetry with quark mixing

$$g_{ud} = g_{cs} = g_W \cos \theta_C \quad (139)$$

$$g_{us} = -g_{cd} = g_W \sin \theta_C \quad (140)$$

Cabibbo angle is measured experimentally, for example, comparing decay rates:

$$\frac{\Gamma(K^- \rightarrow \mu^- \bar{\nu}_\mu)}{\Gamma(\pi^- \rightarrow \mu^- \bar{\nu}_\mu)} \propto \frac{g_{us}^2}{g_{ud}^2} = \tan^2 \theta_C$$

which corresponds to

$$\theta_C = 12.7^\circ \pm 0.1^\circ \quad (141)$$

Charmed quark couplings g_{cd} and g_{cs} are measured in neutrino scattering experiments and give

$$\theta_C = 12^\circ \pm 1^\circ$$

It can be seen that decays involving couplings (140) are suppressed: their rates are reduced by an order

$$\frac{g_{us}^2}{g_{ud}^2} = \frac{g_{cd}^2}{g_{cs}^2} = \tan^2 \theta_C = \frac{1}{20}$$

On the other hand, decays like $c \rightarrow sl^+ \nu_l$ and $c \rightarrow s\bar{u}d$ are Cabibbo-allowed, hence charmed particles almost always decay into strange ones.

The third generation

- ▣▣▣ Existence of c -quark was first predicted from the lepton-quark symmetry
- ▣▣▣ After discovery of τ , ν_τ , and b , the sixth quark has been predicted to complete the symmetry: the top-quark was confirmed in 1995 with mass of $180 \text{ GeV}/c^2$.

Form (138) is conveniently written in matrix form as:

$$\begin{pmatrix} d' \\ s' \end{pmatrix} = \begin{pmatrix} \cos \theta_C & \sin \theta_C \\ -\sin \theta_C & \cos \theta_C \end{pmatrix} \begin{pmatrix} d \\ s \end{pmatrix} \quad (142)$$

Adding the third generation, mixing between all of them must be allowed:

$$\begin{pmatrix} d' \\ s' \\ b' \end{pmatrix} = \begin{pmatrix} V_{ud} & V_{us} & V_{ub} \\ V_{cd} & V_{cs} & V_{cb} \\ V_{td} & V_{ts} & V_{tb} \end{pmatrix} \begin{pmatrix} d \\ s \\ b \end{pmatrix} \quad (143)$$

➡ 3x3 matrix of (143) is the so-called CKM matrix $V_{\alpha\beta}$ (Cabibbo-Kobayashi-Maskawa)

Coupling constants are then:

$$g_{\alpha\beta} = g_W V_{\alpha\beta} \quad (\alpha = u, c, t; \beta = d, s, b) \quad (144)$$

In the limit that mixing between the b quark and (d,s) ones can be neglected, the CKM matrix is

$$\begin{pmatrix} V_{ud} & V_{us} & V_{ub} \\ V_{cd} & V_{cs} & V_{cb} \\ V_{td} & V_{ts} & V_{tb} \end{pmatrix} \approx \begin{pmatrix} \cos\theta_C & \sin\theta_C & 0 \\ -\sin\theta_C & \cos\theta_C & 0 \\ 0 & 0 & 1 \end{pmatrix} \quad (145)$$

and hence $b'=b$

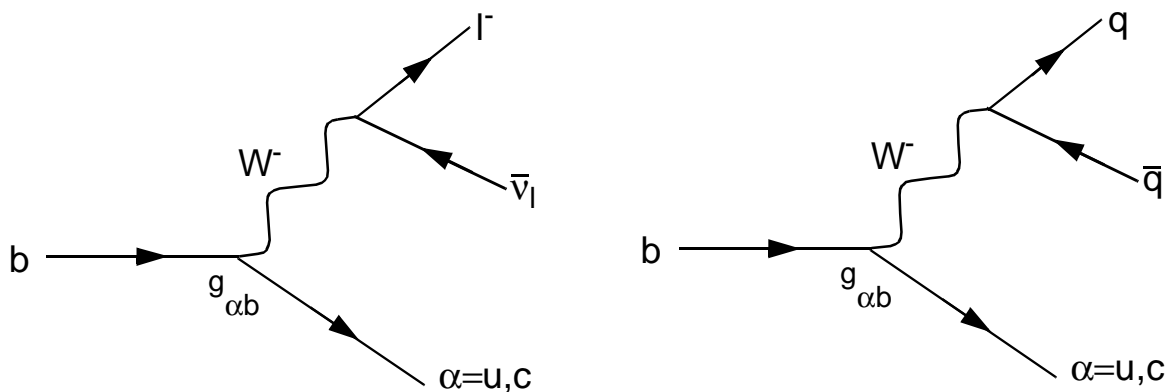
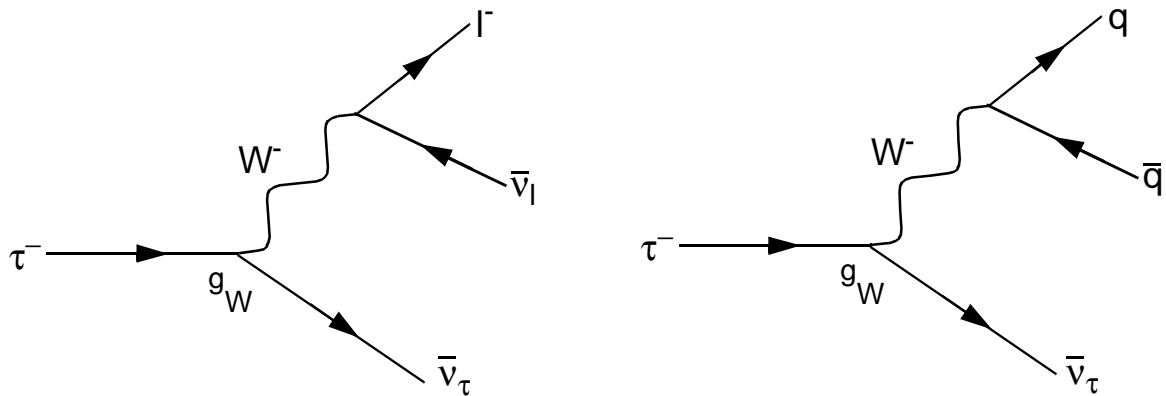


Figure 92: Dominant decays of b-quark

Figure 93: Dominant decays of τ lepton

Decay modes of Fig.92 have rates proportional to squared couplings:

$$|g_{ub}|^2 = |V_{ub}|^2 g_W^2 \text{ or } |g_{cb}|^2 = |V_{cb}|^2 g_W^2 \quad (146)$$

Since V_{ub} and V_{cb} are 0, b-quark should be stable. Experimentally,

$$\tau_b \approx 10^{-12} \text{ s} \quad (147)$$

If otherwise $g_{ub}=g_{cb}=g_W$, lifetime has to be shorter, like in case of τ decays (Fig.93).

Knowing the lifetime of τ lepton $\tau_\tau \approx 3 \times 10^{-13}$ s, and assuming there is no suppression of b decay, lifetime of b-quark will be:

$$\tau_b \approx \frac{1}{N} \left(\frac{m_\tau}{m_b} \right)^5 \approx 10^{-15} \text{ s}$$

where N is number of possible b-quark decays per analogous t-decays (3 or 4)

This contradicts experimental results; more precise measurements yield

$$|V_{ub}|^2 \approx 10^{-5} \quad \text{and} \quad |V_{cb}|^2 \approx 2 \times 10^{-3} \quad (148)$$

❖ The top-quark is much heavier than even W bosons and can decay by

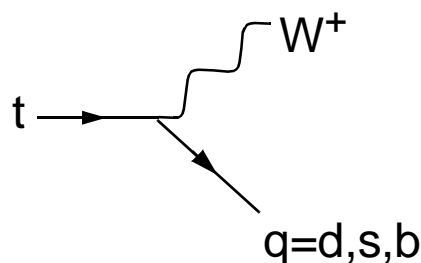


Figure 94: Decay $t \rightarrow W^+ + q$

As can be seen from CKM matrix, the only significant decay mode of t-quark is

$$t \rightarrow W^+ + b \tag{149}$$

with a rate proportional to

$$\alpha_W = g_W^2 / 4\pi \approx 4.2 \times 10^{-3}$$

Estimate of decay width $\Gamma \sim \alpha_W m_t \sim 1 \text{ GeV}$ suggests very short lifetime; more precisely:

$$\tau_t \approx 4 \times 10^{-25} \text{ s} \tag{150}$$

❖ Top-quarks do not form hadrons because of too short lifetime

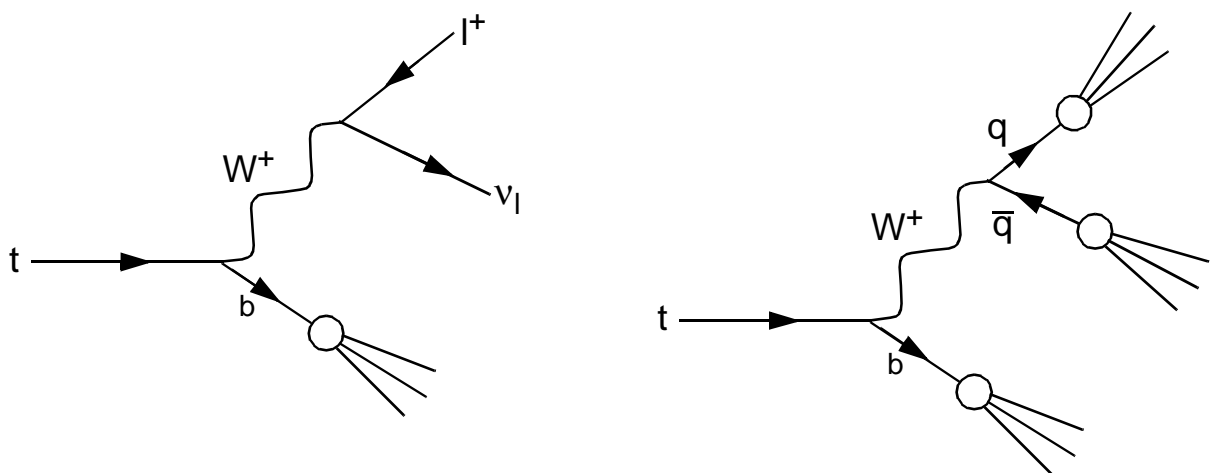


Figure 95: Decays of top-quark

IX. Electroweak unification

❖ Theory of weak interactions only by means of W^\pm bosons leads to infinities

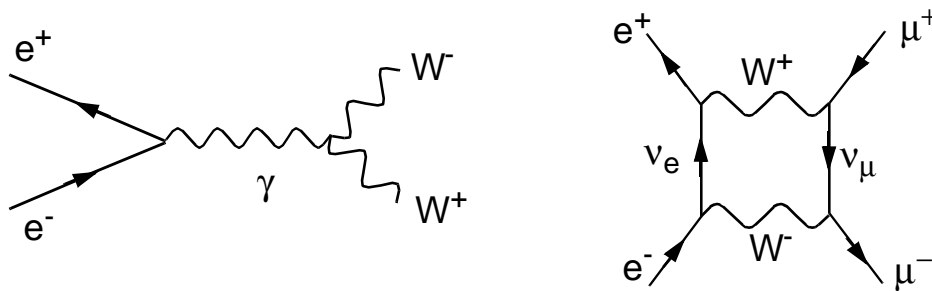


Figure 96: Examples of divergent processes

➡ A “good” theory (such as QED) must be *renormalisable*: all expressions can be made finite by reexpressing them in a finite number of physical parameters (e, m_e and \hbar in QED)

➡ Introduction of Z^0 boson fixes the problem:

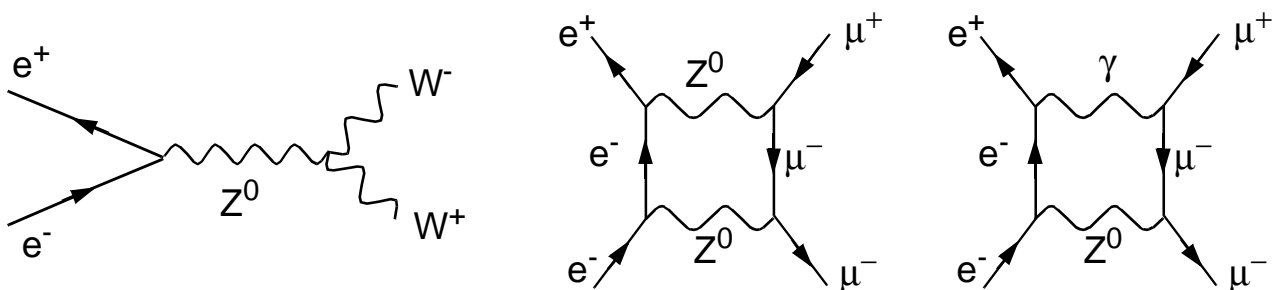


Figure 97: Additional processes to cancel divergence

Basic vertices for Z^0 boson:

- Conserved lepton numbers
- Conserved flavour

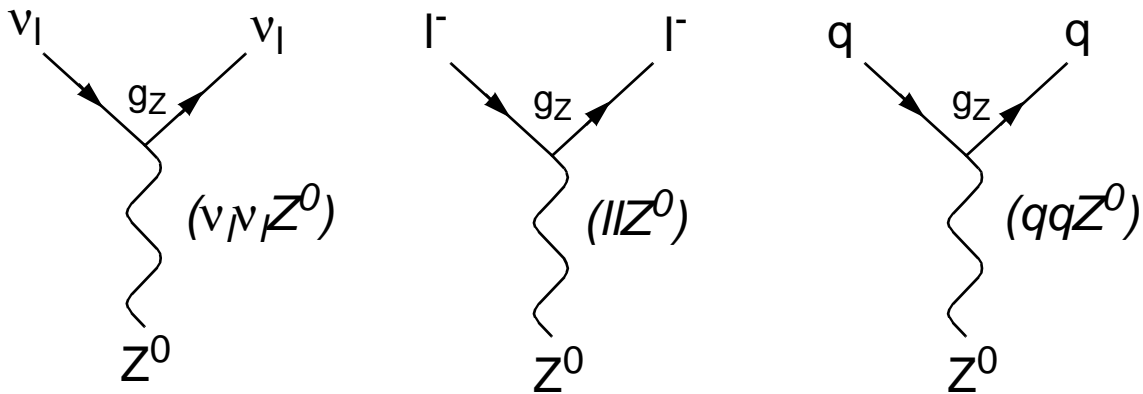


Figure 98: Z^0 -lepton and Z^0 -quark basic vertices

❖ By applying quark-lepton symmetry and quark mixing:

$$\begin{aligned}
 d'd'Z^0 + s's'Z^0 &= (d \cos \theta_C + s \sin \theta_C)(d \cos \theta_C + s \sin \theta_C)Z^0 + \\
 &+ (-d \sin \theta_C + s \cos \theta_C)(-d \sin \theta_C + s \cos \theta_C)Z^0 = \\
 &= ddZ^0 + ssZ^0
 \end{aligned}$$

It is not necessary to appeal to quark mixing in Z^0 vertices; even if applied it does not yield contradictions

Experimental test of flavour conservation at Z^0 vertex: considering two possible processes changing strangeness

$$K^+ \rightarrow \pi^0 + \mu^+ + \nu_\mu \quad (\text{a})$$

and

$$K^+ \rightarrow \pi^+ + \nu_l + \bar{\nu}_l \quad (\text{b})$$

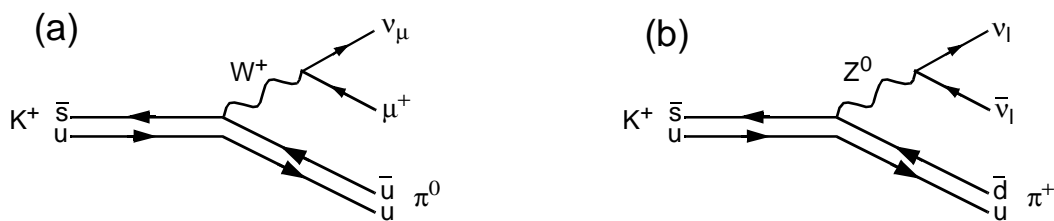


Figure 99: Decay (a) is allowed; decay (b) – forbidden

Measured upper limit on the ratio of the decay rates (b) to (a) is:

$$\frac{\sum_l \Gamma(K^+ \rightarrow \pi^+ + \nu_l + \bar{\nu}_l)}{\Gamma(K^+ \rightarrow \pi^0 + \mu^+ + \nu_\mu)} < 10^{-7}$$

❖ Comparing vertices involving γ , W^\pm and Z^0 , one can conclude that they all are governed by the same coupling constant $g \approx e$

➡ The *unification condition* establishes relation between coupling constants ($\alpha_{em} = e^2/4\pi\epsilon_0$):

$$\frac{e}{2\sqrt{2}\epsilon_0} = g_W \sin\theta_W = g_Z \cos\theta_W \quad (151)$$

θ_W is the *weak mixing angle*, or *Weinberg angle*:

$$\cos\theta_W = \frac{M_W}{M_Z} \quad (152)$$

➡ The *anomaly condition* relates electric charges:

$$\sum_l Q_l + 3 \sum_q Q_q = 0 \quad (153)$$

In the zero-range approximation (see Eq.(134)):

$$\frac{G_F}{\sqrt{2}} = \frac{g_W^2}{M_W^2} \Rightarrow M_W^2 = \frac{g_W^2 \sqrt{2}}{G_F} = \frac{\pi\alpha}{\sqrt{2} G_F \sin^2\theta_W} \quad (154)$$

Introducing the neutral current coupling (also in low energy zero-range approximation)

$$\frac{G_Z}{\sqrt{2}} = \frac{g_Z^2}{M_Z^2} \quad (155)$$

the weak mixing angle can be expressed as

$$\frac{G_Z}{G_W} = \frac{g_Z^2 M_W^2}{g_W^2 M_Z^2} = \sin^2 \theta_W \quad (156)$$

From measurements of rates of charged and neutral currents reactions,

$$\sin^2 \theta_W = 0.227 \pm 0.014$$

which allowed to predict masses of W and Z:

$$M_W = 78.3 \pm 2.4 \text{ GeV}/c^2; M_Z = 89.0 \pm 2.0 \text{ GeV}/c^2$$

The most precise result:

$$\sin^2 \theta_W = 0.2255 \pm 0.0021 \quad (157)$$

However, the most precise value for mass ratio is

$$1 - \frac{M_W^2}{M_Z^2} = 0.22318 \pm 0.0052$$

The difference comes from higher-order diagrams:

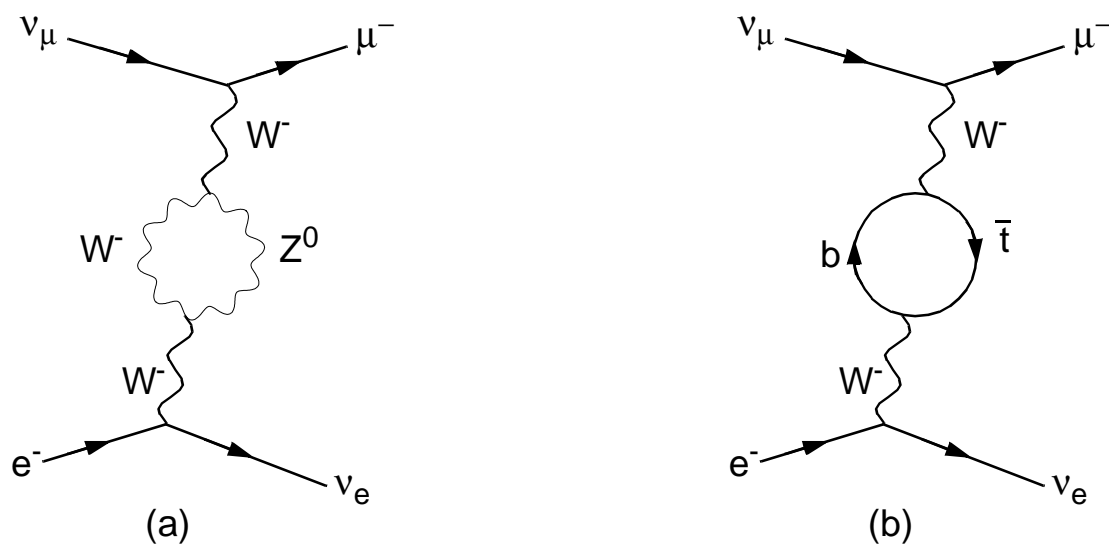


Figure 100: Examples of higher order contributions to inverse muon decay

From higher order corrections, the estimate of top-quark mass is:

$$m_t = 170 \pm 30 \text{ GeV}/c^2 \quad (158)$$

Measured value is $m_t = 174 \pm 5 \text{ GeV}/c^2$

► In any process in which a photon is exchanged, a Z^0 boson can be exchanged as well

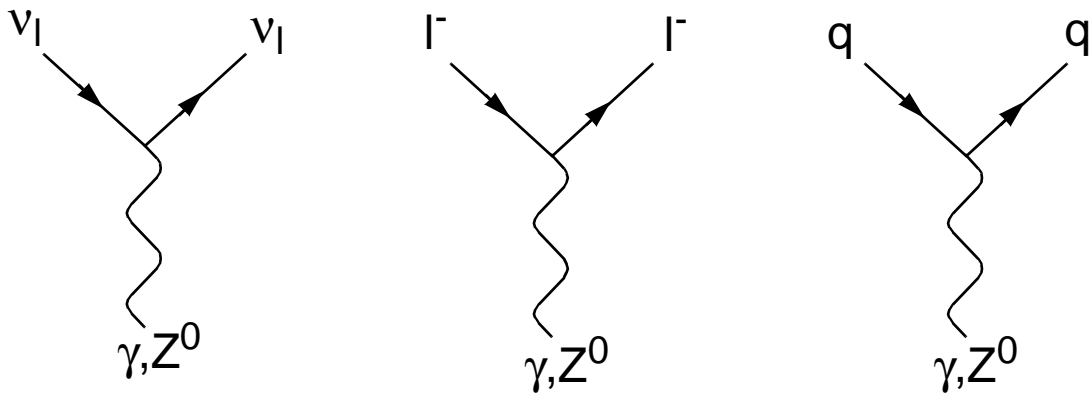


Figure 101: Z^0 and γ couplings to leptons and quarks

Example: reaction $e^+e^- \rightarrow \mu^+\mu^-$ has two dominant contributions:

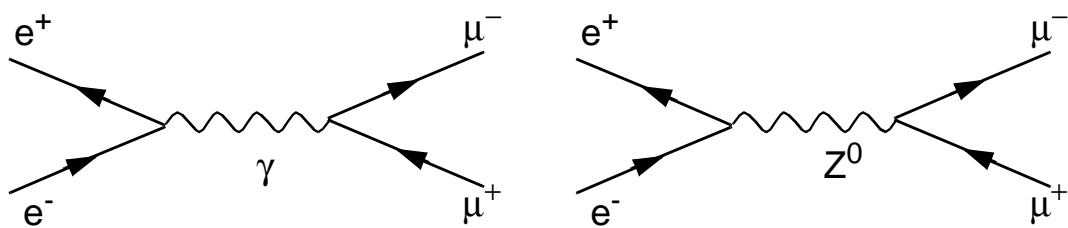
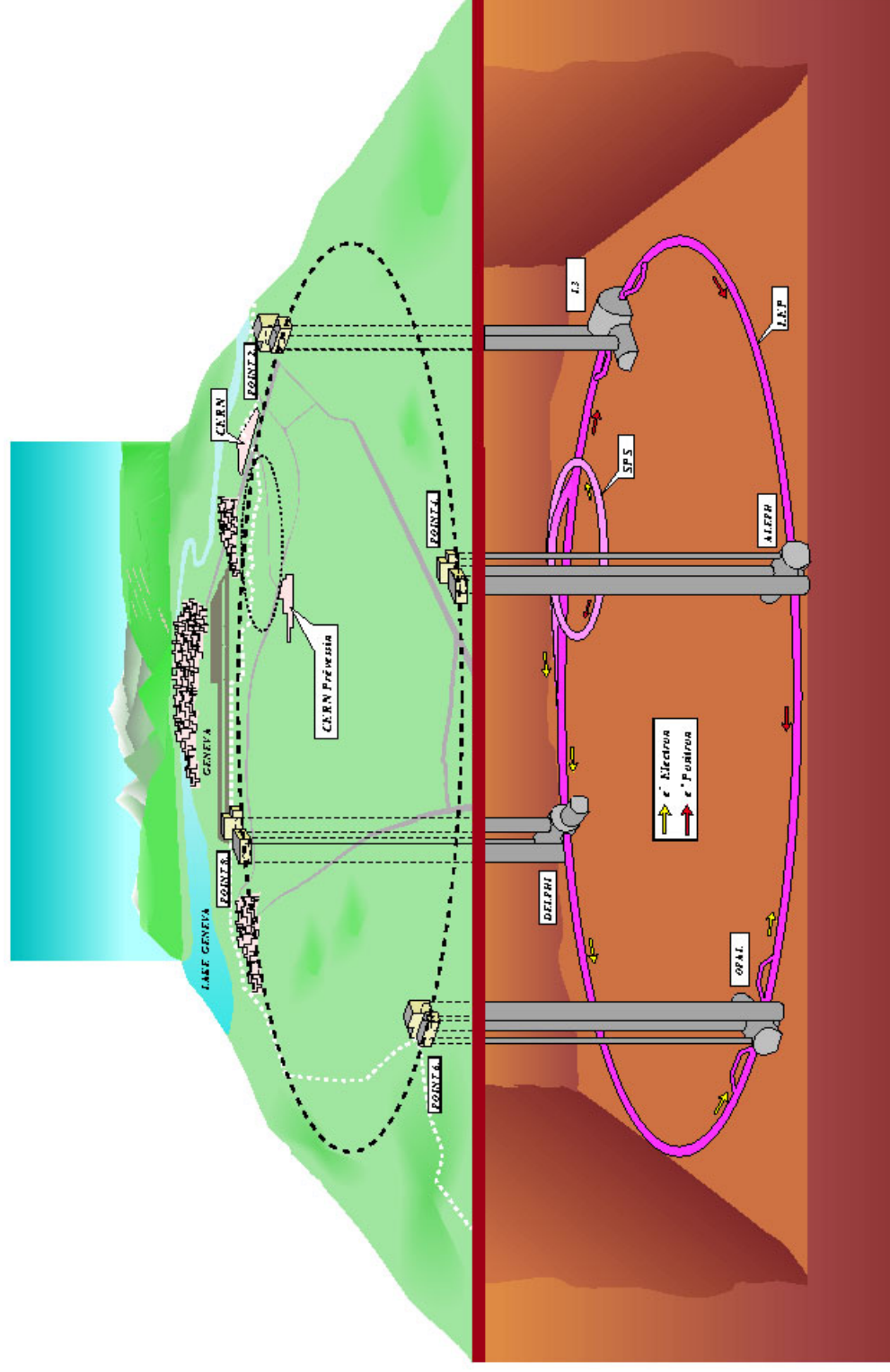


Figure 102: Dominant contributions to the e^+e^- annihilation into muons

$$\sigma_\gamma \approx \frac{\alpha^2}{E^2} \quad \sigma_Z \approx G_Z^2 E^2 \quad (159)$$

Figure 103: Schematic layout of the e^+e^- collider LEP at CERN

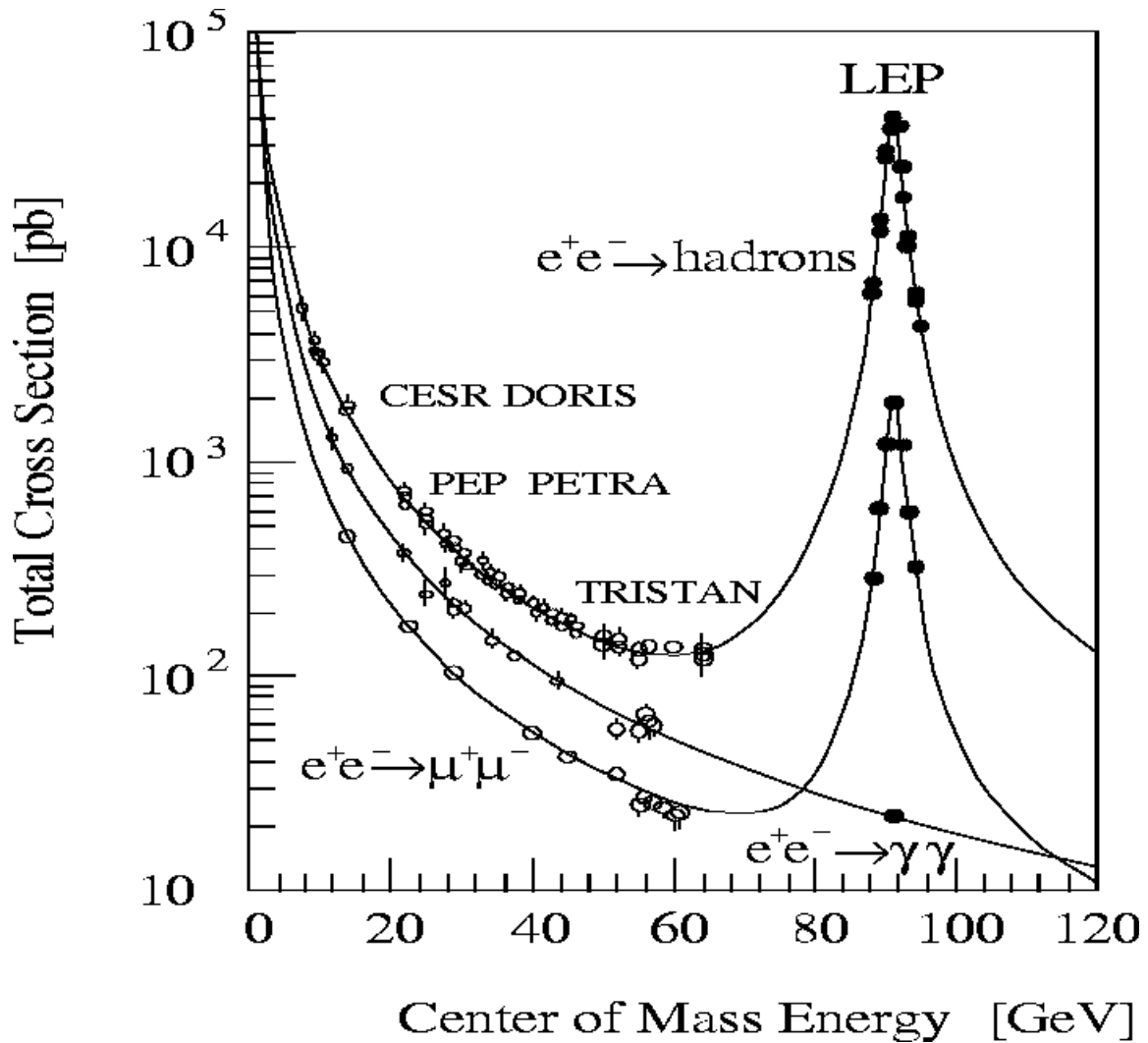


Figure 104: Total cross sections of e^+e^- annihilation

From Eq.(159), ratio of σ_Z and σ_γ is:

$$\frac{\sigma_Z}{\sigma_\gamma} \approx \frac{E^4}{M_Z^4} \tag{160}$$

At energies $E_{CM}=M_Z$, low-energy approximation fails

❖ Z^0 peak is described by the Breit-Wigner formula:

$$\sigma(e^+e^- \rightarrow X) = \frac{12\pi M_Z^2}{E_{CM}^2} \left[\frac{\Gamma(Z^0 \rightarrow e^+e^-)\Gamma(Z^0 \rightarrow X)}{(E_{CM}^2 - M_Z^2)^2 + M_Z^2\Gamma_Z^2} \right] \quad (161)$$

Here Γ_Z is the total Z^0 decay rate, and $\Gamma_Z(Z^0 \rightarrow X)$ are decay rates to other final states.

Height of the peak (at $E_{CM}=M_Z$) is then proportional to the product of branching ratios:

$$B(Z^0 \rightarrow e^+e^-)B(Z^0 \rightarrow X) \equiv \frac{\Gamma(Z^0 \rightarrow e^+e^-)\Gamma(Z^0 \rightarrow X)}{\Gamma_Z^2} \quad (162)$$

Fitted parameters of the Z^0 peak:

$$\begin{aligned} M_Z &= 91.187 \pm 0.007 \text{ GeV}/c^2 \\ \Gamma_Z &= 2.490 \pm 0.007 \text{ GeV} \end{aligned} \quad (163)$$

❖ Fitting the peak with Eq.(161), not only M_Z and Γ_Z can be found, but also partial decay rates:

$$\Gamma(Z^0 \rightarrow \text{hadrons}) = 1.741 \pm 0.006 \text{ GeV} \quad (164)$$

$$\Gamma(Z^0 \rightarrow l^+ l^-) = 0.0838 \pm 0.0003 \text{ GeV} \quad (165)$$

⇒ Decays $Z^0 \rightarrow l^+ l^-$ and $Z^0 \rightarrow \text{hadrons}$ account for only about 80% of all Z^0 decays

⇒ Remaining decays are those containing only neutrinos in the final state

$$\Gamma_Z = \Gamma(Z^0 \rightarrow \text{hadrons}) + 3\Gamma(Z^0 \rightarrow l^+ l^-) + N_\nu \Gamma(Z^0 \rightarrow \nu_l \bar{\nu}_l) \quad (166)$$

From Eqs.(163)-(165):

$$N_\nu \Gamma(Z^0 \rightarrow \nu_l \bar{\nu}_l) = 0.498 \pm 0.009 \text{ GeV}$$

Decay rate to neutrino pairs is calculated from diagrams of Fig.101:

$$\Gamma(Z^0 \rightarrow \nu_l \bar{\nu}_l) = 0.166 \text{ GeV} \quad (167)$$

which means that $N_\nu \approx 3$. More precisely,

$$N_\nu = 2.994 \pm 0.011 \quad (168)$$

▣▣▣▣ There are no explicit restrictions on number of generations in the Standard Model

▣▣▣▣ However, analysis of Z^0 line shape shows that there are 3 and only 3 kinds of massless neutrinos.

❖ If neutrinos are assumed having negligible masses as compared with the Z^0 mass, there must be only THREE generations of leptons and quarks within the Standard Model.

Gauge invariance and the Higgs boson

▣▣▣▣ Renormalisable theories are *gauge invariant* theories

❖ Gauge transformation: certain alteration of a quantum field variables that leave basic properties of the field unchanged; a symmetry transformation

❖ There are several forms of gauge invariance corresponding to different interactions

In QED, Schrödinger equation must be invariant under the phase transformation of the wavefunction:

$$\psi(\vec{x}, t) \rightarrow \psi'(\vec{x}, t) = e^{iq\alpha(\vec{x}, t)} \psi(\vec{x}, t) \quad (169)$$

Here $\alpha(\vec{x}, t)$ is an arbitrary continuous function.

If a particle is free, then

$$i\frac{\partial\psi(\vec{x}, t)}{\partial t} = -\frac{1}{2m}\nabla^2\psi(\vec{x}, t) \quad (170)$$

- ▣▣▣▣ Transformed wavefunction $\psi'(\vec{x}, t)$ can not be a solution of the Schrödinger equation (170)
- ▣▣▣▣ *Gauge principle*: to keep the invariance condition satisfied, a minimal field should be added to the Schrödinger equation, i.e., an interaction should be introduced

In QED, the transition from one electron state to another with different phase, $e^- \rightarrow e^-$, demands emission (or absorption) of a photon: $e^- \rightarrow e^- \gamma$

More generally, transformations like

$$e^- \rightarrow \nu_e \quad \nu_e \rightarrow e^- \quad e^- \rightarrow e^- \quad \nu_e \rightarrow \nu_e$$

lead via the gauge principle to interactions

$$e^- \rightarrow \nu_e W^- \quad \nu_e \rightarrow e^- W^+ \quad e^- \rightarrow e^- W^0 \quad \nu_e \rightarrow \nu_e W^0$$

W^+ , W^- and W^0 are corresponding spin-1 gauge bosons.

While W^+ and W^- are well-known charged currents, W^0 has not been identified.

Electroweak unification regards both Z^0 and γ as mixtures of W^0 and yet another neutral boson B^0 :

$$\begin{aligned}\gamma &= B^0 \cos \theta_W + W^0 \sin \theta_W \\ Z^0 &= -B^0 \sin \theta_W + W^0 \cos \theta_W\end{aligned}\quad (171)$$

The corresponding gauge transformation is:

$$\psi_l(\vec{x}, t) \rightarrow \psi_l'(\vec{x}, t) = e^{ig_Z y_l \alpha(\vec{x}, t)} \psi_l(\vec{x}, t) \quad (172)$$

Here l stands for electron or neutrino and y_l are corresponding constants

This will lead to extra vertices

$$e^- \rightarrow e^- B^0 \quad \nu_e \rightarrow \nu_e B^0$$

with new couplings $g_Z y_{e^-}$ and $g_Z y_{\nu_e}$ and they satisfy the unification condition (151).

- ▣▣▣▣▶ Electroweak theory can be made gauge-invariant by introducing neutral bosons W^0 and B^0 .
 - ❖ Generally, experimental data agree with gauge invariant electroweak theory predictions.
- ▣▣▣▣▶ However, gauge invariance implies that spin-1 bosons have zero masses if they are only bosons in theory (photon and gluon comply with this)



a new field should be introduced

- ❖ The scalar *Higgs field* solves the problem:
 - *Higgs boson* H^0 is a spin-0 particle
 - Higgs field has a **non-zero** value ϕ_0 in vacuum

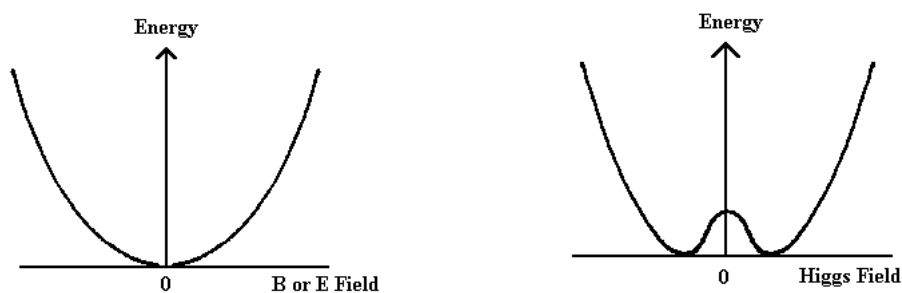


Figure 105: Comparison of the electric and Higgs fields

- ❖ The vacuum value ϕ_0 is not gauge invariant \Rightarrow *hidden gauge invariance*, or *spontaneously broken*.
- ➡ Vacuum hence is supposed to be populated with massive Higgs bosons \Rightarrow **when a gauge field interacts with the Higgs field it acquires mass.**
- ➡ In the same way, fermions acquire masses by interacting with Higgs bosons:

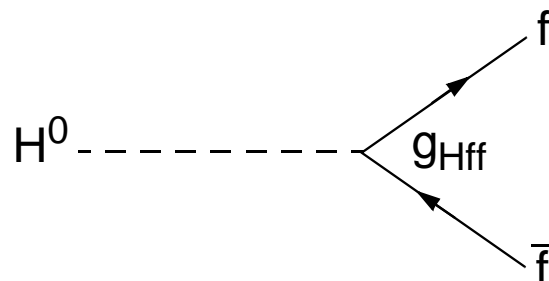


Figure 106: Basic vertex for Higgs-fermion interactions

The coupling constant is related to the fermion mass:

$$g_{Hff}^2 = \sqrt{2} G_F m_f^2 \quad (173)$$

- ❖ The mass of the Higgs itself is not predicted by the theory, only couplings to other particles. (Eq.(173))
- ❖ Existence of the Higgs has not been (yet) confirmed by experiment

Possible signatures of the Higgs:

- a) If H^0 is lighter than Z^0 (rather, $M_H \leq 50 \text{ GeV}/c^2$), then Z^0 can decay by

$$Z^0 \rightarrow H^0 + l^+ + l^- \quad (174)$$

$$Z^0 \rightarrow H^0 + \nu_l + \bar{\nu}_l \quad (175)$$

But the branching ratio is very low:

$$3 \times 10^{-6} \leq \frac{\Gamma(Z^0 \rightarrow H^0 l^+ l^-)}{\Gamma_{tot}} \leq 10^{-4}$$

With the LEP statistics they still must be detectable; since reactions (174) and (175) had not been observed, the *lower limit* is $M_H > 58 \text{ GeV}/c^2$

b) If H^0 is significantly heavier than $60 \text{ GeV}/c^2$, it can be produced in e^+e^- annihilation at higher energies:

$$e^+ + e^- \rightarrow H^0 + Z^0 \quad (176)$$

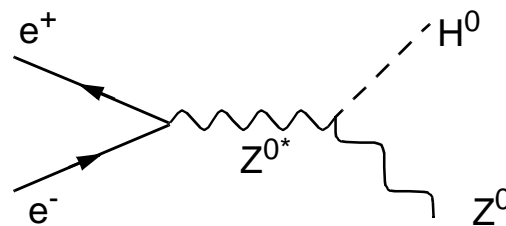


Figure 107: “Higgsstrahlung” in e^+e^- annihilation

In such a reaction, Higgs with mass up to $90 \text{ GeV}/c^2$ could have been detected. Up-to-date limit is:

$$M_H > 109.7 \text{ GeV}/c^2 \quad (177)$$

c) Higgs with masses up to 1 TeV can be observed at the future proton-proton collider LHC at CERN:

$$p + p \rightarrow H^0 + X \quad (178)$$

where H^0 is produced in electroweak interaction between the quarks

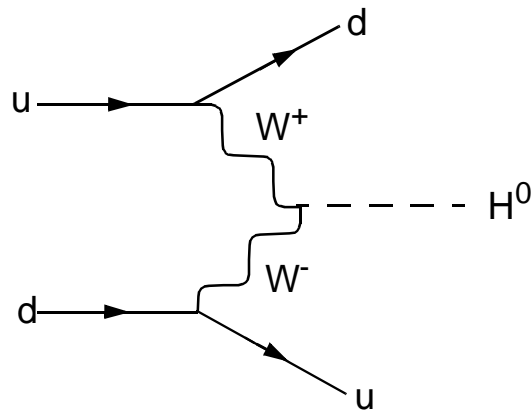


Figure 108: An example of Higgs production process at LHC

Due to heavy background, a good signatures have to be considered:

– If $M_H > 2M_Z$, then dominant decay modes are:

$$H^0 \rightarrow Z^0 + Z^0 \quad (179)$$

$$H^0 \rightarrow W^- + W^+ \quad (180)$$

The most clear signal is when both Z^0 decay into electron or muon pairs:

$$H^0 \rightarrow l^+ + l^- + l^+ + l^- \quad (181)$$

This will mean $200 \text{ GeV}/c^2 \leq M_H \leq 500 \text{ GeV}/c^2$, but only 4% of all decays

– If $M_H < 2M_W$, the dominant decay mode is

$$H^0 \rightarrow b + \bar{b} \quad (182)$$

but this gives indistinguishable signal. Other mode is

$$H^0 \rightarrow \gamma + \gamma \quad (183)$$

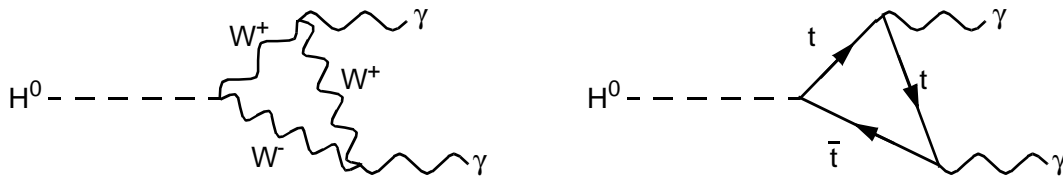


Figure 109: The dominant mechanisms for the decay (183)

Branching ratio of this kind of processes is about 10^{-3}

- ❖ The neutral Higgs is the minimal requirement; there might exist more complicated variants, including charged higgs-particles.

X. Charge conjugation and parity

While conserved in strong and electromagnetic interactions, parity is violated in weak processes:

Some known decays of K^+ are:

$$K^+ \rightarrow \pi^0 + \pi^+ \quad \text{and} \quad K^+ \rightarrow \pi^+ + \pi^+ + \pi^-$$

Intrinsic parity of a pion $P_\pi = -1$, and for the $\pi^0\pi^+$ and $\pi^+\pi^+\pi^-$ states parities are

$$P_{0+} = P_\pi^2 (-1)^L = 1, \quad P_{++-} = P_\pi^3 (-1)^{L_{12} + L_3} = -1$$

where $L=0$ since kaon has spin-0.

❖ One of the K^+ decays **violates** parity!

– 1956: Lee & Yang indicated that parity is violated in weak processes

– 1957: Wu carried out studies of parity violation in β -decay

- ^{60}Co β -decay into $^{60}\text{Ni}^*$ was studied
- ^{60}Co was cooled to 0.01 K to prevent thermal disorder
- Sample was placed in a magnetic field \Rightarrow nuclear spins were aligned along the field direction

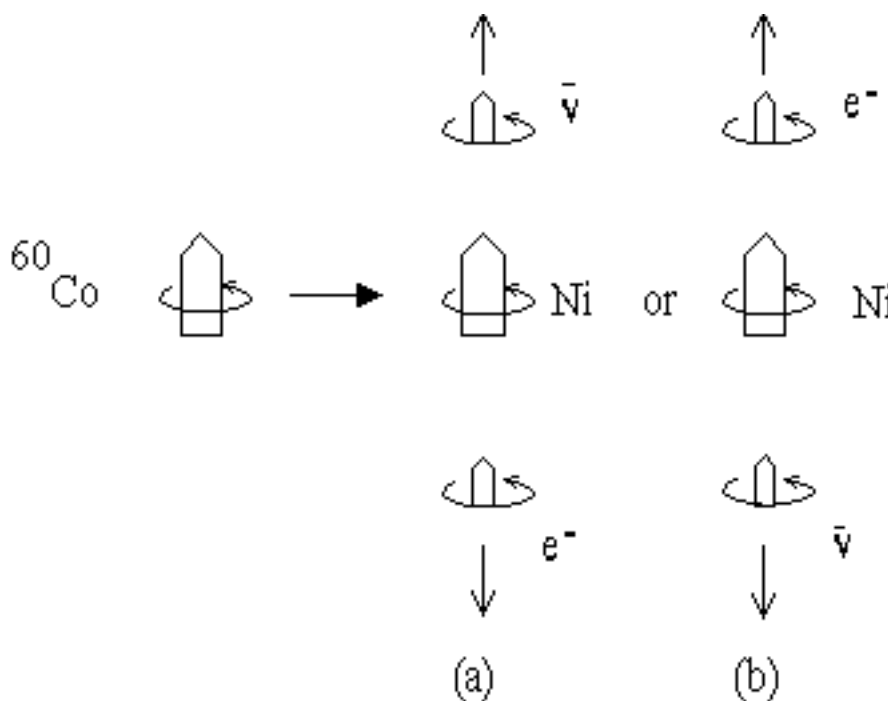


Figure 110: Possible β -decays of ^{60}Co : case (a) is preferred.
 – If parity is conserved, processes (a) and (b) must have equal rates

❖ Electrons were emitted predominantly in the direction opposite the ^{60}Co spin

Another case of parity and C-parity violation was observed in muon decays:

$$\mu^- \rightarrow e^- + \bar{\nu}_e + \nu_\mu \tag{184}$$

$$\mu^+ \rightarrow e^+ + \nu_e + \bar{\nu}_\mu \tag{185}$$

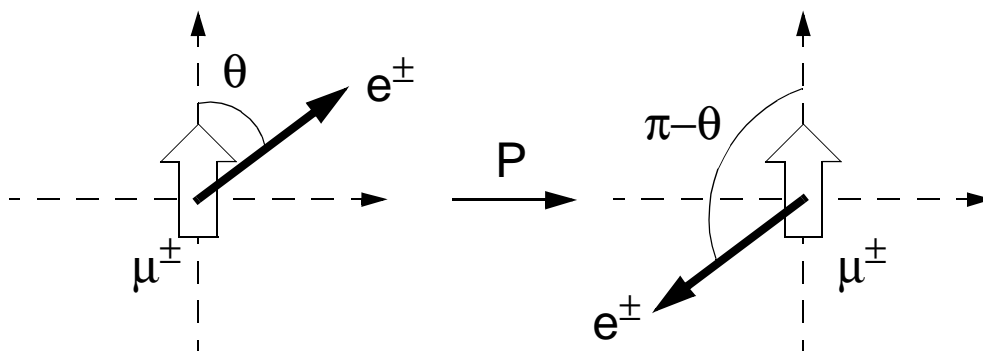


Figure 111: Effect of a parity transformation on the muon decays (184) and (185)

Angular distribution of electrons (positrons) emitted in μ^- (μ^+) decay has a form of

$$\Gamma_{\mu^\pm}(\cos\theta) = \frac{1}{2}\Gamma_\pm \left(1 - \frac{\xi_\pm}{3} \cos\theta \right) \tag{186}$$

here ξ_\pm are constants – “*asymmetry parameters*”, and Γ_\pm are total decay rates \Rightarrow inverse lifetimes

$$\Gamma_{\pm} = \int_{-1}^1 \Gamma_{\pm}(\cos\theta) d\cos\theta \equiv \frac{1}{\tau_{\pm}} \quad (187)$$

❖ If the process is invariant under charge conjugation (C-invariance) \Rightarrow

$$\Gamma_{+} = \Gamma_{-} \quad \xi_{+} = \xi_{-} \quad (188)$$

(rates and angular distributions are the same for e^{-} and e^{+})

❖ If the process is P-invariant, then angular distributions in forward and backward directions are the same:

$$\Gamma_{\mu^{\pm}}(\cos\theta) = \Gamma_{\mu^{\pm}}(-\cos\theta) \quad \xi_{+} = \xi_{-} = 0 \quad (189)$$

⇒ Experimental results:

$$\Gamma_{+} = \Gamma_{-} \quad \xi_{+} = -\xi_{-} = 1.00 \pm 0.04 \quad (190)$$

Both C- and P-invariance are violated!

❖ Solution: combined operation CP is conserved

$$\Gamma_{\mu^+}(\cos\theta) = \Gamma_{\mu^-}(-\cos\theta) \tag{191}$$

⇓

$$\Gamma_+ = \Gamma_- \quad \xi_+ = -\xi_- \tag{192}$$

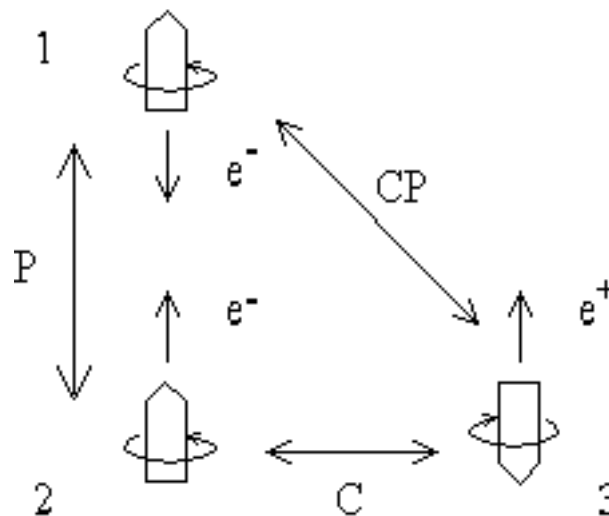


Figure 112: P-, C- and CP-transformation of an electron

➡ It appears that electrons prefer to be emitted with momentum opposite to their spin

Corresponding characteristics: *helicity* – projection of particle’s spin to its direction of motion

$$\Lambda = \frac{\vec{J} \cdot \vec{p}}{|\vec{p}|} = \frac{\vec{s} \cdot \vec{p}}{|\vec{p}|} \tag{193}$$

Eigenvalues of helicity are $h = -s, -s+1, \dots, +s$, \Rightarrow for spin-1/2 electron it can be either -1/2 or 1/2



Figure 113: Helicity states of spin-1/2 particle

Helicity of neutrino

– 1958: Goldhaber et al. measured helicity of the neutrino using reaction



– In reaction (194), ${}^{152}\text{Sm}^*$ and ν_e recoil in opposite directions



Figure 114: Spin of ${}^{152}\text{Sm}^*$ has to be opposite to the neutrino spin (parallel to the electron spin)

– In initial state electron has spin-1/2, ^{152}Eu – spin-0, in final state: $^{152}\text{Sm}^*$ has spin-1 and ν_e – spin-1/2 \Rightarrow spin of $^{152}\text{Sm}^*$ is parallel to the electron spin and opposite to the neutrino spin.

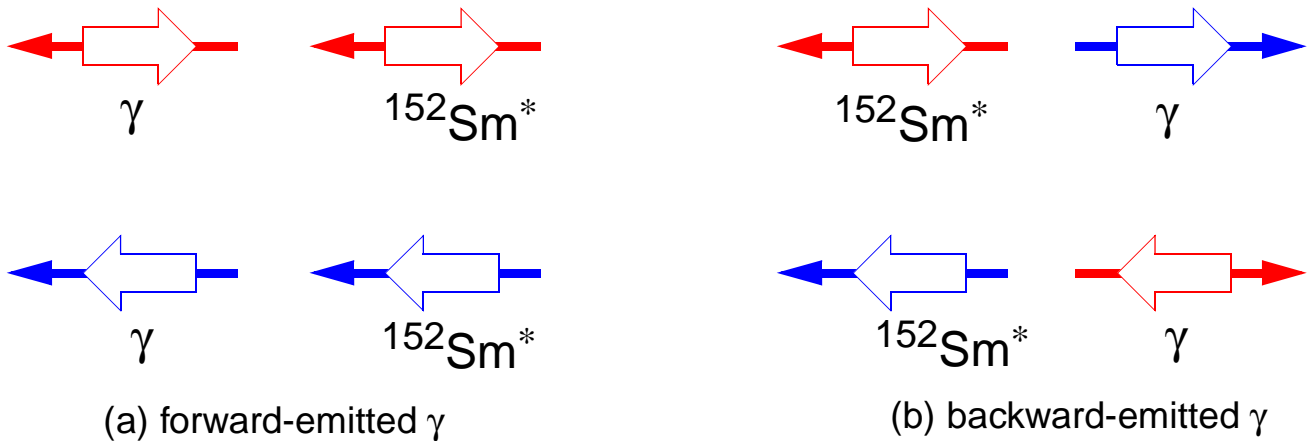


Figure 115: Forward-emitted γ has the same helicity as ν_e

– Events with γ emitted in the direction of motion of $^{152}\text{Sm}^*$ were selected.

– Polarization of photons was determined by studying their absorption in magnetized iron.

➡ It turned out that neutrinos can be only **left-handed!**

➡ Antineutrinos were found to be always right-handed.

V-A interaction

- ❖ V-A interaction theory was introduced by Fermi as an analytic description of spin dependence of charged current interactions.
- ❖ It denotes “polar Vector - Axial vector” interaction
 - *Polar vector* is any which direction is reversed by parity transformation: momentum \vec{p}
 - *Axial vector* is that which direction is not changed by parity transformation: spin \vec{s} or orbital angular momentum $\vec{L} = \vec{r} \times \vec{p}$
 - Weak current has both vector and axial components, hence parity is not conserved in weak interactions
- ➡ Main conclusion: if $v \approx c$, only left-handed fermions ν_L, e_L^- etc. are emitted, and right-handed antifermions.
- ➡ *The very existence of preferred states violates both C- and P- invariance*

- ❖ Neutrinos (antineutrinos) are always relativistic and hence always left(right)-handed
- ❖ For other fermions, preferred states are left-handed, and right-handed states are not completely forbidden but suppressed by factors

$$\left(1 - \frac{v}{c}\right) \approx \frac{m^2}{2E^2} \tag{196}$$

Consider pion decay modes:

$$\pi^+ \rightarrow l^+ + \nu_l \quad (l=e, \mu) \tag{197}$$

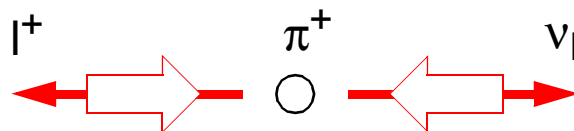


Figure 116: Helicities of leptons emitted in a pion decay

- π^+ has spin-0, \Rightarrow spins of charged lepton and neutrino must be opposite
- Neutrino is always left-handed \Rightarrow charged lepton has to be left-handed as well. BUT: e^+ and μ^+ ought to be right-handed!

It follows that the relativistic charged lepton can not be emitted in a pion decay!

❖ Muons are rather heavy \Rightarrow non-relativistic \Rightarrow can be right-handed (see Eq.(196))

❖ Suppression factor for positron is of order 10^{-5}

Measured ratio:

$$\frac{\Gamma(\pi^+ \rightarrow e^+ \nu_e)}{\Gamma(\pi^+ \rightarrow \mu^+ \nu_\mu)} = (1.230 \pm 0.004) \times 10^{-4} \quad (198)$$

Muons emitted in pion decays are always polarized (μ^+ are left-handed)

This can be used to measure muon decay (184), (185) symmetries by detecting highest-energy (relativistic) electrons with energy

$$E = \frac{m_\mu}{2} \left(1 + \frac{m_e^2}{m_\mu^2} \right) \gg m_e \quad (199)$$

❖ Highest-energy electrons are emitted in decays when both ν_μ and $\bar{\nu}_e$ are emitted in the direction opposite to e^- :

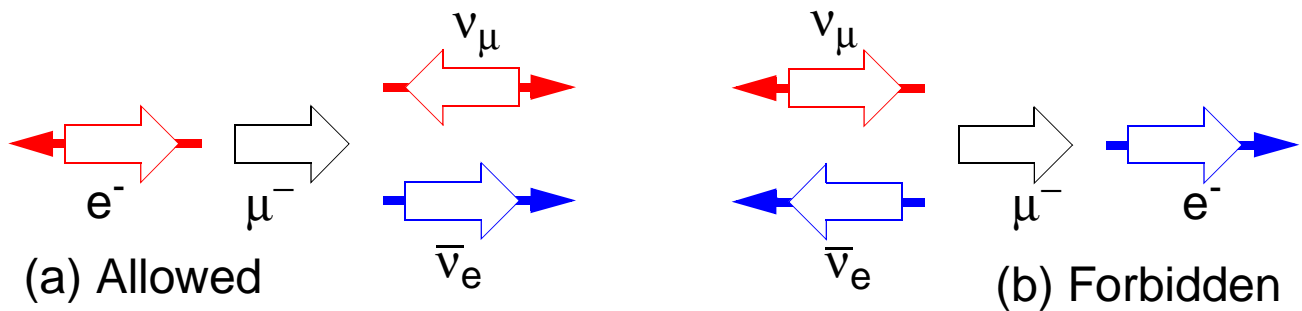


Figure 117: Muon decays with highest-energy electron emission

– Electron must have spin parallel to the muon spin \Rightarrow configuration (a) is strongly preferred \Rightarrow observed experimentally forward-backward asymmetry (190)

Neutral kaons

➡ CP symmetry apparently can be violated in weak interactions

❖ Neutral kaons $K^0(498)=d\bar{s}$ and $\bar{K}^0(498)=s\bar{d}$ can be converted into each other because they have same quantum numbers

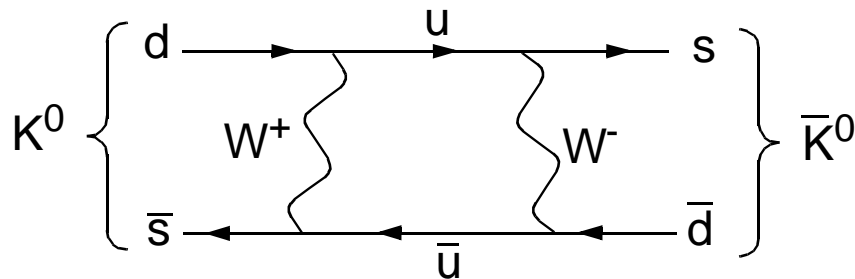


Figure 118: Example of a process converting K^0 to \bar{K}^0 .

❖ Phenomenon of $K^0-\bar{K}^0$ mixing: observed physical particles are linear combinations of K^0 and \bar{K}^0 , since there is no conserved quantum number to distinguish them

➡ The same is true for neutral B-mesons: $B^0 = d\bar{b}$, $\bar{B}^0 = \bar{d}b$, $B_s = s\bar{b}$ and $\bar{B}_s = \bar{s}b$, and for neutral D-mesons $D^0 = c\bar{u}$ and $\bar{D}^0 = \bar{c}u$.

C-transformation changes a quark into antiquark \Rightarrow

$$C|K^0, \vec{p}\rangle = -|\bar{K}^0, \vec{p}\rangle \quad \text{and} \quad C|\bar{K}^0, \vec{p}\rangle = -|K^0, \vec{p}\rangle \quad (200)$$

* Here signs are chosen for further convenience and do not affect physical predictions

Intrinsic parity of a kaon is $P_K = -1 \Rightarrow$ for $\vec{p} = (0, 0, 0)$

$$P|K^0, \vec{p}\rangle = -|K^0, \vec{p}\rangle \quad \text{and} \quad P|\bar{K}^0, \vec{p}\rangle = -|\bar{K}^0, \vec{p}\rangle \quad (201)$$

and the CP transformation is

$$CP|K^0, \vec{p}\rangle = |\bar{K}^0, \vec{p}\rangle \quad \text{and} \quad CP|\bar{K}^0, \vec{p}\rangle = |K^0, \vec{p}\rangle \quad (202)$$

\Rightarrow there are two CP eigenstates :

$$|K_1^0, \vec{p}\rangle = \frac{1}{\sqrt{2}} \{ |K^0, \vec{p}\rangle + |\bar{K}^0, \vec{p}\rangle \} \quad (203)$$

$$|K_2^0, \vec{p}\rangle = \frac{1}{\sqrt{2}} \{ |K^0, \vec{p}\rangle - |\bar{K}^0, \vec{p}\rangle \} \quad (204)$$

so that

$$CP|K_1^0, \vec{p}\rangle = |K_1^0, \vec{p}\rangle \quad \text{and} \quad CP|K_2^0, \vec{p}\rangle = -|K_2^0, \vec{p}\rangle \quad (205)$$

Experimental observations are two types of neutral kaons: K_S^0 ("S" for "short", lifetime $\tau = 0.9 \times 10^{-10} \text{ s}$) and K_L^0 ("long", $\tau = 5 \times 10^{-8} \text{ s}$).

❖ K_S^0 is identified with K_1^0 CP-eigenstate, and K_L^0 – with K_2^0

⇒ If CP-invariance holds for neutral kaons, K_S^0 should decay only to states with CP=1, and K_L^0 – to states with CP=-1:

$$K_S^0 \rightarrow \pi^+ \pi^-, K_S^0 \rightarrow \pi^0 \pi^0 \tag{206}$$

– Parity of a two-pion state is $P = P_\pi^2 (-1)^L = 1$ (kaon has spin-0)

– C-parity of $\pi^0 \pi^0$ state is $C = (C_{\pi^0})^2 = 1$, and of a $\pi^+ \pi^-$ state: $C = (-1)^L = 1, \Rightarrow$ for final states in (206) CP=1

$$K_L^0 \rightarrow \pi^+ \pi^- \pi^0, K_L^0 \rightarrow \pi^0 \pi^0 \pi^0 \tag{207}$$

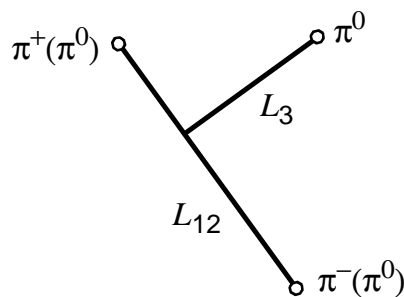


Figure 119: Angular momenta in the 3-pion system

- Parity of a 3-pion state is $P = P_\pi^3 (-1)^{L_{12} + L_3} = -1$
- C-parity of $\pi^0\pi^0\pi^0$ is $C = (C_{\pi^0})^3 = 1$, and of the state $\pi^+\pi^-\pi^0$: $C = C_{\pi^0}(-1)^{L_{12}} = (-1)^{L_{12}}$. L_{12} can be defined experimentally: $L_{12}=0 \Rightarrow$ for final states in (207) $CP=-1$

⇒ However, the *CP-violating* decay

$$K_L^0 \rightarrow \pi^+ \pi^- \quad (208)$$

was observed in 1964, with a branching ratio $B \approx 10^{-3}$.

❖ In general, physical states K_S^0 and K_L^0 don't have to correspond to CP-eigenstates K_1^0 and K_2^0 : K_S^0 has admixture of K_2^0 and K_L^0 – of K_1^0 .

❖ There can be different mechanisms for CP-violation, esp. in B^0 - \bar{B}^0 systems; no experimental data is available yet though.

XI. Beyond the Standard Model

- ▣▣▣▣ While Standard Model appears to be confirmed in all ways, there are some unclear points and possible extensions
 - ❖ Why observed quarks and leptons have the masses they do?
 - ❖ Do neutrino have actually masses?
 - ❖ If yes, are they the *Dark Matter*?

Neutrino masses

- ▣▣▣▣ If neutrinos have non-zero masses, they must be subject to *neutrino-mixing*

Recall: quark mixing in weak interactions

$$d' = d \cos \theta_C + s \sin \theta_C$$

$$s' = -d \sin \theta_C + s \cos \theta_C$$

By analogy, neutrinos can be represented as linear combinations:

$$\begin{aligned} \nu_e &= \nu_1 \cos \alpha + \nu_2 \sin \alpha \\ \nu_\mu &= -\nu_1 \sin \alpha + \nu_2 \cos \alpha \end{aligned} \quad (209)$$

if neutrinos ν_1 and ν_2 have masses m_1 and m_2 .

- ▣▣▣▣► Mixing angle α must be determined from experiment; *neutrino oscillation* can be observed
- ❖ Neutrino oscillation: a beam of ν_e develops ν_μ component as it travels through space, and vice versa

In Dirac notation,

$$|\nu_e, \vec{p}\rangle = \cos \alpha |\nu_1, \vec{p}\rangle + \sin \alpha |\nu_2, \vec{p}\rangle \quad (210)$$

and after period of time t it evolves to:

$$e^{-iE_1 t} \cos \alpha |\nu_1, \vec{p}\rangle + e^{-iE_2 t} \sin \alpha |\nu_2, \vec{p}\rangle \quad (211)$$

where $e^{-iE_i t}$ are oscillating time factors

Form (211) is not a pure ν_e state anymore:

$$A(t)|\nu_e, \vec{p}\rangle + B(t)|\nu_\mu, \vec{p}\rangle \quad (212)$$

where the ν_μ states are, as in (210):

$$|\nu_\mu, \vec{p}\rangle = -\sin\alpha|\nu_1, \vec{p}\rangle + \cos\alpha|\nu_2, \vec{p}\rangle \quad (213)$$

and hence

$$\begin{aligned} A(t) &= e^{-iE_1 t} \cos^2 \alpha + e^{-iE_2 t} \sin^2 \alpha \\ B(t) &= \sin\alpha \cos\alpha [e^{-iE_2 t} - e^{-iE_1 t}] \end{aligned} \quad (214)$$

Squares of $A(t)$ and $B(t)$ are probabilities to find ν_e respective ν_μ in a beam of electron neutrinos:

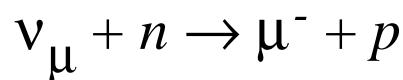
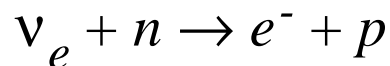
$$P(\nu_e \rightarrow \nu_e) = |A(t)|^2 = 1 - P(\nu_e \rightarrow \nu_\mu) \quad (215)$$

$$P(\nu_e \rightarrow \nu_\mu) = |B(t)|^2 = \sin^2(2\alpha) \sin^2 \frac{(E_2 - E_1)t}{2} \quad (216)$$

▣▣▣▣ If neutrinos have equal (zero) masses $\Rightarrow E_1 = E_2$
 \Rightarrow no oscillations

Ways to detect neutrino oscillations:

❖ ν_e and ν_μ can be distinguished by their interaction with neutrons: former produce electrons and latter - muons



❖ Time t is determined by the distance between the detector and the source of neutrinos

➡ Several neutrino sources can be considered:

- Sun
- Cosmic rays (“atmospheric neutrinos”)
- Secondary accelerator beams
- Nuclear reactors
- Natural radioactivity
- Supernova
- Big Bang

Atmospheric neutrino anomaly

- ▣▣▣▣ Was first detected in 1980's: instead of predicted $N(\nu_\mu) \approx 2N(\nu_e)$, rates of both neutrinos were approximately equal.

- ❖ Super-Kamiokande detector: measures rates and flavours of neutrinos coming both from zenith and nadir
 - A neutrino created in cosmic rays travels at maximum 20 km in the atmosphere \Rightarrow have no time to oscillate (proven by other experiments)
 - A similar neutrino created on the other side of the Earth travels ≈ 13000 km \Rightarrow has good chances to oscillate
 - If ratio of ν_e and ν_μ is different in two cases above \Rightarrow there are oscillations \Rightarrow at least one neutrino is massive.

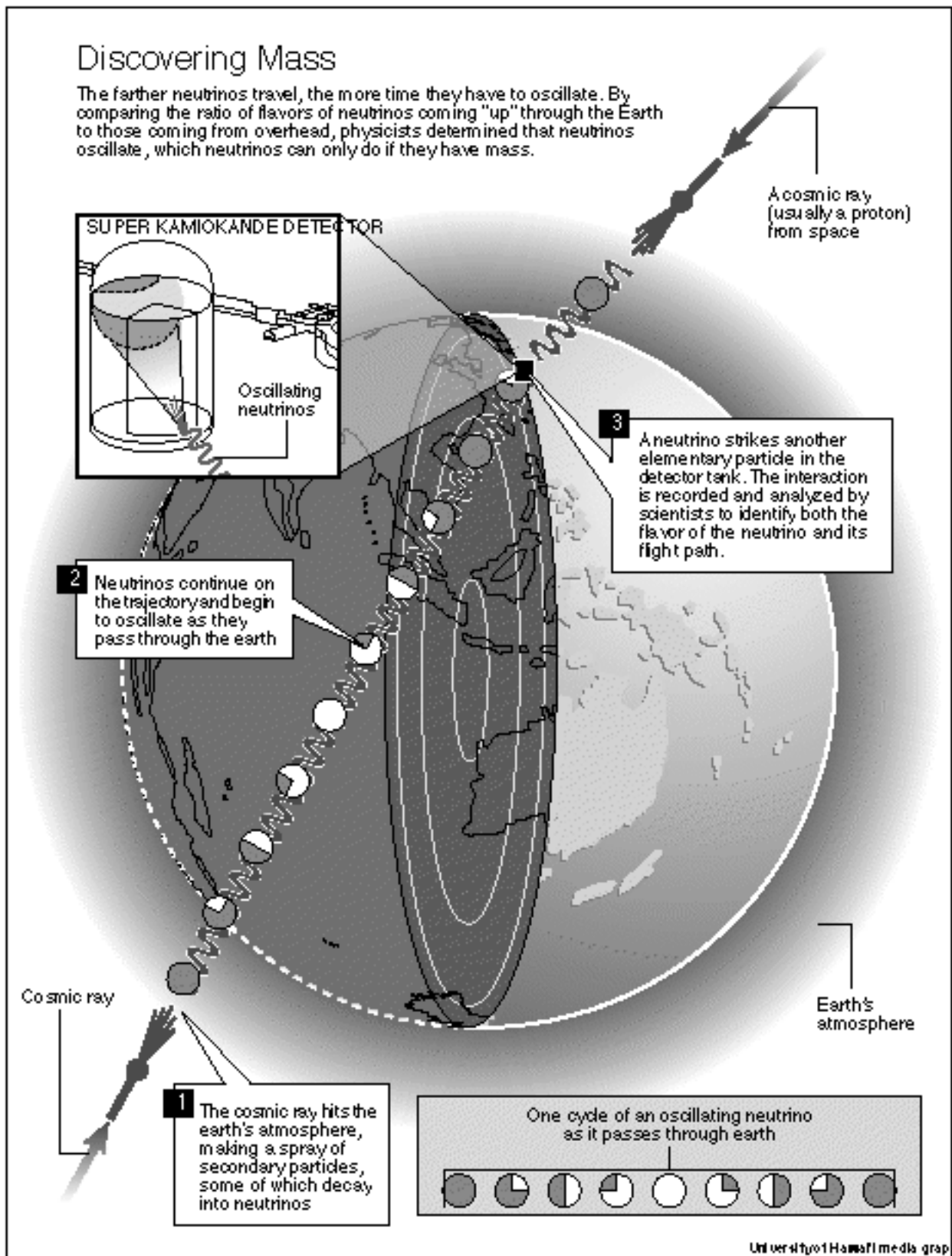
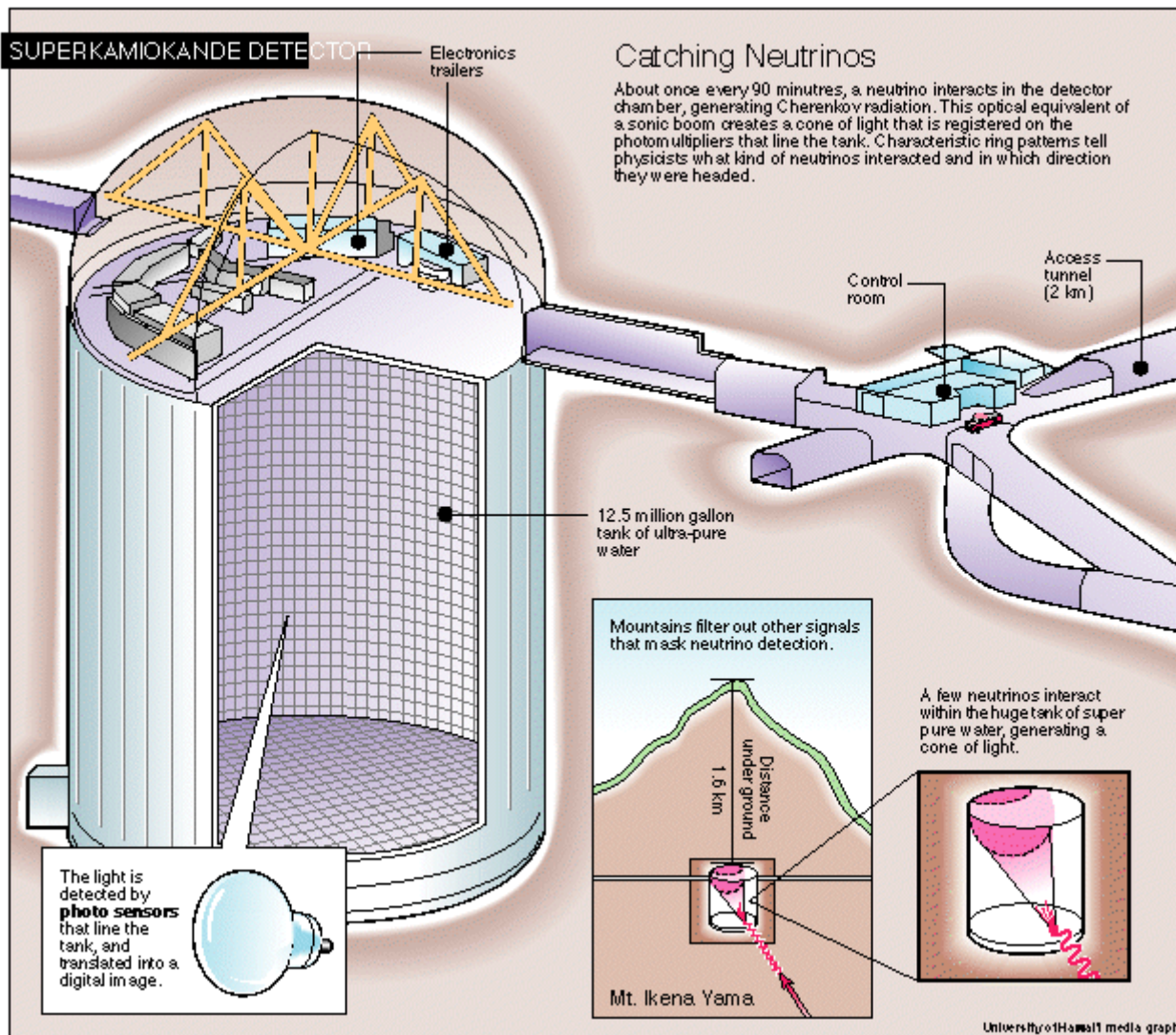


Figure 120: Neutrino oscillations through Earth



- Figure 121: Schematics of the Super-Kamiokande detector
- Detector placed in a deep mine to reduce the background
 - $50\,000\text{ m}^3$ of water and 13 000 photomultipliers work at the Cherenkov detector

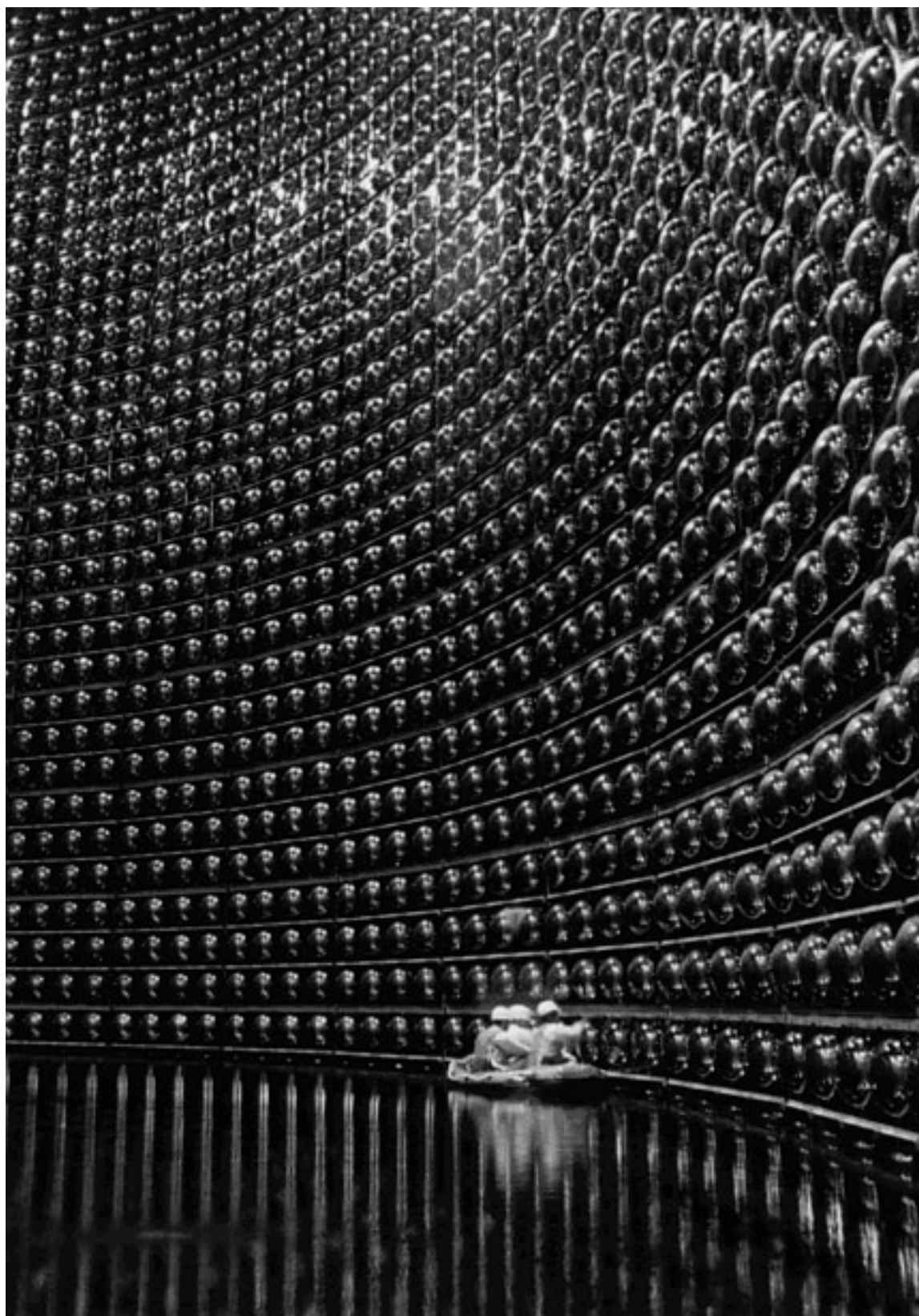


Figure 122: Interior of the Super-Kamiokande detector (during construction)

- ▣ In 1998, the Super-Kamiokande Collaboration announced:
- a) 4654 observed events – by far the largest statistical sample
 - b) data exhibit zenith angle dependence of ν_μ deficit
 - c) hence the “atmospheric neutrino anomaly” can only be explained by oscillations $\nu_\mu \leftrightarrow \nu_\tau$, which leads to muonic neutrino deficiency in cosmic rays.
 - d) the mixing angle and neutrino mass difference Δm estimated at

$$\begin{aligned} \sin^2(2\alpha) &> 0.82 \\ 5 \times 10^{-4} < \Delta m^2 < 6 \times 10^{-3} \text{ eV}^2 \end{aligned} \tag{217}$$

Solar neutrino problem

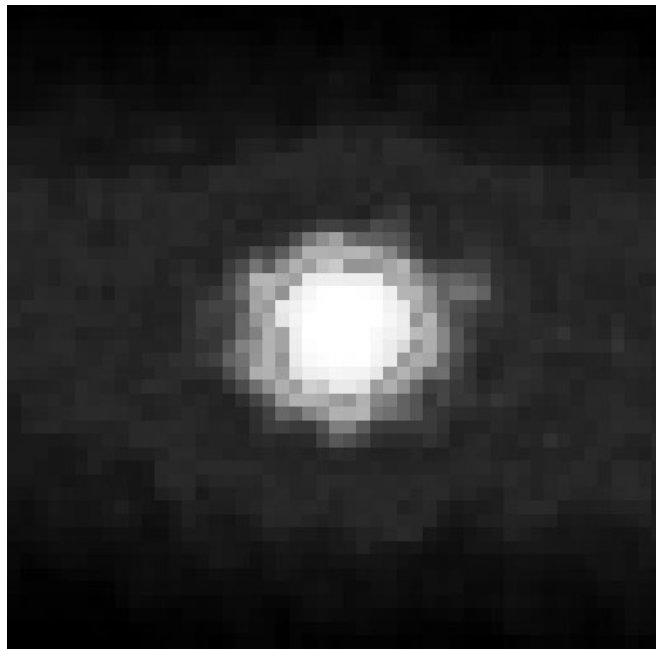
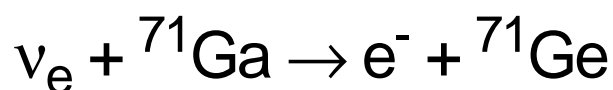
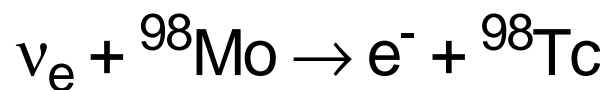
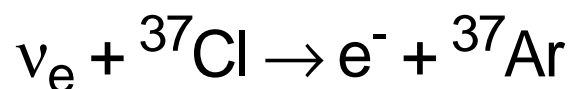
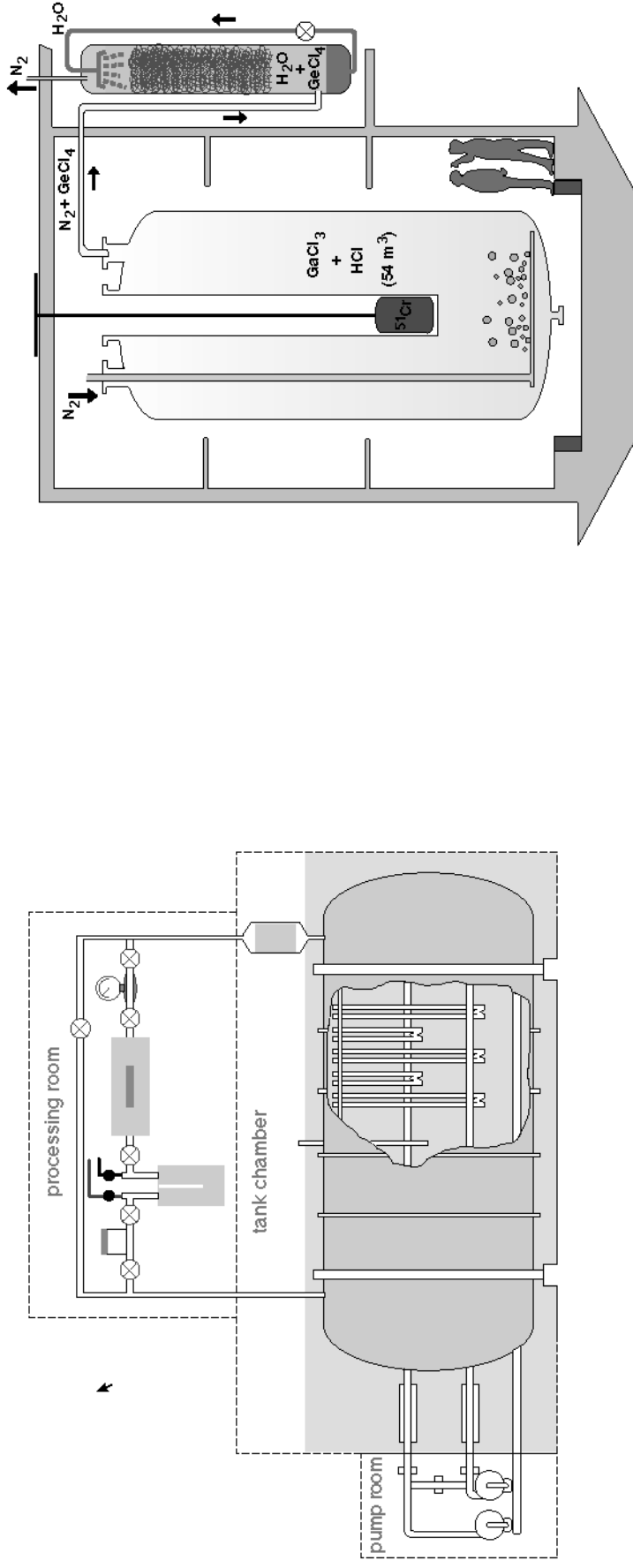


Figure 123: “Portrait” of the Sun in neutrinos

Several (similar) methods are used to detect solar neutrinos:



Experimental installations typically are tanks filled with corresponding medium and placed underground



Homestake gold mine detector (data taking since 1970, USA)

GALLEX detector under the Gran Sasso mountain (Italy)

Figure 124: Typical layouts of solar neutrino detectors

Solar neutrino flux is measured in SNU (“solar neutrino unit”):

$$1 \text{ SNU} = 1 \text{ capture} / 1 \text{ second} / 10^{36} \text{ target atoms}$$

“Solar neutrino problem”:

- ▣▣▣▣ For the Homestake detector, predicted neutrino flux is 7.3 ± 2.3 SNU, measured 2.5 ± 0.2 SNU
- ▣▣▣▣ GALLEX: predicted 132 ± 9 SNU, measured 79 ± 11 SNU

Reactions producing solar neutrinos are:



GALLEX measures all of them, Homestake – only the last one.

- ▣▣▣▣ **Neutrino oscillations seems to be the most appealing explanation, although there are many other hypotheses**

- ▣▣▣▣ Detection of neutrinos from supernovae can provide information about neutrino mass
- ▣▣▣▣ Simultaneous observation of neutrinos from the SN1987a on February 23, 1987 by two experiments (IMB and Kamiokande) set the upper limit on the neutrino mass of 20 eV

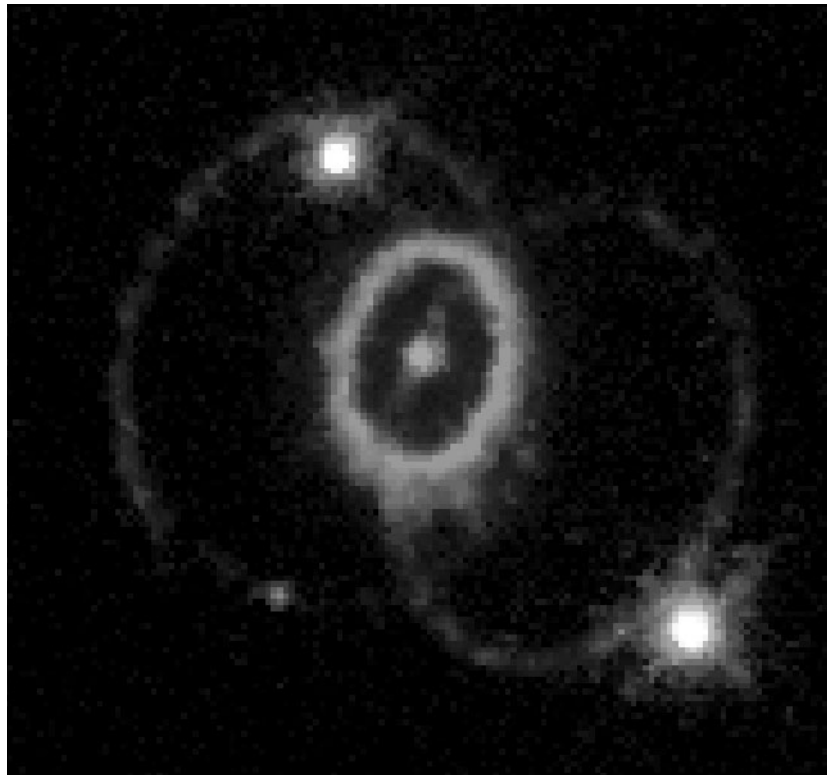


Figure 125: SN1987a as seen by the Hubble Space Telescope in 1994

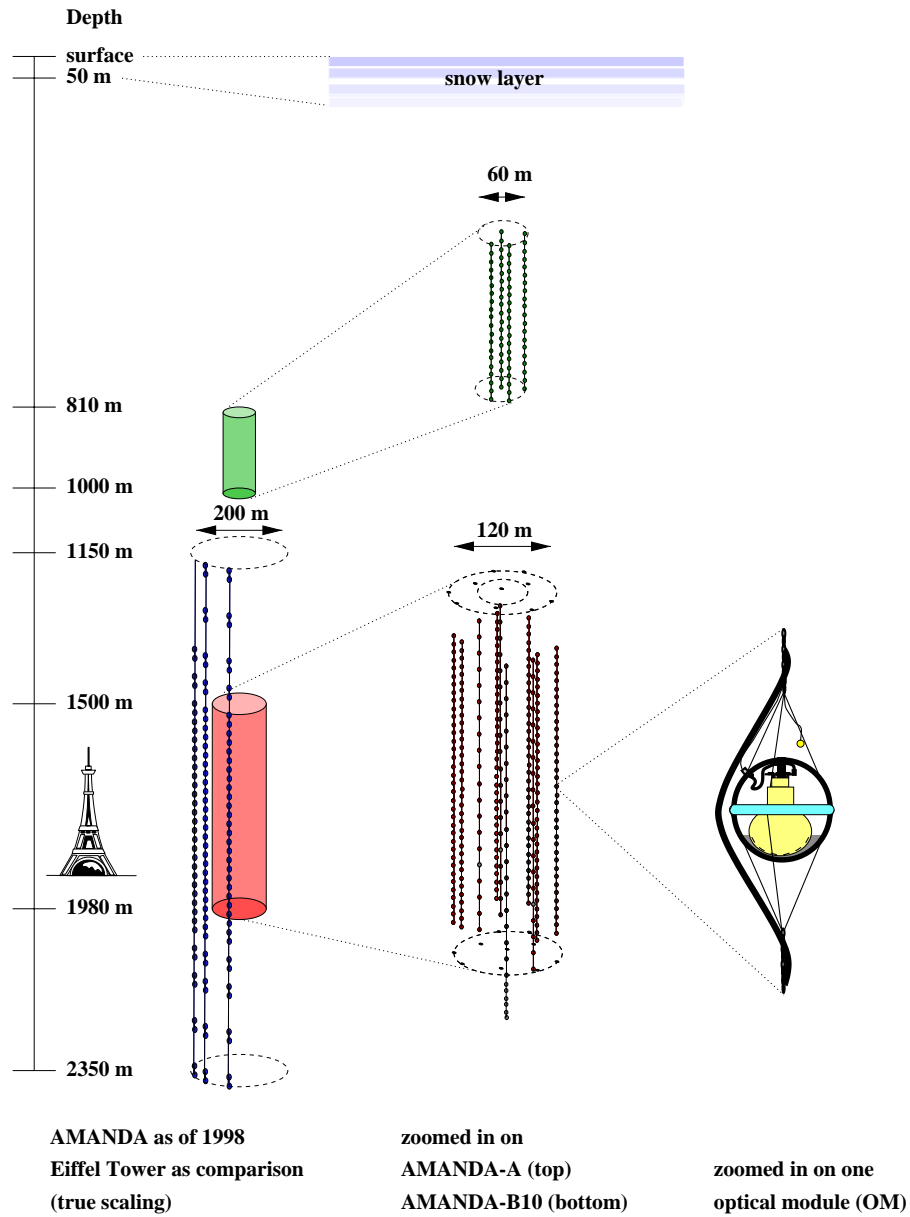


Figure 126: Schematics of the AMANDA neutrino telescope at the South Pole

Dark matter

Experimental evidence for the Big Bang model:

- Universe expands
- Cosmic background radiation
- Abundance of light elements

Expansion will halt at the critical density of the Universe:

$$\rho_c = \frac{3H_0^2}{8\pi G} = O(10^{-26}) \text{ kg m}^3$$

H_0 is Hubble constant and G is the gravitational constant.

The relative density is estimated to be close to 1:

$$\Omega \equiv \rho / \rho_c = 1$$

- ▣▣▣▣▶ Relative density of observable (i.e. emitting electromagnetic radiation) matter in the Universe is only $\Omega_L \approx 0.01$
- ▣▣▣▣▶ The rest is called “dark matter”

Possible components of the dark matter:

- a) *Baryonic matter* that emit little or no e.m. radiation: brown dwarfs, small black holes – MACHO's (for MAssive Compact Halo Object). There is evidence that $\Omega_B \approx 0.06$ only.
- b) Massive neutrinos (“*hot dark matter*”): at the big bang, rate of neutrino production is the same as of photons \Rightarrow knowing the density of photons and the expansion rate of the Universe:

$$\sum m_\nu \leq 100 \text{ eV}/c^2$$

Apparently, neutrinos can not be the dominant dark matter either.

- c) “*Cold dark matter*”: WIMP's (Weakly Interacting Massive Particles), non-baryonic objects, non-relativistic at early stages of the Universe evolution. Still to be detected...

Grand Unified Theories (GUTs)

- ▣▣▣▣ Weak and electromagnetic interactions are unified, why not to add the strong one?
- ▣▣▣▣ At some very high “unification mass” electroweak and strong couplings might become equal

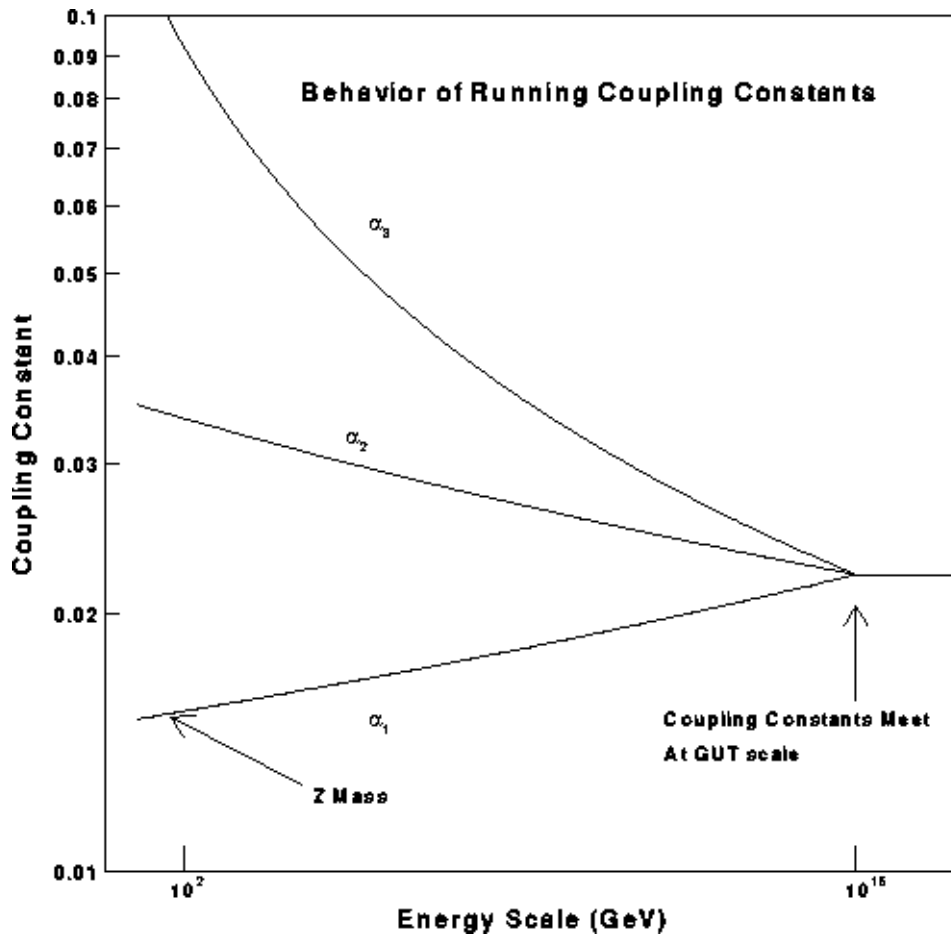


Figure 127: Behavior of coupling constants in GUT; α_1 and α_2 denote couplings at Z and W respectively

Grand unified theories can be constructed in many different ways.

❖ Georgi-Glashow model combines coloured quarks and leptons in single families, like

$$(d_r, d_g, d_b, e^+, \bar{\nu}_e)$$

and hence new gauge bosons appear:

X with $Q=-4/3$ and Y with $Q=-1/3$, $M_X \approx 10^{15} \text{ GeV}/c^2$:

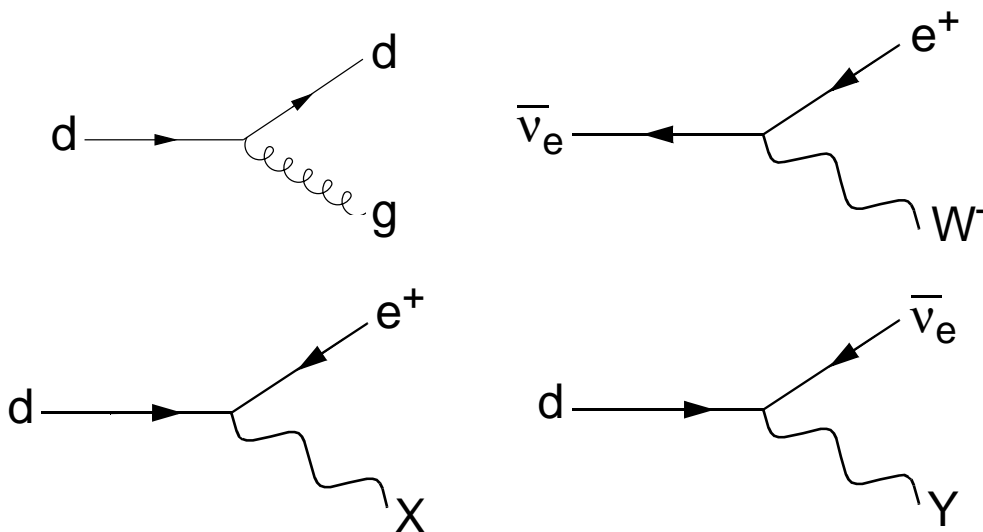


Figure 128: Standard processes together with predicted by GUT

The single unified coupling constant is g_U , and

$$\alpha_U \equiv \frac{g_U^2}{4\pi} \approx \frac{1}{42} \tag{218}$$

Georgi-Glashow model explains equal magnitudes of electron and proton charge

Sum of electric charges in any given family must be zero $\Rightarrow 3Q_d + e = 0 \Rightarrow$ down-quark has charge $-e/3$.

Factor of 3 arises simply from the number of colors

This model also predicts the weak mixing angle using values of the coupling constants:

$$\sin^2 \theta_W = 0.21 \tag{219}$$

which is very close to experimental results, but not precisely.

GUT predict that proton is unstable and can decay by a process involving X or Y bosons

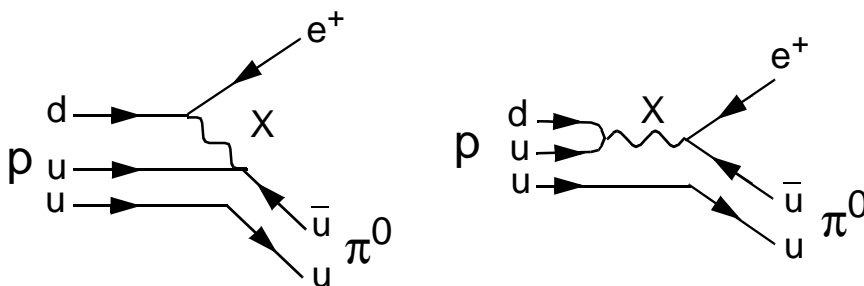


Figure 129: Proton decays in GUT

❖ In processes like those on Fig.129, baryon and lepton numbers are not conserved, but their combination is:

$$B - L \equiv B - \sum_{\alpha} L_{\alpha} \quad (\alpha = e, \mu, \tau) \quad (220)$$

❖ From the simple zero-range approximation, lifetime of the proton is (from different GUTs):

$$\tau_p = 10^{29} \div 10^{30} \text{ years} \quad (221)$$

while the age of the universe is about 10^{10} years...

❖ Same detectors as used in the neutrino physics (IMB, Kamiokande) are looking for the proton decays, but have not observed a clear example so far.

➡ Baryon number non-conservation allows explanation of excess of baryons in the universe as compared to antibaryons. However, CP-violation must be present as well.

Supersymmetry (SUSY)

➡ Most popular GUTs incorporate SUSY

❖ Every known elementary particle has a supersymmetric partner - "superparticle" - with different spin:

| Particle | Symbol | Spin | Superparticle | Symbol | Spin |
|----------|----------|-------|---------------|------------------|-------|
| Quark | q | $1/2$ | Squark | \tilde{q} | 0 |
| Electron | e | $1/2$ | Selectron | \tilde{e} | 0 |
| Muon | μ | $1/2$ | Smuon | $\tilde{\mu}$ | 0 |
| Tauon | τ | $1/2$ | Stauon | $\tilde{\tau}$ | 0 |
| W | W | 1 | Wino | \tilde{W} | $1/2$ |
| Z | Z | 1 | Zino | \tilde{Z} | $1/2$ |
| Photon | γ | 1 | Photino | $\tilde{\gamma}$ | $1/2$ |
| Gluon | g | 1 | Gluino | \tilde{g} | $1/2$ |
| Higgs | H | 0 | Higgsino | \tilde{H} | $1/2$ |

Supersymmetric particles however have to be much heavier than their counterparts

- ➡ SUSY shifts grand unification mass from 10^{15} to 10^{16} GeV/c², and hence the lifetime of the proton increases:

$$\tau_p = 10^{32} \div 10^{33} \text{ years} \quad (222)$$

which is more consistent with experimental (non)observations.

- ➡ SUSY also modifies value of the weak mixing angle (219) to be closer to experimental results.
- ➡ SUSY even attempts at unifying ALL forces, including gravity, at the *Planck mass* of order 10^{19} GeV/c² by replacing particles with *superstrings*
- ➡ Lightest superparticles can be candidates for the cold dark matter; most models introduce *neutralino* $\tilde{\chi}_0$, which is the mixture of photino, Higgsino and zino:

$$e^+ + e^- \rightarrow \tilde{e}^+ + \tilde{e}^- \quad (223)$$

$$\tilde{e}^+ \rightarrow e^+ + \tilde{\chi}_0 \quad \tilde{e}^- \rightarrow e^- + \tilde{\chi}_0 \quad (224)$$

SUSY predictions for reactions (223)-(224):

- 1) Cross-section of (223) is comparable with producing ordinary charged particles of the same mass
- 2) Selectrons decay before they can reach a detector
- 3) Neutralinos are virtually undetectable due to very weak interaction

Thus only final state electrons in (224) can be detected, so that they:

- a) carry only half of the initial energy of e^+e^- state,
 - b) should not be emitted in opposite directions in CM frame
- ⇒ No signature of this kind has been observed so far, tests at higher energies needed